Chitosan–Cellulose Nanocrystal Polyelectrolyte Complex Particles: Preparation, Characterization, and *In Vitro* Drug Release Properties

Hezhong Wang

Dissertation submitted to the faculty of the
Virginia Polytechnic Institute and State University
in partial fulfillment of the requirements for the degree of

Doctor of Philosophy
In
Forest Products

Maren Roman, Chair
Richey M. Davis
Susan E. Duncan
Sean F. O'Keefe
Scott H. Renneckar

October 22, 2009
Blacksburg, VA

Keywords: cellulose nanocrystals, chitosan, polyelectrolyte complex, drug delivery, caffeine, ibuprofen

Chitosan–Cellulose Nanocrystal Polyelectrolyte Complex Particles: Preparation, Characterization, and *In Vitro* Drug Release Properties

Hezhong Wang

ABSTRACT

Polyelectrolyte complexes (PECs) between chitosan, a mucoadhesive, intestinal mucosal permeability-enhancing polysaccharide, and cellulose nanocrystals, rod-like cellulose nanoparticles with sulfate groups on their surface, have potential applications in oral drug delivery. The purpose of this research was to develop an understanding of the formation and properties of chitosan–cellulose nanocrystal PECs and determine their *in vitro* drug release properties, using caffeine and ibuprofen as model drugs. Cellulose nanocrystals were prepared by sulfuric acid hydrolysis of bleached wood pulp. Chitosans with three different molecular weights (81, $3 \cdot 10^3$, $6 \cdot 10^3$ kDa) and four different degrees of deacetylation (77, 80, 85, 89%) were used. PEC formation was studied by turbidimetric titration. PEC particles were characterized by FT-IR spectroscopy, scanning electron microscopy, dynamic light scattering, and laser Doppler electrophoresis. The formation and properties of chitosan–cellulose nanocrystal PEC particles were governed by the strong mismatch in the densities of the ionizable groups. The particles were composed primarily of cellulose nanocrystals. Particle shape and size strongly depended on the mixing ratio and pH of the surrounding medium. The ionic strength of the surrounding medium, and the molecular weight and degree of deacetylation of chitosan had a minor effect. Release of caffeine from the chitosan–cellulose nanocrystal PEC particles was rapid and uncontrolled. Ibuprofen-loaded PEC particles showed no release in simulated gastric fluid and rapid release in simulated intestinal fluid. Further evaluation studies should focus on the expected mucoadhesive and permeability-enhancing properties of chitosan–cellulose nanocrystal PEC particles.

ACKNOWLEDGMENTS

I sincerely thank my advisor, Dr. Maren Roman, for giving me the opportunity to work on this project, and for her guidance, which was essential to the completion of my dissertation. I am grateful to Drs. Richey Davis, Susan E. Duncan, Sean F. O'Keefe, and Scott H. Renneckar for serving on my graduate committee, providing valuable suggestions, and reviewing my dissertation.

I thank Dr. Paul M. Winistorfer (the department head) for being approachable and supportive of graduate students in the department. I also thank the professors of the Department of Wood Science and Forest Products for their help, support, and patience throughout the last four years. I further thank Debbie Garnand for her assistance with administrative issues. Particular thanks go to Stephen R. McCartey for training me in the operation of the FE-SEM at the Nanoscale Characterization and Fabrication Laboratory.

Thanks go also to all students and postdoctoral associates in the Departments of Wood Science and Forest Products, Chemistry, Chemical Engineering, Food Science and Technology, and the Virginia Tech Writing Center, who have provided access to and training in the use of laboratory equipment, help in sample preparation, and with technical problems that I have encountered with regard to AFM, SEM, DLS, NMR spectroscopy, as well as help in the preparation of my dissertation.

Above all, I must acknowledge my family for their unwavering love and support throughout my life. Special thanks go to my son, Ban Wang, for his assistance in solving computer problems and correcting my writing.

The research was supported in part by the USDA/CSREES under Grant No. 2005-35504-16088, the National Science Foundation under Grant No. CHE-0724126, and the Institute for Critical Technology and Applied Science at Virginia Tech. Additional support from Omnova, Inc. and Tembec, Inc. is also acknowledged.

TABLE OF CONTENTS

LIST OF FIGURES

Chapter 2

Chapter 3

Chapter 4

Chapter 5

Chapter 6

LIST OF TABLES

Chapter 6

CHAPTER 1

INTRODUCTION

Polyelectrolytes are polymers that contain functional groups capable of dissociating into ions. Mixing polyelectrolytes of opposite charge results in the formation of polyelectrolyte complexes due to attractive Coulomb forces between the opposite charges. Polyelectrolyte complexes between e.g. gelatin and gum acacia or alginate have long been used in the food industry for the encapsulation of sensitive ingredients in food products. Recently, polyelectrolyte complexes have been studied for use in drug, gene, and protein delivery, enzyme immobilization, and cell encapsulation, among other areas.

A bio-based polyelectrolyte that has received considerable attention is chitosan, an amino group ($–NH_2$) containing polysaccharide. In acidic media, the amino groups of chitosan are protonated and carry a positive charge ($–NH_3^+$). Chitosan has many properties that render it attractive for applications in the food and pharmaceutical industries. For example, chitosan has been shown to be non-toxic, biocompatible, and biodegradable. In addition, chitosan has been shown to enhance the intestinal absorption of nutrients and drugs by increasing the residence time in the intestine and the permeability across mucosal membranes.

Many synthetic and natural polymers bearing negative charges have been studied for the formation of polyelectrolyte complexes with chitosan. The goal of this research is to explore a novel polyelectrolyte complex consisting of chitosan and cellulose nanocrystals.

Cellulose nanocrystals are nanoscale, rod-like, crystalline particles of cellulose bearing a small number of sulfate groups ($–OSO_3H$) on their surface. The sulfate groups

are the result of a side reaction during the preparation of the nanocrystals with sulfuric acid. In aqueous media, at most pH levels, these sulfate groups are deprotonated and carry a negative charge ($–OSO_3^-$). Cellulose has been used as a food additive and excipient in drug tablets for decades. Polyelectrolyte complexes of chitosan and cellulose are therefore promising candidates as controlled release systems in food products and oral drug formulations. Moreover, the research represents one of the first studies on the complexation of a polyelectrolyte and rod-like nanoparticles. Thus, the results of this research are likely to yield new insights into the mechanisms of ionic self-assembly. The objectives of this research are to:

1. Develop a method for the preparation of chitosan–cellulose nanocrystal polyelectrolyte complexes;
2. Determine the effects of pH and ionic strength on the formation and properties of the polyelectrolyte complexes;
3. Determine the effects of chitosan molecular weight and degree of deacetylation on the formation and properties of the polyelectrolyte complexes;
4. Evaluate the drug release properties of the polyelectrolyte complexes for selected model drugs.

The research results are reported in four chapters, namely Chapters 3 through 6, written in manuscript format. Chapter 2 reviews the relevant literature and Chapter 7 presents the overall conclusions.

CHAPTER 2

LITERATURE REVIEW

2.1. CHITOSAN

2.1.1. Origin of Chitosan

Chitosan was first reported by Rouget in 1859 upon boiling chitin in a concentrated potassium hydroxide solution (Rouget, 1859). However, detailed studies of chitosan did not start until a century later (Li *et al.*, 1992). Before 1970, less than 10 papers per year related to the study of chitosan had been listed in Chemical Abstracts. By 1999, the number had increased to more than 2000 (Muzzarelli, 1977; Li *et al.*, 1992; Domard and Domard, 2002). Chitosan is the second most abundant polymer in nature, after cellulose, and the primary structural component of the outer skeletons of crustaceans and of many other species, such as mollusks, insects, and fungi. Chitosan has attracted interest because of its abundance and renewability but also because of its unique physicochemical properties.

Chitosan is produced from chitin, a linear homopolysaccharide of β(1–4) linked 2-acetamido-2-deoxy-D-glucopyranose (GlcNAc) residues (Figure 2.1). There are three crystalline forms of chitin, α-, β-, and γ-chitin. Of the three forms, α-chitin has been studied most extensively because of its abundance and accessibility (Shimojoh *et al.*, 1998). Chitosan prepared from β-chitin has been reported to have high bactericidal activity and a higher reactivity than chitosan prepared from α-chitin (Kurita *et al.*, 1993; Shimojoh *et al.*, 1996). Nevertheless, the preparation of chitosan from crustacean shells,

composed of α-chitin, is economically and ecologically preferred over the preparation of chitosan from β-chitin, because large amounts of α-chitin are available as a waste product of the food industry. In recent years, the production of chitosan from fungi using fermentation methods also has attracted attention (Roberts, 1992; Nwe *et al.*, 2002; Säkkinen, 2003).

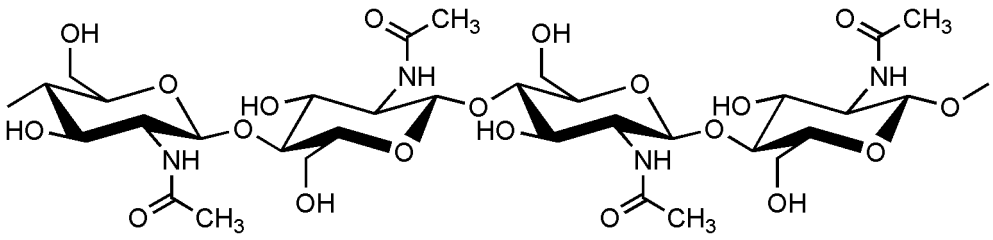

Figure 2.1. Molecular structure of chitin.

2.1.2. Structure of Chitosan

2.1.2.1. Molecular Structure

Chitosan is a linear copolysaccharide of β(1–4) linked GlcNAc and 2-amino-2-deoxy-D-glucopyranose (GlcN) residues (Figure 2.2).

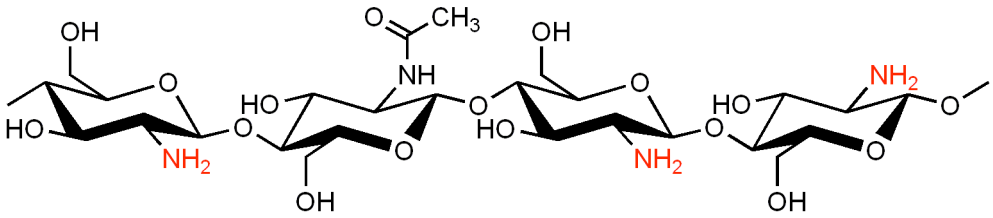

Figure 2.2. Molecular structure of chitosan.

Chitosan is obtained by heating chitin in a concentrated (> 40%) solution of sodium hydroxide at high temperature (90–120 °C) (Roberts, 1992). This harsh treatment removes some of the acetyl groups on the GlcNAc residues, converting them into GlcN

residues. Different hydrolysis processes result in chitosans with different GlcNAc and GlcN proportions and sequences. Hydrolysis under heterogeneous conditions has been reported to give block-type copolymers with several-residue-long GlcNAc or GlcN sequences, whereas hydrolysis under homogeneous conditions has been found to produce copolymers with a random sequence of GlcNAc and GlcN residues (Kurita *et al.*, 1977; Aiba, 1991).

2.1.2.2. Solid-State Structure

The solid-state structure of chitosan depends strongly on the molecular properties, in particular the proportions, sequence, and number of GlcNAc and GlcN residues. Chitosan with equal proportions and a random sequence of GlcNAc and GlcN residues has been reported to be completely amorphous and highly soluble (Kurita *et al.*, 1991). Chitosan with a high proportion of GlcN residues and short chain length (low molecular weight) has been observed to be highly crystalline (Ogawa, 1991; Ogawa and Yui, 1993). Two crystalline forms of chitosan can be distinguished: hydrated (Okuyama *et al.*, 1997) and anhydrous (Ogawa *et al.*, 1984). In both cases, the chitosan chains have a fully extended two-fold helical conformation (Okuyama *et al.*, 2000). The structure of the hydrated crystalline form of chitosan is shown in Figure 2.3.

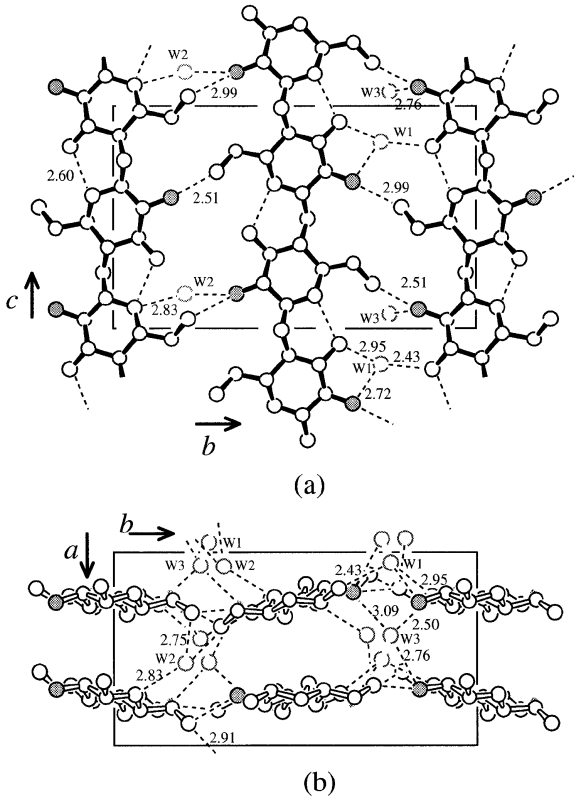

Figure 2.3. Packing structure of hydrated chitosan projected along the *a*-axis (a) and along the *c*-axis (b). Filled circles denote nitrogen atoms. For the sake of clarity, only three polymer chains of the lower layer in (b) are shown in (a). (Reprinted from Okuyama *et al.*, 1997; fair use; Copyright 1997 American Chemical Society)

2.1.2.3. Chitosan Conformation in Solution

The conformation of chitosan molecules in solution depends on two kinds of parameters: parameters related to the molecular structure, such as the chain length (molecular weight) and proportions of GlcNAc and GlcN residues, and parameters related to the molecular environment, such as type of solvent, pH, ionic strength, and temperature. It is commonly accepted that chitosan molecules behave like more or less stiff wormlike chains (Sorlier *et al.*, 2002).

In acidic solutions, the amino groups of the GlcN residues are protonated and positively charged (Figure 2.4).

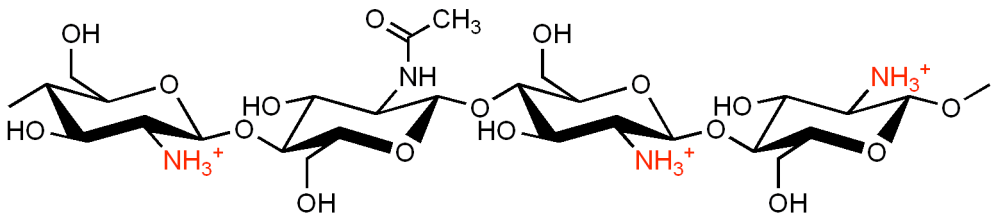

Figure 2.4. Protonated structure of chitosan occurring in acidic aqueous solutions.

Repulsive electrostatic forces between the charges along the chain reduce the molecular flexibility and result in a more extended conformation (Buhler and Rinaudo, 2000). Random coil conformation has been reported for chitosan in dilute HCl solution at temperatures between 10 and 50 °C (Chen and Tsaih, 1998). Temperature-induced conformational transitions were not observed in this study. By intrinsic viscosity measurements, the authors found the flexibility of chitosan molecules to be correlated with the molecular weight (chain length) (Tsaih and Chen, 1997; Chen and Tsaih, 1998). The results indicated that chitosan molecules of a molecular weight equal to or greater than 223 kDa had a random coil conformation, whereas molecules with a molecular weight of 148 kDa or lower had an extended rod-like conformation (Tsaih and Chen, 1997). The authors attributed the observed molecular weight-induced conformational transition to differences in the intramolecular hydrogen bonding patterns and charge distributions below and above the transition. In a later study, Tsaih and Chen (1999a) reported that neither the ionic strength, nor the pH, or temperature substantially affected the conformation of chitosan molecules. Berth and Dautzenberg (2002), on the other hand, found that the proportions of GlcNAc and GlcN residues and the ionic strength had an insignificant effect on the chain conformation of chitosan.

Due to the many –OH groups in the molecule, polysaccharides have a tendency to form intra- and interchain hydrogen bonds, causing insolubility or molecular aggregation in solutions (Rinaudo, 2008). Moreover, polysaccharides have hydrophobic properties due to –CH groups, which are the basis for hydrophobic interactions (Rinaudo, 2006).

2.1.3. Molecular Weight

As mentioned above, chitosan is obtained by alkali hydrolysis (N-deacetylation) of chitin at high temperature. The harsh chemical treatment leads to a reduction in molecular weight from many million Daltons (Da) in chitin to molecular weights in the range 10–1,000 kDa (George and Abraham, 2006) for commercial chitosans. Chitosans from Fluka (Biochemika, Switzerland), for example, are classified as high-molecular-weight with a molecular weight of about 2,000 kDa; medium-molecular-weight with a weight of about 750 kDa, and low-molecular-weight with weight of about 70 kDa.

A number of analytical techniques have been used to measure the molecular weight of chitosan, including size exclusion chromatography (Wu *et al.*, 1976; Mima *et al.*, 1983; Beri *et al.*, 1993; Niola *et al.*, 1993; Ottoy *et al.*, 1996; Knaul *et al.*, 1998; Schatz *et al.*, 2003), dynamic light scattering (Berth *et al.*, 1998; Buhler and Rinaudo, 2000; Pa and Yu, 2001), and viscometry (Wang *et al.*, 1991; Anthonsen *et al.*, 1993; Wang and Xu, 1994; Lamarque *et al.*, 2005). Of these methods, the viscosity method is the easiest and fastest. It measures the viscosity-average molecular weight and is based on the Mark-Houwink equation, describing the relationship between the intrinsic viscosity, i.e. the viscosity at zero concentration, and the molecular weight of the solute (Wang *et al.*, 1991; Tsaih and Chen, 1999b). A small amount of salt in the solution is required to minimize the electrostatic contributions, screen ionic sites along the chain, hinder electrostatic repulsion, and prevent chains from aggregation (Domard and Rinaudo, 1984; Rinaudo *et al.*, 1993; Anthonsen *et al.*, 1994). Nevertheless, commercial samples used without further purification may yield high and variable polydispersity indices and show aggregate formation by self-association, leading to erroneous molecular weight values (Anthonsen *et al.*, 1994; Berth *et al.*, 1998; Shimojoh *et al.*, 1998; Lamarque *et al.*, 2005). However, most aggregates can be removed by centrifugation or filtration (Berth and Dautzenberg, 2002). In addition to sample purity, the type of solvent, ionic strength, and pH of the solution influence the consistency and reliability of the results (Beri *et al.*, 1993; Brugnerotto *et al.*, 2001b). If the solvent used is not a good solvent, aggregates are formed, which lead to an overestimation of molecular weight. Rinaudo *et al.* (1993) reported that the solvent system 0.1 M acetic acid/0.2 M NaCl was a bad solvent, which

promoted aggregation and caused errors in the determination of the intrinsic viscosity. Filar and Wirick (1978) reported that the solvent system 0.3 M acetic acid/0.2 M sodium acetate minimized the presence of aggregates.

2.1.4. Degree of Deacetylation

The degree of deacetylation (DD) is defined as the average number of GlcN residues per 100 residues (Sabnis and Block, 1997) and is generally expressed as a percentage. Sometimes the DD is expressed as the degree of acetylation (DA) with DA = 100 – DD. The DD is an important parameter for chitosan applications and varies for commercial chitosans from about 70 to 95% (Domard, 1987a; George and Abraham, 2006), depending on the manufacturing and determination methods. Chitosan is soluble in dilute acidic solutions when the DD exceeds 40% (Wang and Xu, 1994).

The effects of the DD and sequence of GlcN and GlcNAc residues, i.e. distribution of N-acetyl groups along the polymeric backbone, on the physical, chemical, and biological properties of chitosan, such as acid–base and electrostatic properties, biodegradability, self-aggregation properties, and sorption properties, have been studied extensively (Bodek, 1995; Kristiansen *et al.*, 1998; Sorlier *et al.*, 2001; Schatz *et al.*, 2003; Guibal, 2004; Balazs and Sipos, 2007; Tajik *et al.*, 2008). The effect of the DD on the solution behavior of chitosan has been described by defining three domains (Schatz *et al.*, 2003): (a) a polyelectrolyte domain (DD > 80%), where electrostatic interactions were predominant but decreased with DD; (b) a transition domain (50% < DD < 80%), where chitosan lost its hydrophilicity or displayed behavior between hydrophilic and hydrophobic; and (c) a hydrophobic domain (DD < 50%), where hydrogen bonding and hydrophobic interactions, primarily between GlcNAc residues, resulted in polymer association and aggregation. The predominance of attractive van der Waals forces in chitosans with a DD below 30% have also been observed by Brunel et al. (2008). The relationship between the viscosity of chitosan solutions and the molecular weight has reported as both dependent (Wang *et al.*, 1991) and independent of the DD (Berth and Dautzenberg, 2002).

Many different methods for measuring the DD of a chitosan sample have been evaluated. These methods include gel permeation chromatography (Aiba, 1986); IR spectroscopy (Sannan, 1978; Miya *et al.*, 1980; Moore and Roberts, 1980; Domszy and Roberts, 1985; Baxter *et al.*, 1992; Sabnis and Block, 1997; Khan *et al.*, 2002; Sahu *et al.*, 2009); potentiometric and conductometric titration (Raymond *et al.*, 1993; Kuang and Liu, 2006; Balazs and Sipos, 2007); ^{1}H NMR spectroscopy (Hirai *et al.*, 1991; Bodek, 1995; Budovskaya *et al.*, 1997; Jia and Li, 2002; ASTM, 2003; Jiang *et al.*, 2003; Lavertu *et al.*, 2003; Kuang and Liu, 2006; Balazs and Sipos, 2007); ninhydrin reaction (Prochazkova *et al.*, 1999); and UV or first derivative UV spectrophotometry (Muzzarelli and Rocchetti, 1985; Aiba, 1986; Tan *et al.*, 1998; Liu *et al.*, 2006; Wu and Zivanovic, 2008). It has been recognized, however, that different methods frequently yield different DD values for the same chitosan sample (Khan *et al.*, 2002).

Of the different methods, IR spectroscopy-based ones rank among the most convenient. The method by Domszy and Roberts (1985) uses the absorption band at 1655 cm $^{-1}$, attributed to the vibrations of the C=O groups of the GlcNAc residues, as a measure for the proportion of GlcNAc residues, and the absorption band at 3450 cm^{-1}, arising from the vibrations for the –OH groups, as an internal standard. The DD is calculated from

$$\mathrm{DD} = 100 - \left[\left(A_{1655} / A_{3450}\right) \cdot 100/1.33\right] \qquad [2.1]$$

where A_{1655} and A_{3450} are the absorbances at 1655 and 3450 cm^{-1}, respectively, and the factor '1.33' is the value of A_{1655}/A_{3450} for chitin (DD = 0%).

The method by Baxter *et al.* (1992) uses the same absorption bands but a different baseline for the absorption band at 1655 cm $^{-1}$. The DD is calculated form the empirical equation

$$DD = 100 - \left[\left(A_{1655} / A_{3450}\right) \cdot 115\right] \qquad [2.2]$$

Sabnis and Block (1997) have proposed a further modification of the method, involving the use of a calibration curve instead of empirical equations for the determination of DD. The method has been shown to yield superior results.

2.1.5. Persistence Length

The persistence length of a polymer is the maximum length of an uninterrupted chain persisting in a particular direction. It is a measure of the molecular rigidity and determines the viscosity of a solution of the polymer. The persistence length of polyelectrolytes is strongly influenced by ionic strength and polyelectrolyte concentration (Buhler and Rinaudo, 2000).

The actual persistence length (L_t) of a polyelectrolyte has an intrinsic contribution (L_p), due to the rigidity of the uncharged chain, and an electrostatic contribution (L_e) arising from the repulsive forces between the charges along the chain. For polysaccharides, L_e is much smaller than L_p (Buhler and Rinaudo, 2000) because of extensive intramolecular hydrogen bonding. Molecular modeling studies showed a moderate dependence of L_p on the DD of chitosan (Mazeau *et al.*, 2000; Mazeau and Rinaudo, 2004). L_p increased from 9 nm for DD = 100 % to 12.5 nm for DD = 40 %, after which it remained constant until DD = 0 % (completely acetylated) (Mazeau and Rinaudo, 2004). Schatz *et al.* (2004), on the other hand, observed no specific trend for L_p at different DDs but the chain stiffness was found to decrease with an increase in temperature. Brugnerotto et al. (2001a; 2001b) reported experimental L_p values, measured by size exclusion chromatography, of 11 nm for 75% > DD > 100 % and 15 nm for DD = 40 %. The L_p value reported by Terbojevich *et al.* (1991) was 22 nm for DD = 58 and 85 %. Berth and Dautzenberg (2002) investigated the chain conformation of chitosan in salt-containing solutions (pH = 4.5, ionic strength = 0.12 M) and found that L_p was approximately 6 nm, irrespective of DD. For heterogeneously acetylated chitosan, L_p was 11 nm independent of the DD in the range 75 < DD < 100 % (Brugnerotto *et al.*, 2001b; Rinaudo, 2008). For homogeneously acetylated chitosans, L_p was found to increase slightly from 11 to 15 nm when DD decreased to 40% (Brugnerotto *et al.*, 2001b).

2.1.6. Solubility

Chitosan is insoluble in water, alkali, and organic solvents, but soluble in many dilute aqueous organic acids at concentration in the range of 0.25 to 10% (Filar and Wirick, 1978) and some inorganic acids such as HCl, acetic acid, and dilute H_2SO_4 (Wu *et al.*, 1976; Gamzazade *et al.*, 1985; Amiji, 1995; Rinaudo *et al.*, 1999; Zamani *et al.*, 2007). As mentioned above, in acidic aqueous media, the amino groups of chitosan are protonated. The pK_a values reported for chitosan are in the range 6.2–7 (Hejazi and Amiji, 2002). The intrinsic pK_a of chitosan has been found to be independent of the DD (Domard, 1987b; Domard and Domard, 2002). If the pH of the solution approaches the pK_a, the amino groups become deprotonated and chitosan precipitates. The solubility of chitosan also depends on the hydrolysis conditions, molecular weight, and DD (Terbojevich *et al.*, 1991; Brugnerotto *et al.*, 2001a). The effect of DD is related to the molecular hydrophilicity, which increases with increasing DD (Sannan *et al.*, 1976; Aiba, 1989). However, samples with the same DD may have different solubilities if they were obtained with different hydrolysis processes (Kurita *et al.*, 1977). In this case, the difference in solubility would be related to differences in chain length or the distrubution of GlcN and GlcNAc residues along the chain. Kurita *et al.* (1977) reported chitosans obtained under heterogeneous hydrolysis conditions to be insoluble in water and chitosans produced under homogeneous conditions to be water-soluble.

Most commercial chitosans obtained by heterogeneous deacetylation of chitin have a tendency to form molecular aggregates in solution (Anthonsen *et al.*, 1994). The aggregation activity of chitosan obtained from β-chitin was found to be higher than that obtained from α-chitin (Shimojoh *et al.*, 1998). Shimojoh *et al.*(1998) also reported that even low-molecular-weight chitosan obtained from β-chitin formed aggregates in dilute solution. The critical aggregation concentration has been reported as 10^{-4} kg/L (Qun and Ajun, 2006). Wu *et al.* (1995) observed by dynamic laser light scanning that even in dilute solution, chitosan forms a certain amount of large aggregates.

The mechanism of aggregate formation is not well understood. Hydrophobic moieties in chitosan, such as the acetyl groups and glucosidic rings, are believed to play a significant role by promoting hydrophobic interactions (Aiba, 1991; Amiji, 1995; Ottoy

et al., 1996; Philippova *et al.*, 2001; Schatz *et al.*, 2003). Low-molecular-weight electrolytes shield the repulsive interactions allowing attractive interactions to dominate (Philippova *et al.*, 2001).

2.1.7. Biological Properties

Chitosan is an unusual polysaccharide because it bears exclusively positive charges. Chitosan shows notable bioactivities including the promotion of wound healing, hemostatic activity, immune enhancement, hypolipidemic activity, mucoadhesion, and antimicrobial activity (Kurita, 2006; Klossner *et al.*, 2008). Chitosan is largely indigestible and non-absorbable by humans but shows lysozymic digestibility (Aiba, 1992). It can be degraded by certain enzymes, such as chitinases, chitobiases, chitosanases, and glucosaminidases (Hirano *et al.*, 1989; Aiba, 1993; Domard and Domard, 2002; Roncal *et al.*, 2007; Zhang and Sun, 2007). Aiba (1992) proposed an increase in degradation rate with decreasing DD (Figure 2.5).

Deuchi *et al.* (1994) proposed that chitosan was soluble in the stomach to form an emulsion with intragastric oil droplets and precipitated in the small intestine at pH 6–6.5. Chitosan is not degraded in the human intestine due to the absence of suitable enzymes and behaves as a dietary fiber (Shahidi *et al.*, 1999). Shimojoh *et al.* (1998) found that low-molecular-weight chitosan (11–436 kDa) derived from α-chitin was less susceptible to degradation than chitosan from β-chitin. Hirano *et al.* (1990) reported chitosan to be digestible and hypolipidemic at an appropriate dosage by oral administration in rabbits, hens, and broilers. In a recent study, Yang *et al.*(2007) investigated the biodegradation of chitosan fiber and its acetylated derivatives *in vitro* and *in vivo* and reported that the degradation rate of chitosan fibers was strongly dependent on DD. A higher degradability was observed for lower DDs of chitosan.

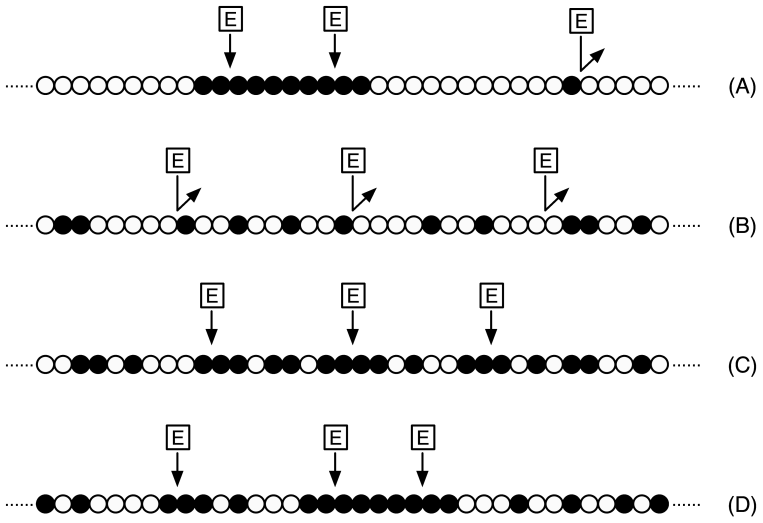

Figure 2.5. Speculative representation of the action of lysozyme on the various types of chitosans: (○) D-glucosamine; (●) N-acetyl-D-glucosamine; (E) lysozyme; (A) chitosan (DD ≈ 70%) prepared by deacetylation of chitin; (B) chitosan (DD ≈ 70%) prepared by acetylation of high-DD chitosan; (C) chitosan (DD < 50%) prepared by acetylation of high-DD chitosan; (D) chitosan (DD < 50%) prepared by acetylation of medium-DD chitosan. (Reprinted from Aiba, 1992; fair use; Copyright 1992 Elsevier B.V.)

Chitosan also exhibits antimicrobial activities. Chitosan constitutes a source of carbon and nitrogen for various kinds of bacteria and fungi such as *Aspergillus oryzae, Mucor mucedo,* and *Phycomyces blakesleeanus* (Chung *et al.*, 1994). The growth of *Escherichia coli*, *Fuarium, Alternaria* was inhibited by chitosan at a concentration of 0.025% (Hirano and Nagao, 1989; Hirano, 1999). The cationic amino groups of chitosan were proposed to bind to anionic chemical groups on these microorganisms resulting in growth inhibition.

2.2. CELLULOSE

2.2.1. Origin of Cellulose

Cellulose, first characterized by Anselme Payen in 1838, is the main component of the cell walls of higher plants (French *et al.*, 2004). It is one of the few natural compounds the structure of which is the same regardless whether its source is wood, cotton, grass, or any of a number of other plants. Acetic acid bacteria (*Acetobacter xylinum*), some animals (tunicates), many forms of algae, as well as the oomycetes are also known to synthesize cellulose (Hirano *et al.*, 2003). Cellulose occurs in nature in the form of highly crystalline microscopic fibrils.

2.2.2. Structure of Cellulose

Cellulose is a linear homopolysaccharide of β(1–4) linked D-glucopyranose (Glc) residues (Figure 2.6). Unlike amylase, a component of starch and linear homopolysaccharide of α(1–4) linked Glc residues, cellulose molecules do not form coils but adopt an extended rod-like conformation. There are two natural crystalline polymorphs of cellulose, known as I_α and I_β. In both polymorphs, cellulose molecules have a twofold screw symmetry in chain direction (Salmon and Hudson, 1997; Baker *et al.*, 2000).

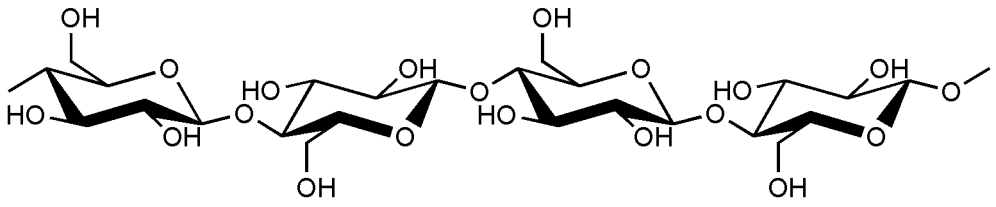

Figure 2.6. Molecular structure of cellulose.

2.2.3. Morphology of Native Cellulose

Macroscopic cellulose fibers are aggregates of small microfibrils of 2–20 nm in width, a crystallinity of 65–95%, lengths depending on the cellulose origin (Helbert *et al.*, 1996; Grunert, 2002; Saito *et al.*, 2007). In the crystalline structures, cellulose molecules form inter-, and intramolecular hydrogen bonds (Heiner *et al.*, 1995) (Figure 2.7). Intramolecular hydrogen bonds are formed between O(3)H and O(5), and between O(2)H and O(6) of adjacent anhydroglucose residues (Grunert, 2002). Intermolecular hydrogen bonds are formed between O(6)H and O(3) of anhydroglucose residues in neighboring chains. The intermolecular hydrogen bonds are believed to be the primary factor holding cellulose chains together cellulose microfibrils.

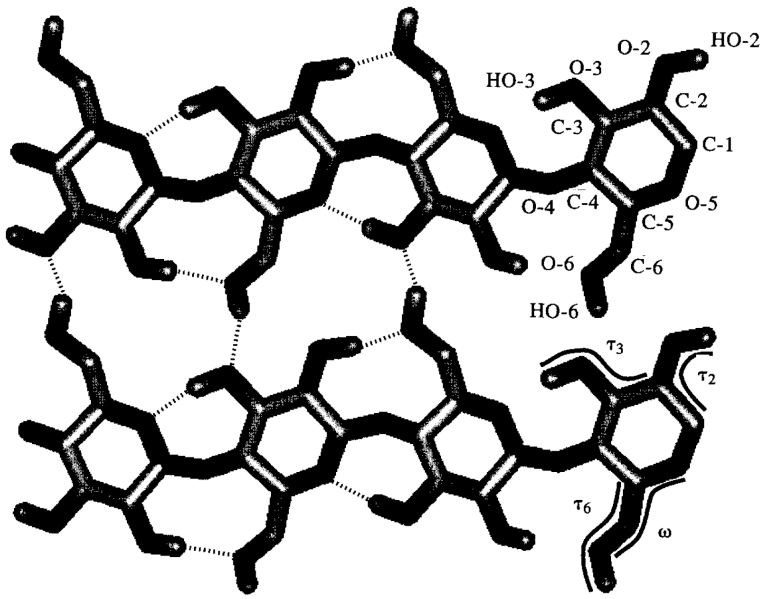

Figure 2.7. Intra- and intermolecular hydrogen bonding in native cellulose. (Reprinted from Heiner *et al.*, 1995; fair use; Copyright 1995 Elsevier Science Ltd.)

2.2.4. Degree of Polymerization

Many properties of cellulose depend on its degree of polymerization (DP), i.e. average number of glucose residues per cellulose molecule. Cellulose from wood pulp has typical DPs between 300 and 1700. Cotton and other plant fibers as well as bacterial celluloses have DPs ranging from 800 to 10,000 (Klemm *et al.*, 2005). Molecules with very low DPs can be obtained by acidic breakdown of cellulose.

2.2.5. Cellulose Nanocrystals

Rånby and Ribi (1950) were the first to produce stable suspensions of colloidal-sized cellulose crystals by sulfuric acid hydrolysis of wood and cotton cellulose. Acid hydrolysis of the cellulose microfibrils is a complex heterogeneous reaction. Early studies of the homogeneous and heterogeneous hydrolysis of cellulose, have shown that wood cellulose is depolymerized at a faster rate than cotton cellulose (Rånby and Marchessault, 1959). In a heterogeneous hydrolysis reaction, acid first penetrates into the amorphous regions and breaks down the elementary fibrils into highly crystalline fragments. As more glycosidic bonds in the fibers are hydrolyzed, the rate of the reaction slows down significantly, leveling off at a certain level-off-degree of polymerization. Thus, acid hydrolysis of cellulose fibers yields highly crystalline rod-like particles termed cellulose nanocrystals (Figure 2.8) (Marchessault *et al.*, 1961; Fan *et al.*, 1987; Revol *et al.*, 1992; Revol *et al.*, 1994; Favier *et al.*, 1995; Camacho *et al.*, 1996; Dong *et al.*, 1996; Araki *et al.*, 1998; French *et al.*, 2004; Roman and Winter, 2004; Beck-Candanedo *et al.*, 2005; Coffey *et al.*, 2006).

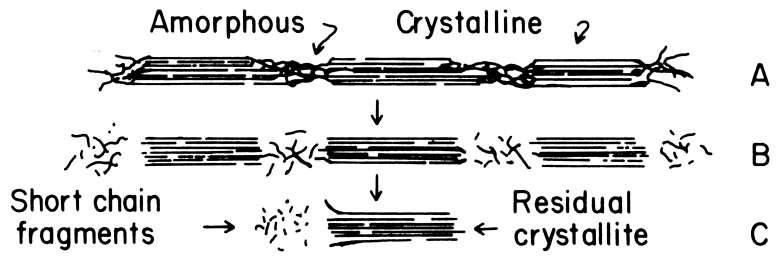

Figure 2.8. Schematic degradation pattern of a cellulose microfibril subjected to acid: A, original cellulose microfibril; B, initial attack in the amorphous regions; C, residual crystallites and digestion of short chain fragments. (Reprinted from Fan *et al.*, 1987; fair use; Copyright 1987 Springer Verlag)

The mechanism for cleavage of β(1–4) glycosidic bonds in acid medium involves three steps (Rånby and Marchessault, 1959; Fan *et al.*, 1987; Grunert, 2002; Xiang *et al.*, 2003), as illustrated in Figure 2.9. The reaction begins with the protonization of the acetal oxygen by the acid interacting rapidly with the glycosidic oxygen, linking two sugar residues, thus forming a conjugate acid. Cleavage of the C–O bond is related to a shift of an electron pair to the anomeric carbon. Finally, water attacks the carbonium ion to form a neutral endgroup and a proton. According to Xiang *et al.* (2003), the formation of the intermediate carbonium ion takes place more rapidly at the end than in the middle of the polysaccharide chain. Accordingly, the yield of monosaccharides after partial hydrolysis is higher than that calculated on the basis of a random bond cleavage.

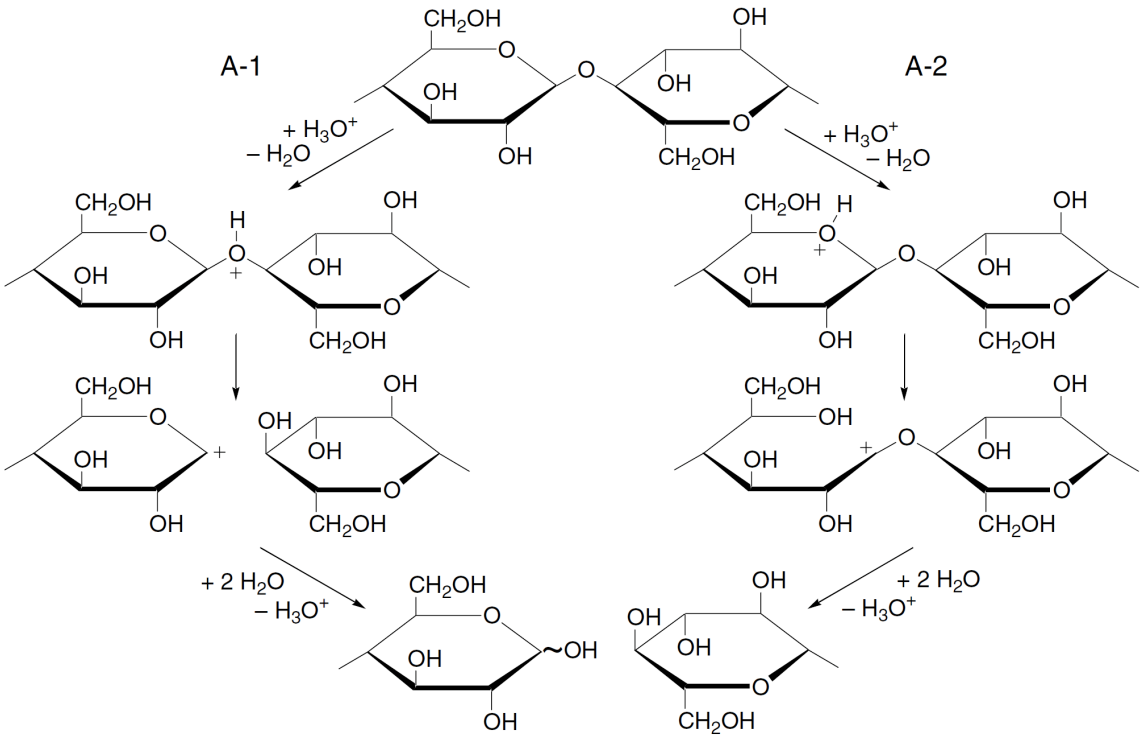

Figure 2.9. Mechanisms of the acidic hydrolysis of cellulose. (Adapted from Fan *et al.*, 1987; fair use; Copyright 1987 Springer Verlag)

2.2.5.1. Particle Charge

During the process of hydrolysis with sulfuric acid, sulfuric ester groups are introduced to the surface of the cellulose nanocrystals (Figure 2.10).

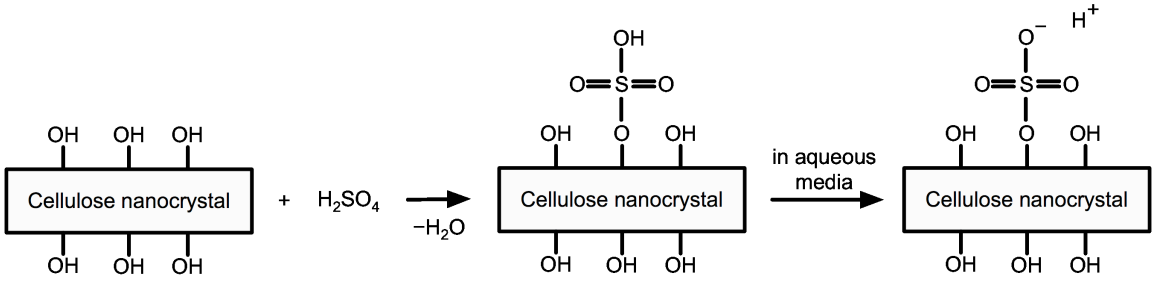

Figure 2.10. Partial esterification of surface hydroxyl groups by sulfuric acid during cellulose hydrolysis.

The sulfur content in cellulose nanocrystals produced with H_2SO_4 depends on the hydrolysis conditions, such as time, temperature, acid concentration, and acid-to-substrate ratio, and can reach 0.5–2% (Marchessault *et al.*, 1961; Revol *et al.*, 1992; Revol *et al.*, 1994; Favier *et al.*, 1995; Dong *et al.*, 1996). In aqueous solution, the sulfate groups are deprotonated and negatively charged.

2.2.5.2. Suspension Properties

Cellulose nanocrystals form stable aqueous suspensions because of repulsive electrostatic interactions between the negatively charged rods (Beck-Candanedo *et al.*, 2005; Beck-Candanedo *et al.*, 2006; Beck-Candanedo *et al.*, 2007). The interparticle forces depend on the ionic strength of the system (Dong and Gray, 1997). In salt free condition cellulose nanocrystal suspensions form chiral nematic ordered phases above a critical concentration beginning at around 5–7% cellulose (Marchessault *et al.*, 1959; Dong *et al.*, 1998; Beck-Candanedo *et al.*, 2006).

2.2.5.3. Particle Size

It is generally accepted that cellulose molecules in wood form long crystalline elements with cross-sectional dimensions around 2–5 nm (sometimes called elementary fibrils) that aggregate into larger microfibrils with lateral dimensions in the tens of nanometers (de Souza Lima and Borsali, 2004; French *et al.*, 2004; Beck-Candanedo *et al.*, 2005; Roman and Gray, 2005). The dimensions of cellulose nanocrystals depend mainly on cellulose origin and the preparation methods (de Souza Lima *et al.*, 2003; Beck-Candanedo *et al.*, 2005). It has been reported that cellulose nanocrystals made from cotton have typical dimensions of 100–300 nm in length and 8–10 nm in diameter, while those of tunicate cellulose nanocrystals range from 100 nm to a few micrometers in length and 10 to 20 nm in diameter (Beck-Candanedo *et al.* 2005). Ultrasonic treatment of cellulose nanocrystal suspensions was found to break down aggregates but did not cause a reduction in the average length of the particles (Marchessault *et al.*, 1961).

Determining the exact dimensions of cellulose microfibrils is challenging. Several different analytical methods have been evaluated in the past decades including atomic force microscopy (Hanley *et al.*, 1992; Beck-Candanedo *et al.*, 2005; Kvien *et al.*, 2005; Lefebvre and Gray, 2005; Shutava *et al.*, 2005; Kontturi *et al.*, 2007), transmission electron microscopy (Hanley *et al.*, 1992; Grunert and Winter, 2002; Roman and Winter, 2004; Shin *et al.*, 2007a), field emission scanning electron microscope (Shin *et al.*, 2007b), scanning electron microscopy (Matsumura *et al.*, 2000; Xiang *et al.*, 2003; Samir *et al.*, 2004), and dynamic and static light scattering techniques (de Souza Lima and Borsali, 2004).

2.2.6. Applications

Applications of cellulose and its derivatives have involved many areas of chemistry, biology, and technology in paper, textiles, water-soluble adhesives and binders, as thickeners and stabilizers in processed foods, and in the pharmaceutical industry (Favier *et al.*, 1995; Helbert *et al.*, 1996; Dong *et al.*, 1998; Suzuki and Makino, 1999; Iijima and Takeo, 2000; Biermann *et al.*, 2001). Microcrystalline cellulose has been listed as a GRAS (Generally Recognized As Safe) substance by the U.S. Food and Drug Administration.

Cellulose nanocrystals, with their ability to form stable aqueous suspensions, have a number of potential applications in drug/bioactives delivery as well as in controlled release applications. By reason of their small dimensions, high aspect ratio, and high modulus, cellulose nanocrystals have been studied as reinforcing particles in polymeric materials (Helbert *et al.*, 1996; Chazeau *et al.*, 1999). Cellulose nanocrystals from tunicate cellulose have been mixed with polymer latexes to yield nanocomposite materials with superior mechanical properties (Favier *et al.*, 1995; Heux *et al.*, 2000).

2.3. POLYELECTROLYTE COMPLEXES IN DRUG DELIVERY

2.3.1. Polyelectrolytes

A polymer the repeat units of which bear electrical charges is called a polyelectrolyte (Walstra, 2003). There are three types of polyelectrolytes, namely polybases, polyacids, and polyampholytes. Polybases, or cationic polyelectrolytes, mainly contain $–NH_2$ or =NH groups that are protonated at sufficiently low pH. The most common charged groups in polyacids, or anionic polyelectrolytes, are carboxyl groups (–COOH), or sulfate groups ($–OSO_3H$). Polyampholytes, such as proteins, DNA, and RNA, contain both positively and negatively charged groups. Polyelectrolytes exhibit properties of both polymers and electrolytes, providing them with a range of physicochemical behaviors, from those of neutral long chain polymers to those of simple electrolytes (Fuoss, 1951). Like salts, their solutions are electrically conductive; like polymers, their solutions are often viscous.

The physical properties of polyelectrolyte solutions are usually strongly affected by the degree of ionization or charge density. Intramolecular repulsive Coulomb interactions cause the chain to adopt a more expanded, rigid-rod-like conformation. If the solution contains low-molecular-weight electrolytes, the intramolecular electrostatic interactions will be screened and the polyelectrolyte chain takes on a more coiled conformation (Fuoss, 1951; Philipp *et al.*, 1989).

2.3.2. Polyelectrolyte Complexes

Polyelectrolytes of opposite charge, when mixed, form polyelectrolyte complexes (PECs). Studies on the interaction between oppositely charged polyelectrolytes date back to 1896 when Kossel (1896) precipitated egg albumin with protamine. Since then, PECs have been studied extensively (Tsuchida and Abe, 1982). In the early 1930's, researchers focused their attention on aqueous solutions of oppositely charged natural polyelectrolytes. When those polyelectrolytes, having a relatively low charge density, were mixed, phase separation and the formation of aggregates took place under certain

conditions (Zezin and Kabanov, 1982). Willstatter and Rohdewald (1934) coined the term “simplex” for polyanion-polycation-complexes. Systematic studies of simplex formation started in the early 1960’s with the work of Michaels and Miekka (1961), who discovered the formation of stoichiometric polysalts between oppositely charged synthetic polyelectrolytes. Mixing of strong polyelectrolytes with high charge densities resulted in the formation of PECs that precipitated from solution. In the following decades, a large number of new simplex-forming systems have been patented (Philipp *et al.*, 1984). In recent years, more and more interdisciplinary research has focused again on polyelectrolytes occurring in nature.

The reaction between polyelectrolytes can be represented schematically as shown in Figure 2.11.

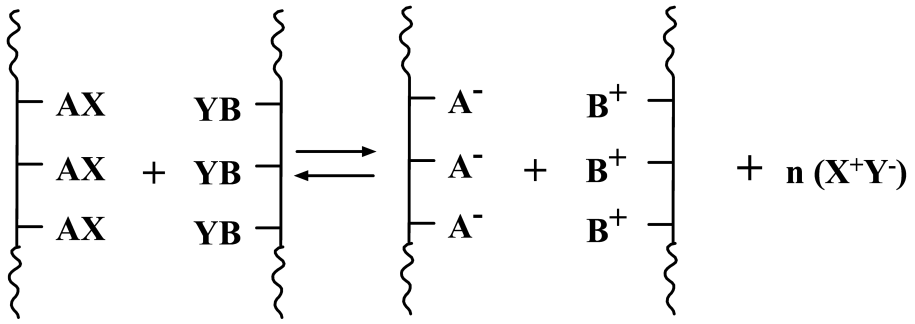

Figure 2.11. Reaction between polyelectrolytes. AX is a unit of a polymeric acid or its salt and YB is a unit of the polymeric base or its salt. (Reprinted from Zezin and Kabanov, 1982; fair use; Copyright 1982 Turpion Ltd.)

Coulomb forces between the oppositely charged polyelectrolytes and the release of the small counter ions are considered the main driving forces for PEC formation (Philipp *et al.*, 1984; Raspaud *et al.*, 1998; Quemeneur *et al.*, 2007). Other intermolecular interactions may also be involved in the formation of PEC structures, including hydrogen bonding, hydrophobic interactions, van der Waals forces (Schatz *et al.*, 2004).

The concentration, pH, and ionic strength of polyelectrolyte solutions are the major factors influencing PEC formation (Dautzenberg *et al.*, 1996). Concentrated polyelectrolyte solutions lead to macroscopic flocculation. Dilute solutions, mixed at

non-stoichiometric ratios, yield colloidal PEC particles with a neutral core surrounded by excess polyelectrolyte, stabilizing the PEC particles against further coalescence. With a small amount of salt present in the solution, the process of PEC formation is thermodynamically controlled and results in non-stoichiometric polyelectrolyte complexes (N-PECs) (Dautzenberg and Karibyants, 1999; Nordmeier and Beyer, 1999). In salt free solutions, the formation of PECs is rapid and leads to non-equilibrium structures. Changes in solution pH result in changes in the charge densities of the polyelectrolytes causing structural changes in the PECs (Zezin and Kabanov, 1982).

Kabanov and Zezin (1984b) have demonstrated that the types of ionic groups and the relative molecular dimensions of the polyelectrolytes also play an important role. Polyelectrolytes with strong ionic groups and comparable molecular dimensions yield insoluble and highly aggregated PECs whereas polyelectrolytes with weak ionic groups and large differences in molecular dimensions yield water-soluble PECs at non-stoichiometric ratios (Kabanov and Zezin, 1984a). Soluble, non-stoichiometric polyanion-polycation aggregates have been termed "soluble simplexes" by Tsuchida *et al.* (1972). Kabanov and Zezin (1984a) proposed that soluble simplexes consisted of very long "host-polyions" and shorter, sequentially attached "guest-polyions" of opposite charge.

In general, three types of PEC systems can be distinguished: (a) macroscopically homogeneous systems containing small complex aggregates (soluble complex); (b) turbid colloidal systems with suspended complex particles in a transition range to phase separation; (c) two-phase systems of a liquid supernatant and precipitated polysalt, easily separated and obtainable in the solid state after washing and drying (Philipp *et al.*, 1989).

2.3.3. Stable Colloidal Dispersions

In a colloidal system, colloidal particles of well-defined size can self-assemble into ordered, crystalline structures under non-equilibrium conditions, originating from various forces including van der Waals, electrostatic, hydrodynamic, and capillary forces, as well as Brownian motions (Li *et al.*, 2008). Many interactions act simultaneously. A stable

colloidal system is one in which the particles resist flocculation or aggregation. The stability of a colloidal system depends on the balance of repulsive and attractive forces that exist between particles due to Brownian motion (van Driessche and Hoste, 2006). If all particles have a mutual repulsion, the dispersion will remain stable. However, if the particles have little or no repulsive force then some instability mechanism, such as flocculation or aggregation, will eventually take place. In that case the particles in the colloidal system adhere to one another and form aggregates that settle out under the influence of gravity.

2.3.4. Chitosan in Controlled Release Systems

Controlled release is a recent technology used to increase the effectiveness of many drugs and bioactives in food and drug delivery (Pothakamury and Barbosa-Cánovas, 1995). Controlled release may be defined as a method by which one or more active agents or ingredients are made available at a desired site and time at a specific rate (Grattard *et al.*, 2002). Controlled release systems generally involve an enclosed solid or liquid active in a water-soluble or meltable matrix (matrix system) or shell (core-shell system). Most controlled release devices currently used in the food industry are core-shell systems with temperature or solvent activated (triggered) release, depending on the shell material. With the emergence of controlled-release technology, some heat-, temperature- or pH-sensitive additives can be used very conveniently in food systems and drug delivery (Figure 2.12) (Pothakamury and Barbosa-Cánovas, 1995; Brannon-Peppas, 1997).

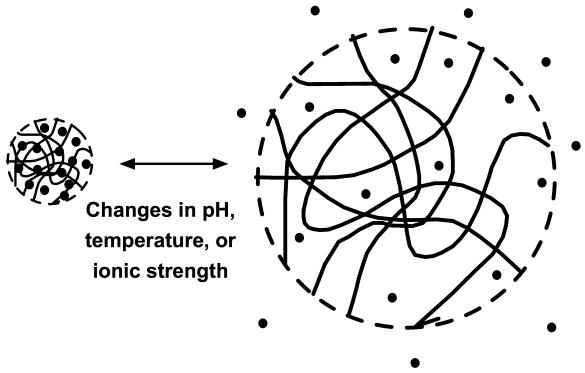

Figure 2.12. Drug delivery from environmentally sensitive release systems. (Adapted from Brannon-Peppas, 1997; fair use; Copyright 1997 Medical Plastics and Biomaterials)

Passive absorption of drug across mucosal tissues involves either trans- or paracellular diffusion through one or several epithelial cell layers. The transcellular route is mainly restricted to small hydrophobic compounds capable of passing through the lipophilic cell membranes (Schipper *et al.*, 1996). In contrast, the absorption of orally administered hydrophilic drugs is limited by low permeability of the intestinal mucosal to such compounds. Recently, many efforts have been made to improve the uptake of poorly absorbed drugs. Chitosan, an acidic polycationic polyelectrolyte, has been employed in many studies as a pharmaceutical excipient for the dissolution and sustained release of drugs (Schipper *et al.*, 1996).

The use of colloidal carriers made of hydrophilic polysaccharides has arisen as a promising alternative for improving the transport of such macromolecules across biological surfaces (Janes *et al.*, 2001). Chitosan has been shown to form colloidal particles and entrap macromolecules through a number of mechanisms, including ionic crosslinking, desolvation, or ionic complexation. The particular advantages of chitosan for developing micro/nanoparticles include low toxicity, ability to control the release of active agents, cationic nature in aqueous solution for ionic cross-linking with multivalent anions, and mucoadhesive character that increases residual time at the site of absorption (Agnihotri *et al.*, 2004). Ohya *et al.* (1994) was the first researcher to present data involving chitosan nanospheres for drug delivery applications. Chitosan capsules as

controlled release vectors for applications in food processing and biochemical reagents were developed in the early 1990's (He *et al.*, 1998). These pioneering studies demonstrated the feasibility of synthesizing stable, reproducible, nanosized chitosan particles that could entrap and deliver drugs. However, negative effects of glutaraldehyde, used as chitosan cross-linker, discovered in cell viability studies, shifted the general interest to less harsh procedures for the synthesis of chitosan nanospheres (Janes *et al.*, 2001). Ionic crosslinking with negatively charged polyelectrolytes has the advantage that it allows tailoring the properties of the resulting particles, such as the size, swelling behavior, and pH sensitivity.

2.4. REFERENCES

Agnihotri, S. A., N. N. Mallikarjuna and T. M. Aminabhavi (2004). "Recent advances on chitosan-based micro- and nanoparticles in drug delivery." Journal of Controlled Release **100**(1): 5–28.

Aiba, S. (1986). "Studies on chitosan. 1. Determination of the degree of N-acetylation of chitosan by ultraviolet spectrphotometry and gel-permeation chromatography." International Journal of Biological Macromolecules **8**(3): 173–176.

Aiba, S. (1989). "Studies on chitosan. 2. Solution stability and reactivity of partially N-acetylated chitosan derivatives in aqueous-media." International Journal of Biological Macromolecules **11**(4): 249–252.

Aiba, S. (1991). "Studies on chitosan. 3. Evidence for the presence of random and block copolymer structures in partially N-acetylated chitosans." International Journal of Biological Macromolecules **13**(1): 40–44.

Aiba, S. (1992). "Studies on chitosan. 4. Lysozymic hydrolysis of partially N-acetylated chitosans." International Journal of Biological Macromolecules **14**(4): 225–228.

Aiba, S. (1993). "Studies on chitosan. 6. Relationship between N-acetyl group distribution pattern and chitinase digestibility of partially N-acetylated chitosans " International Journal of Biological Macromolecules **15**(4): 241–245.

Amiji, M. M. (1995). "Pyrene fluorescence study of chitosan self-association in aqueous solution." Carbohydrate Polymers **26**(3): 211–213.

Anthonsen, M. W., K. M. Varum, A. M. Hermansson, O. Smidsrod and D. A. Brant (1994). "Aggregates in acidic solutions of chitosans detected by static laser light scattering." Carbohydrate Polymers **25**(1): 13–23.

Anthonsen, M. W., K. M. Varum and O. Smidsrod (1993). "Solution properties of chitosans: conformation and chain stiffness of chitosans with different degrees of N-acetylation." Carbohydrate Polymers **22**(3): 193–201.

Araki, J., M. Wada, S. Kuga and T. Okano (1998). "Flow properties of microcrystalline cellulose suspension prepared by acid treatment of native cellulose." Colloids and Surfaces, A: Physicochemical and Engineering Aspects **142**(1): 75–82.

ASTM (2003). "Standard test method for determining degree of deacetylation in chitosan salts by proton nuclear magnetic resonance (^{1}H NMR) spectroscopy." Annual book of ASTM standards, Designation: F2260 - 03 **13**(01): 1318–1323.

Baker, A. A., W. Helbert, J. Sugiyama and M. J. Miles (2000). "New insight into cellulose structure by atomic force microscopy shows the I alpha crystal phase at near-atomic resolution." Biophysical Journal **79**(2): 1139–1145.

Balazs, N. and P. Sipos (2007). "Limitations of pH-potentiometric titration for the determination of the degree of deacetylation of chitosan." Carbohydrate Research **342**(1): 124–130.

Baxter, A., M. Dillon, K. D. Anthony Taylor and G. A. F. Roberts (1992). "Improved method for i.r. determination of the degree of N-acetylation of chitosan." International Journal of Biological Macromolecules **14**(3): 166–169.

Beck-Candanedo, S., M. Roman and D. G. Gray (2005). "Effect of reaction conditions on the properties and behavior of wood cellulose nanocrystal suspensions." Biomacromolecules **6**(2): 1048–1054.

Beck-Candanedo, S., D. Viet and D. G. Gray (2006). "Induced phase separation in cellulose nanocrystal suspensions containing ionic dye species." Cellulose **13**(6): 629–635.

Beck-Candanedo, S., D. Viet and D. G. Gray (2007). "Triphase equilibria in cellulose nanocrystal suspensions containing neutral and charged macromolecules." Macromolecules **40**(9): 3429-3436.

Beri, R. G., J. Walker, E. T. Reese and J. E. Rollings (1993). "Characterization of chitosans via coupled size-exclusion chromatography and multiple-angle laser light-scattering technique." Carbohydrate Research **238**(1): 11–26.

Berth, G. and H. Dautzenberg (2002). "The degree of acetylation of chitosans and its effect on the chain conformation in aqueous solution." Carbohydrate Polymers **47**(1): 39–51.

Berth, G., H. Dautzenberg and M. G. Peter (1998). "Physico-chemical characterization of chitosans varying in degree of acetylation." Carbohydrate Polymers **36**(2-3): 205–216.

Biermann, O., E. Hadicke, S. Koltzenburg and F. Muller-Plathe (2001). "Hydrophilicity and lipophilicity of cellulose crystal surfaces." Angewandte Chemie-International Edition **40**(20): 3822–3825.

Bodek, K. H. (1995). "Evaluation of potentiometric titration in anhydrous medium for determination of chitosan seacetylation degree." Acta poloniae pharmaceutica-drug research **52**(4): 337–343.

Brannon-Peppas, L. (1997). "Polymers in controlled drug delivery." Medical Plastics and Biomaterials **Nov**: 34–45.

Brugnerotto, J., J. Desbrieres, L. Heux, K. Mazeau and M. Rinaudo (2001a). "Overview on structural characterization of chitosan molecules in relation with their behavior in solution." Macromolecular Symposia **168**(1): 1–20.

Brugnerotto, J., J. Desbrieres, G. Roberts and M. Rinaudo (2001b). "Characterization of chitosan by steric exclusion chromatography." Polymer **42**(25): 9921–9927.

Brunel, F., L. Véron, L. David, A. Domard and T. Delair (2008). "A novel synthesis of chitosan nanoparticles in reverse emulsion." Langmuir **24**(20): 11370–11377.

Budovskaya, K., I. Gorbacheva, G. Vikhoreva and L. Gal'braikh (1997). "Conductometric titration of chitosan sulfate polyanions in the presence of extraneous electrolytes." Fibre Chemistry **29**(2): 106–109.

Buhler, E. and M. Rinaudo (2000). "Structural and dynamical properties of semirigid polyelectrolyte solutions: A light-scattering study." Macromolecules **33**(6): 2098–2106.

Camacho, F., P. González-Tello, E. Jurado and A. Robles (1996). "Microcrystalline-cellulose hydrolysis with concentrated sulphuric acid." Journal of Chemical Technology & Biotechnology **67**(4): 350–356.

Chazeau, L., J. Y. Cavaillé, G. Canova, R. Dendievel and B. Boutherin (1999). "Viscoelastic properties of plasticized PVC reinforced with cellulose whiskers." Journal of Applied Polymer Science **71**(11): 1797–1808.

Chen, R. H. and M. L. Tsaih (1998). "Effect of temperature on the intrinsic viscosity and conformation of chitosans in dilute HCl solution." International Journal of Biological Macromolecules **23**(2): 135–141.

Chung, L. Y., R. J. Schmidt, P. F. Hamlyn, B. F. Sagar, A. M. Andrew and T. D. Turner (1994). "Biocompatibility of potential wound management products: Fungal mycelia as a source of chitin/chitosan and their effect on the proliferation of human F1000 fibroblasts in culture." Journal of Biomedical Materials Research **28**(4): 463–469.

Coffey, D. G., D. A. Bell and A. Henderson (2006). Cellulose and cellulose derivatives. In: Stephen, A. M., G. O. Phillips and P. A. Williams, Eds., Food polysaccharides and their applications. 2nd ed., pp. 147–180. Boca Raton, FL: CRC Press, Taylor and Francis Group.

Dautzenberg, H., J. Hartmann, S. Grunewald and F. Brand (1996). "Stoichiometry and structure of polyelectrolyte complex particles in diluted solution." Berichte der Bunsen-Gesellschaft fuer Physikalische Chemie **100**(6): 1024–1032.

Dautzenberg, H. and N. Karibyants (1999). "Polyelectrolyte complex formation in highly aggregating systems. Effect of salt: response to subsequent addition of NaCl." Macromolecular Chemistry and Physics **200**(1): 118-125.

de Souza Lima, M. M. and R. Borsali (2004). "Rodlike cellulose microcrystals: Structure, properties, and applications." Macromolecular Rapid Communications **25**(7): 771–787.

de Souza Lima, M. M., J. T. Wong, M. Paillet, R. Borsali and R. Pecora (2003). "Translational and rotational dynamics of rodlike cellulose whiskers." Langmuir **19**(1): 24–29.

Deuchi, K., O. Kanauchi, Y. Imasato and E. Kobayashi (1994). "Decreasing effect of chitosan on the apparent fat digestibility by rats fed on a high-fat diet." Bioscience Biotechnology and Biochemistry **58**(9): 1613–1616.

Domard, A. (1987a). "Determination of N-acetyl content in chitosan samples by c.d. measurements." International Journal of Biological Macromolecules **9**(6): 333–336.

Domard, A. (1987b). "pH and c.d. measurements on a fully deacetylated chitosan: Application to CuII-polymer interactions." International Journal of Biological Macromolecules **9**(2): 98–104.

Domard, A. and M. Domard (2002). Chitosan: Structure-properties relationship and biomedical application. In: Dumitriu, S., Ed., Polymeric Biomaterials. 2nd ed., pp. 187–212. New York: Marcel Dekker.

Domard, A. and M. Rinaudo (1984). "Gel-permeation chromatography of cationic polymer on cationic porous silica-gels." Polymer Communications **25**(2): 55–58.

Domszy, J. G. and G. A. F. Roberts (1985). "Evaluation of infrared spectroscopic techniques for analysing chitosan." Makromolekulare Chemie **186**(8): 1671–1677.

Dong, X. M. and D. G. Gray (1997). "Effect of counterions on ordered phase formation in suspensions of charged rodlike cellulose crystallites." Langmuir **13**(8): 2404–2409.

Dong, X. M., T. Kimura, J. F. Revol and D. G. Gray (1996). "Effects of ionic strength on the isotropic-chiral nematic phase transition of suspensions of cellulose crystallites." Langmuir **12**(8): 2076–2082.

Dong, X. M., J. F. Revol and D. G. Gray (1998). "Effect of microcrystallite preparation conditions on the formation of colloid crystals of cellulose." Cellulose **5**(1): 19–32.

Fan, L. T., M. M. Gharpuray and Y.-H. Lee (1987). Cellulose hydrolysis. New York: Springer-Verlag.

Favier, V., H. Chanzy and J. Y. Cavaille (1995). "Polymer nanocomposites reinforced by cellulose whiskers." Macromolecules **28**(18): 6365–6367.

Filar, L. J. and M. G. Wirick (1978). Bulk and solution properties of chitosan. In: Muzzarelli, R. A. A. and E. R. Pariser, Eds., Proceedings of The First International Conference on Chitin/Chitosan, MIT Sea Grant Report MITSG 78-7. pp. 169–181. Cambridge, MA: Massachusetts Institute of Technology.

French, A. D., N. R. Bertoniere, R. M. Brown, H. Chanzy, D. Gray, K. Hattori and W. Glasser (2004). "Cellulose." Kirk-Othmer Encyclopedia of Chemical Technology. 5th ed. **5** 360-394.

Fuoss, R. M. (1951). "Polyelectrolytes." Discussions of the Faraday Society **11**: 125–134.

Gamzazade, A. I., V. M. Slimak, A. M. Skljar, E. V. Stykova, S. S. A. Pavlova and S. V. Rogozin (1985). "Investigation of the hydrodynamic properties of chitosan solutions." Acta Polymerica **36**(8): 420–424.

George, M. and T. E. Abraham (2006). "Polyionic hydrocolloids for the intestinal delivery of protein drugs: Alginate and chitosan - A review." Journal of Controlled Release **114**(1): 1–14.

Grattard, N., M. Pernin, B. Marty, G. Roudaut, D. Champion and M. Le Meste (2002). "Study of release kinetics of small and high molecular weight substances dispersed into spray-dried ethylcellulose microspheres." Journal of Controlled Release **84**(3): 125–135.

Grunert, M. (2002). "Cellulose Nanocrystals: Preparation, surface modification, and application in nanocomposites." PhD Thesis, SUNY College of Environmental Science and Forestry, Syracuse, NY, May 2002.

Grunert, M. and T. W. Winter (2002). "Nanocomposites of cellulose acetate butyrate reinforced with cellulose nanocrystals." Journal of Polymers and the Environment **10**(1-2): 27–30.

Guibal, E. (2004). "Interactions of metal ions with chitosan-based sorbents: A review." Separation and Purification Technology **38**(1): 43–74.

Hanley, S. J., J. Giasson, J.-F. Revol and D. G. Gray (1992). "Atomic force microscopy of cellulose microfibrils: Comparison with transmission electron microscopy." Polymer **33**(21): 4639–4642.

He, P., S. S. Davis and L. Illum (1998). "*In vitro* evaluation of the mucoadhesive properties of chitosan microspheres." International Journal of Pharmaceutics **166**(1): 75–88.

Heiner, A. P., J. Sugiyama and O. Teleman (1995). "Crystalline cellulose I-alpha and I-beta studied by molecular-dynamics simulation." Carbohydrate Research **273**(2): 207–223.

Hejazi, R. and M. Amiji (2002). Chitosan-based delivery system: Physicochemical properties and pharmaceutical applications. In: Dumitriu, S., Ed., Polymeric Biomaterials. 2nd ed., pp. 213–238. New York: Macel Dekker.

Helbert, W., J. Y. Cavaillé and A. Dufresne (1996). "Thermoplastic nanocomposites filled with wheat straw cellulose whiskers. Part I: Processing and mechanical behavior." Polymer Composites **17**(4): 604–611.

Heux, L., G. Chauve and C. Bonini (2000). "Nonflocculating and chiral-nematic self-ordering of cellulose microcrystals suspensions in nonpolar solvents." Langmuir **16**(21): 8210–8212.

Hirai, A., H. Odani and A. Nakajima (1991). "Determination of degree of deacetylation of chitosan by 1H NMR spectroscopy." Polymer Bulletin **26**(1): 87–94.

Hirano, S. (1999). "Chitin and chitosan as novel biotechnological materials." Polymer International **48**(8): 732–734.

Hirano, S. and N. Nagao (1989). "Effects of chitosan, pectic acid, lysozyme, and chitinase on the growth of several phytopathogens." Agricultural and Biological Chemistry **53**(11): 3065–3066.

Hirano, S., H. Seino, Y. Akiyama and I. Nonaka (1990). Chitosan: A biocompatible material for oral and intravenous administration. In: Gebelein, C. G. and R. L. Dunn, Eds., Progress in Biomedical Polymers. pp. 283–290. New York: Plenum Press.

Hirano, S., H. Tsuchida and N. Nagao (1989). "N-acetylation in chitosan and the rate of its enzymic-hydrolysis." Biomaterials **10**(8): 574–576.

Hirano, S., M. Zhang, H. Yamane, Y. Kimura, K. Matsukawa and M. Nakagawa (2003). "Chemical modification and some aligned composites of chitosan in a filament state." Macromolecular Bioscience **3**(10): 620–628.

Iijima, H. and K. Takeo (2000). Microcrystalline cellulose: An overview. In: Phillips, G. O. and P. A. Williams, Eds., Handbook of Hydrocolloids. pp. 331–346. Boca Raton, FL: CRC Press.

Janes, K. A., P. Calvo and M. J. Alonso (2001). "Polysaccharide colloidal particles as delivery systems for macromolecules." Advanced Drug Delivery Reviews **47**(1): 83–97.

Jia, Z. and X. Li (2002). "Determination of the deacetylation degree of chitosan by acid-base conductometric titration." Fenxi Huaxue **30**(7): 846–848.

Jiang, X., L. Chen and W. Zhong (2003). "A new linear potentiometric titration method for the determination of deacetylation degree of chitosan." Carbohydrate Polymers **54**(4): 457–463.

Kabanov, V. A. and A. B. Zezin (1984a). "A new class of complex water-soluble polyelectrolytes." Makromolekulare Chemie, Supplement **6**(S19841): 259–276.

Kabanov, V. A. and A. B. Zezin (1984b). "Soluble interpolymeric complexes as a new class of synthetic poly-electrolytes." Pure and Applied Chemistry **56**(3): 343–354.

Khan, T. A., K. K. Peh and H. S. Ch'ng (2002). "Reporting degree of deacetylation values of chitosan: the influence of analytical methods." Journal of Pharmacy and Pharmaceutical Sciences **5**(3): 205–212.

Klemm, D., B. Heublein, H. P. Fink and A. Bohn (2005). "Cellulose: Fascinating biopolymer and sustainable raw material." Angewandte Chemie-International Edition **44**(22): 3358–3393.

Klossner, R. R., H. A. Queen, A. J. Coughlin and W. E. Krause (2008). "Correlation of chitosan's rheological properties and its ability to electrospin." Biomacromolecules **9**(10): 2947–2953.

Knaul, J. Z., M. R. Kasaai, V. T. Bui and K. A. M. Creber (1998). "Characterization of deacetylated chitosan and chitosan molecular weight review." Canadian Journal of Chemistry **76**(11): 1699–1706.

Kontturi, E., L. S. Johansson, K. S. Kontturi, P. Ahonen, P. C. Thune and J. Laine (2007). "Cellulose nanocrystal submonolayers by spin coating." Langmuir **23**(19): 9674-9680.

Kossel, A. (1896). "Über die basischen Stoffe des Zellkerns." Hoppe-Seyler's Zeitschrift für Physiologische Chemie **22**(9): 176.

Kristiansen, A., K. M. Varum and H. Grasdalen (1998). "The interactions between highly de-N-acetylated chitosans and lysozyme from chicken egg white studied by 1H-NMR spectroscopy." European Journal of Biochemistry **251**(1-2): 335–342.

Kuang, W. and Z. Liu (2006). "Determination of the degree of deacetylation of chitosan by linear potentiometric titration." Guangzhou Huagong **34**(2): 49–51.

Kurita, K. (2006). "Chitin and chitosan: Functional biopolymers from marine crustaceans." Marine Biotechnology **8**(3): 203–226.

Kurita, K., M. Kamiya and S.-I. Nishimura (1991). "Solubilization of a rigid polysaccharide: Controlled partial N-acetylation of chitosan to develop solubility." Carbohydrate Polymers **16**(1): 83–92.

Kurita, K., T. Sannan and Y. Iwakura (1977). "Studies on chitin, 4. Evidence for formation of block and random copolymers of N-acetyl-D-glucosamine and D-glucosamine by hetero- and homogeneous hydrolyses." Makromolekulare Chemie **178**(12): 3197–3202.

Kurita, K., K. Tomita, T. Tada, S. Nishimura and S. Ishii (1993). "Reactivity characteristic of a new form of chitosan - Facile N-phthaloylation of chitosan prepared from squid beta-chitin for efective solubilization." Polymer Bulletin **30**(4): 429–433.

Kvien, I., B. S. Tanem and K. Oksman (2005). "Characterization of cellulose whiskers and their nanocomposites by atomic force and electron microscopy." Biomacromolecules **6**(6): 3160–3165.

Lamarque, G., J. M. Lucas, C. Viton and A. Domard (2005). "Physicochemical behavior of homogeneous series of acetylated chitosans in aqueous solution: Role of various structural parameters." Biomacromolecules **6**(1): 131–142.

Lavertu, M., Z. Xia, A. N. Serreqi, M. Berrada, A. Rodrigues, D. Wang, M. D. Buschmann and A. Gupta (2003). "A validated 1H NMR method for the determination of the degree of deacetylation of chitosan." Journal of Pharmaceutical and Biomedical Analysis **32**(6): 1149–1158.

Lefebvre, J. and D. G. Gray (2005). "AFM of adsorbed polyelectrolytes on cellulose I surfaces spin-coated on silicon wafers." Cellulose **12**(2): 127–134.

Li, Q., E. T. Dunn, E. W. Grandmaison and M. F. A. Goosen (1992). "Applications and properties of chitosan." Journal of Bioactive and Compatible Polymers **7**(4): 370–397.

Li, Q., U. Jonas, X. S. Zhao and M. Kapp (2008). "The forces at work in collodial self-assembly: a review on fundamental interactions between collodial particels." Asia-Pacific Journal of Chemical Engineering **3**(3): 255–268.

Liu, D. S., Y. N. Wei, P. J. Yao and L. B. Jiang (2006). "Determination of the degree of acetylation of chitosan by UV spectrophotometry using dual standards." Carbohydrate Research **341**(6): 782–785.

Marchessault, R. H., F. F. Morehead and M. J. Koch (1961). "Some hydrodynamic properties of neutral suspensions of cellulose crystallites as related to size and shape." Journal of Colloid Science **16**(4): 327–344.

Marchessault, R. H., F. F. Morehead and N. M. Walter (1959). "Liquid crystal systems from fibrillar polysaccharides." Nature **184**(4686): 632–633.

Matsumura, H., J. Sugiyama and W. G. Glasser (2000). "Cellulosic nanocomposites. I. Thermally deformable cellulose hexanoates from heterogeneous reaction." Journal of Applied Polymer Science **78**(13): 2242–2253.

Mazeau, K., S. Pérez and M. Rinaudo (2000). "Predicted influence of N-acetyl group content on the conformational extension of chitin and chitosan chains." Journal of Carbohydrate Chemistry **19**(9): 1269–1284.

Mazeau, K. and M. Rinaudo (2004). "The prediction of the characteristics of some polysaccharides from molecular modeling. Comparison with effective behavior." Food Hydrocolloids **18**(6): 885–898.

Michaels, A. S. and R. G. Miekka (1961). "Polycation-polyanion complexes: Preparation and properties of poly-(vinylbenzyl trimethylammonium) poly-(styrenesulfonate)." Journal of Physical Chemistry **65**(10): 1765–1773.

Mima, S., M. Miya, R. Iwamoto and S. Yoshikawa (1983). "Highly deacetylated chitosan and its properties." Journal of Applied Polymer Science **28**(6): 1909–1917.

Miya, M., R. Iwamoto, S. Yoshikawa and S. Mima (1980). "I.r. spectroscopic determination of CONH content in highly deacylated chitosan." International Journal of Biological Macromolecules **2**(5): 323–324.

Moore, G. K. and G. A. F. Roberts (1980). "Determination of the degree of N-acetylation of chitosan." International Journal of Biological Macromolecules **2**(2): 115–116.

Muzzarelli, R. A. A. (1977). Chitin. Toronto: Pergamon Press.

Muzzarelli, R. A. A. and R. Rocchetti (1985). "Determination of the degree of acetylation of chitosans by first derivative ultraviolet spectrophotometry." Carbohydrate Polymers **5**(6): 461–472.

Niola, F., N. Basora, E. Chornet and P. F. Vidal (1993). "A rapid method for the determination of the degree of N-acetylation of chitin-chitosan samples by acid hydrolysis and HPLC." Carbohydrate Research **238**(1): 1–9.

Nordmeier, E. and P. Beyer (1999). "Nonstoichiometric polyelectrolyte complexes: A mathematical model and some experimental results." Journal of Polymer Science, Part B: Polymer Physics **37**(4): 335–348.

Nwe, N., S. Chandrkrachang, W. F. Stevens, T. Maw, T. K. Tan, E. Khor and S. M. Wong (2002). "Production of fungal chitosan by solid state and submerged fermentation." Carbohydrate Polymers **49**(2): 235–237.

Ogawa, K. (1991). "Effect of heating an aqueous suspension of chitosan on the crystallinity and polymorphs." Agricultural and Biological Chemistry **55**(9): 2375–2379.

Ogawa, K., S. Hirano, T. Miyanishi, T. Yui and T. Watanabe (1984). "A new polymorph of chitosan " Macromolecules **17**(4): 973–975.

Ogawa, K. and T. Yui (1993). "Structure and function of chitosan.3. Crystallinity of partially N-acetylated chitosans " Bioscience Biotechnology and Biochemistry **57**(9): 1466–1469.

Ohya, Y., M. Shiratani, H. Kobayashi and T. Ouchi (1994). "Release behavior of 5-fluorouracil from chitosan-gel nanospheres immobilizing 5-fluorouracil coated with polysaccharides and their cell specific cytotoxicity." Journal of Macromolecular Science-Pure and Applied Chemistry **A31**(5): 629–642.

Okuyama, K., K. Noguchi, M. Kanenari, T. Egawa, K. Osawa and K. Ogawa (2000). "Structural diversity of chitosan and its complexes." Carbohydrate Polymers **41**(3): 237–247.

Okuyama, K., K. Noguchi, T. Miyazawa, T. Yui and K. Ogawa (1997). "Molecular and crystal structure of hydrated chitosan." Macromolecules **30**(19): 5849–5855.

Ottoy, M. H., K. M. Varum, B. E. Christensen, M. W. Anthonsen and O. Smidsrod (1996). "Preparative and analytical size-exclusion chromatography of chitosans." Carbohydrate Polymers **31**(4): 253–261.

Pa, J.-H. and T. L. Yu (2001). "Light scattering study of chitosan in acetic acid aqueous solutions." Macromolecular Chemistry and Physics **202**(7): 985–991.

Philipp, B., H. Dautzenberg, K. J. Linow, J. Kotz and W. Dawydoff (1989). "Polyelectrolyte complexes - Recent developments and open problems." Progress in Polymer Science **14**(1): 91–172.

Philipp, B., K. Linow and H. Dautzenberg (1984). "Polyelectrolyte complexes-Some new results and open problems." Acta Chimica Hungarica-Models in Chemistry **117**(1): 67–83.

Philippova, O. E., E. V. Volkov, N. L. Sitnikova, A. R. Khokhlov, J. Desbrieres and M. Rinaudo (2001). "Two types of hydrophobic aggregates in aqueous solutions of chitosan and its hydrophobic derivative." Biomacromolecules **2**(2): 483–490.

Pothakamury, U. R. and G. V. Barbosa-Cánovas (1995). "Fundamental aspects of controlled release in foods." Trends in Food Science & Technology **6**(12): 397–406.

Prochazkova, S., K. M. Varum and K. Ostgaard (1999). "Quantitative determination of chitosans by ninhydrin." Carbohydrate Polymers **38**(2): 115–122.

Quemeneur, F., A. Rammal, M. Rinaudo and B. Pepin-Donat (2007). "Large and giant vesicles "decorated" with chitosan: Effects of pH, salt or glucose stress, and surface adhesion." Biomacromolecules **8**(8): 2512–2519.

Qun, G. and W. Ajun (2006). "Effects of molecular weight, degree of acetylation and ionic strength on surface tension of chitosan in dilute solution." Carbohydrate Polymers **64**(1): 29–36.

Rånby, B. and E. Ribi (1950). "Über den feinbau der zellulose." Cellular and Molecular Life Sciences **6**(1): 12–14.

Rånby, B. G. and R. H. Marchessault (1959). "Inductive effects in the hydrolysis of cellulose chains." Journal of Polymer Science **36**(130): 561–564.

Raspaud, E., M. O. de la Cruz, L.-J. Sikorav and F. Livolant (1998). "Precipitation of DNA by polyamines: a polyelectrolyte behavior." Biophysical Journal **74**(1): 381–393.

Raymond, L., F. G. Morin and R. H. Marchessault (1993). "Degree of deacetylation of chitosan using conductometric titration and solid-state NMR." Carbohydrate Research **246**(1): 331–336.

Revol, J.-F., L. Godbout, X.-M. Dong, D. G. Gray, H. Chanzy and G. Maret (1994). "Chiral nematic suspensions of cellulose crystallites; phase separation and magnetic field orientation." Liquid Crystals **16**(1): 127–134.

Revol, J. F., H. Bradford, J. Giasson, R. H. Marchessault and D. G. Gray (1992). "Helicoidal self-ordering of cellulose microfibrils in aqueous suspension." International Journal of Biological Macromolecules **14**(3): 170–172.

Rinaudo, M. (2006). "Non-covalent interactions in polysaccharide systems." Macromolecular Bioscience **6**(8): 590–610.

Rinaudo, M. (2008). "Main properties and current applications of some polysaccharides as biomaterials." Polymer International **57**(3): 397–430.

Rinaudo, M., M. Milas and P. L. Dung (1993). "Characterization of chitosan. Influence of ionic strength and degree of acetylation on chain expansion " International Journal of Biological Macromolecules **15**(5): 281–285

Rinaudo, M., G. Pavlov and J. Desbrieres (1999). "Influence of acetic acid concentration on the solubilization of chitosan." Polymer **40**(25): 7029–7032.

Roberts, G. A. F. (1992). Chitin chemistry. London: Macmillan Press.

Roman, M. and D. G. Gray (2005). "Parabolic focal conics in self-assembled solid films of cellulose nanocrystals." Langmuir **21**(12): 5555–5561.

Roman, M. and W. T. Winter (2004). "Effect of sulfate groups from sulfuric acid hydrolysis on the thermal degradation behavior of bacterial cellulose." Biomacromolecules **5**(5): 1671–1677.

Roncal, T., A. Oviedo, I. L. de Armentia, L. Fernández and M. C. Villarán (2007). "High yield production of monomer-free chitosan oligosaccharides by pepsin catalyzed hydrolysis of a high deacetylation degree chitosan." Carbohydrate Research **342**(18): 2750–2756.

Rouget, C. (1859). "Des substances amylacees dans le tissue des animux, specialement les Articules (Chitine)." Comptes Rendus **48**: 792–795.

Sabnis, S. and L. H. Block (1997). "Improved infrared spectroscopic method for the analysis of degree of N-deacetylation of chitosan." Polymer Bulletin **39**(1): 67–71.

Sahu, A., P. Goswami and U. Bora (2009). "Microwave mediated rapid synthesis of chitosan." Journal of Materials Science: Materials in Medicine **20**(1): 171–175.

Saito, T., S. Kimura, Y. Nishiyama and A. Isogai (2007). "Cellulose nanofibers prepared by TEMPO-mediated oxidation of native cellulose." Biomacromolecules **8**(8): 2485–2491.

Säkkinen, M. (2003). "Biopharmaceutical evaluation of microcrystalline chitosan as release-rate-controlling hydrophilic polymer in granules for gastro-retentive drug delivery." PhD Thesis, University of Helsinki, Helsinki, October 2003.

Salmon, S. and S. M. Hudson (1997). "Crystal morphology, biosynthesis, and physical assembly of cellulose, chitin, and chitosan." Journal of Macromolecular Science-Reviews in Macromolecular Chemistry and Physics **C37**(2): 199–276.

Samir, M. A. S. A., F. Alloin, J.-Y. Sanchez and A. Dufresne (2004). "Cellulose nanocrystals reinforced poly(oxyethylene)." Polymer **45**(12): 4149–4157.

Sannan, T., K. Kurita and Y. Iwakura (1976). "Studies on chitin. 2. Effect of deacetylation on solubility." Makromolekulare Chemie-Macromolecular Chemistry and Physics **177**(12): 3589–3600.

Sannan, T., Kurita, Keisuke., Ogura, Katsuyuki., Iwakura, Yoshio. (1978). "Studies on chitin: 7. I.r. spectroscopic determination of degree of deacetylation." Polymer **19**(4): 458–459.

Schatz, C., J. M. Lucas, C. Viton, A. Domard, C. Pichot and T. Delair (2004). "Formation and properties of positively charged colloids based on polyelectrolyte complexes of biopolymers." Langmuir **20**(18): 7766–7778.

Schatz, C., C. Viton, T. Delair, C. Pichot and A. Domard (2003). "Typical physicochemical behaviors of chitosan in aqueous solution." Biomacromolecules **4**(3): 641–648.

Schipper, N. G. M., M. V. Kjell and A. Per (1996). "Chitosans as absorption enhancers for poorly absorbable drugs. 1: Influence of molecular weight and degree of acetylation on drug transport across human intestinal epithelial (Caco-2) cells." Pharmaceutical Research **13**(11): 1686–1692.

Shahidi, F., J. K. V. Arachchi and Y. J. Jeon (1999). "Food applications of chitin and chitosans." Trends in Food Science & Technology **10**(2): 37–51.

Shimojoh, M., K. Fukushima and K. Kurita (1998). "Low-molecular-weight chitosans derived from beta-chitin: preparation, molecular characteristics and aggregation activity." Carbohydrate Polymers **35**(3-4): 223–231.

Shimojoh, M., K. Masaki, K. Kurita and K. Fukushima (1996). "Bactericidal effects of chitosan from squid pens on oral streptococci." Nippon Nogeikagaku Kaishi-Journal of the Japan Society for Bioscience Biotechnology and Agrochemistry **70**(7): 787–792.

Shin, Y., I.-T. Bae, B. W. Arey and G. J. Exarhos (2007a). "Simple preparation and stabilization of nickel nanocrystals on cellulose nanocrystal." Materials Letters **61**(14-15): 3215–3217.

Shin, Y., J. M. Blackwood, I.-T. Bae, B. W. Arey and G. J. Exarhos (2007b). "Synthesis and stabilization of selenium nanoparticles on cellulose nanocrystal." Materials Letters **61**(21): 4297–4300.

Shutava, T., M. Prouty, D. Kommireddy and Y. Lvov (2005). "pH responsive decomposable layer-by-layer nanofilms and capsules on the basis of tannic acid." Macromolecules **38**(7): 2850–2858.

Sorlier, P., A. Denuziere, C. Viton and A. Domard (2001). "Relation between the degree of acetylation and the electrostatic properties of chitin and chitosan." Biomacromolecules **2**(3): 765–772.

Sorlier, P., C. Viton and A. Domard (2002). "Relation between solution properties and degree of acetylation of chitosan: role of aging." Biomacromolecules **3**(6): 1336–1342.

Suzuki, Y. and Y. Makino (1999). "Mucosal drug delivery using cellulose derivatives as a functional polymer." Journal of Controlled Release **62**(1-2): 101–107.

Tajik, H., M. Moradi, S. M. Rohani, A. M. Erfani and F. S. Jalali (2008). "Preparation of chitosan from brine shrimp (Artemia urmiana) cyst shells and effects of different chemical processing sequences on the physicochemical and functional properties of the product." Molecules **13**(6): 1263–1274.

Tan, S. C., E. Khor, T. K. Tan and S. M. Wong (1998). "The degree of deacetylation of chitosan: advocating the first derivative UV-spectrophotometry method of determination." Talanta **45**(4): 713–719.

Terbojevich, M., A. Cosani, G. Conio, E. Marsano and E. Bianchi (1991). "Chitosan: Chain rigidity and mesophase formation." Carbohydrate Research **209**: 251–260.

Tsaih, M. L. and R. H. Chen (1997). "Effect of molecular weight and urea on the conformation of chitosan molecules in dilute solutions." International Journal of Biological Macromolecules **20**(3): 233–240.

Tsaih, M. L. and R. H. Chen (1999a). "Effects of ionic strength and pH on the diffusion coefficients and conformation of chitosans molecule in solution." Journal of Applied Polymer Science **73**(10): 2041–2050.

Tsaih, M. L. and R. H. Chen (1999b). "Molecular weight determination of 83% degree of decetylation chitosan with non-Gaussian and wide range distribution by high-performance size exclusion chromatography and capillary viscometry." Journal of Applied Polymer Science **71**(11): 1905–1913.

Tsuchida, E. and K. Abe (1982). Interations between macromolecules in solution and intermacromolecular complexes. In: Ferry, J. D., H. Fujita, M. Gordon, J. P. Kennedy, W. Kern, S. Okamura, C. G. Overberger, T. Saegusa, G. V. Schulz, W. P. Slichter and J. K. Stille, Eds., Interactions Between Macromolecules in Solution and Intermacromolecular Complexes, Advances in Polymer Science 45. pp. 1–119. New York: Springer-Verlag.

Tsuchida, E., Y. Osada and K. Sanada (1972). "Interaction of poly(styrene sulfonate) with polycations carrying charges in the chain backbone." Journal of Polymer Science, Part A: Polymer Chemistry **10**(11): 3397–3404.

van Driessche, I. and S. Hoste (2006). Encapsulation through the sol-gel technique and their applications in functional coatings In "Functional Coatings by Polymer Microencapsulation" Ed. by Ghosh, Swapan Kumar. WILEY-VCH. pp 259-296.

Walstra, P. (2003). Physical chemistry of foods. New York: Marcel Dekker.

Wang, W., S. Bo, S. Li and W. Qin (1991). "Determination of the Mark-Houwink equation for chitosans with different degrees of deacetylation." International Journal of Biological Macromolecules **13**(5): 281–285.

Wang, W. and D. Xu (1994). "Viscosity and flow properties of concentrated solutions of chitosan with different degree of deacetylation." International Journal of Biological Macromolecules **16**(3): 149–152.

Willstatter, R. and M. Rohdewald (1934). "Über den Zustand des Glykogens in der Leber, im Muskel und in Leukocyten." Hoppe-Seyler's Zeitschrift für Physiologische Chemie **225**: 103–124.

Wu, A. C. M., W. A. Bough, E. C. Conrad and J. K. E. Alden (1976). "Determination of molecular-weght distribution of chitosan by high-performance liquid chromatography." Journal of Chromatography A **128**(1): 87–99.

Wu, C., S. Q. Zhou and W. Wang (1995). "A dynamic laser light-scattering study of chitosan in aqueous solution." Biopolymers **35**(4): 385–392.

Wu, T. and S. Zivanovic (2008). "Determination of the degree of acetylation (DA) of chitin and chitosan by an improved first derivative UV method." Carbohydrate Polymers **73**(2): 248–253.

Xiang, Q., Y. Y. Lee, P. O. Pettersson and R. W. Torget (2003). "Heterogeneous aspects of acid hydrolysis of α-cellulose." Applied Biochemistry and Biotechnology **105-108**: 505 - 514.

Yang, Y., W. Hu, X. Wang and X. Gu (2007). "The controlling biodegradation of chitosan fibers by N-acetylation *in vitro* and *in vivo*." Journal of Materials Science: Materials in Medicine **18**(11): 1573–4838.

Zamani, A., L. Edebo, B. Sjöström and M. J. Taherzadeh (2007). "Extraction and precipitation of chitosan from cell wall of zygomycetes fungi by dilute sulfuric acid." Biomacromolecules **8**(12): 3786–3790.

Zezin, A. B. and V. A. Kabanov (1982). "A new class of complex watersoluble polyelectrolytes." Russian Chemical Reviews **51**(9): 833–855.

Zhang, J. and Y. Sun (2007). "Molecular cloning, expression and characterization of a chitosanase from Microbacterium sp." Biotechnology Letters **29**(8): 1221–1225.

CHAPTER 3

CHITOSAN–CELLULOSE NANOCRYSTAL POLYELECTROLYTE COMPLEX—PART I: FORMATION AND PROPERTIES

3.1. ABSTRACT

This study was conducted to examine a new type of polyelectrolyte complex (PEC) between chitosan, a cationic polysaccharide, and cellulose nanocrystals, anionic rod-like nanoparticles. Cellulose nanocrystals were prepared by sulfuric acid hydrolysis of bleached wood pulp. The sulfate group density of the rod-like nanoparticles was 0.18 mol/kg and the amino group density of chitosan was 5.83 mol/kg. PEC formation was studied by turbidimetric titration using 0.001% (w/v) chitosan solutions and 0.001–0.04% (w/v) cellulose nanocrystal suspensions. The turbidity increased much more rapidly for more concentrated cellulose nanocrystal suspensions than for dilute ones. In titrations of a chitosan solution with a cellulose nanocrystal suspension, the turbidity reached a plateau but had a maximum and then decreased when the direction of titration was reversed. Chitosan–cellulose nanocrystal PEC particles were characterized by FT-IR spectroscopy, scanning electron microscopy, dynamic light scattering, and laser Doppler electrophoresis. The particles were composed primarily of cellulose nanocrystals. Particles formed at high amino/sulfate group molar ratios (N/S ratios) were spherical in shape, positively charged, and had a chitosan shell. Particles formed at low N/S ratios were non-spherical in shape, negatively charged, and had a cellulose nanocrystal shell. The formation and properties of chitosan–cellulose nanocrystal PEC particles were governed by the strong mismatch in the densities of the ionizable groups.

3.2. INTRODUCTION

Polyelectrolytes are polymers that contain functional groups capable of dissociating into ions. Three types of polyelectrolytes can be distinguished: polycations, bearing positive charges; polyanions, bearing negative charges; and polyampholytes, bearing both positive and negative charges. Upon mixing, polycations and polyanions form polyelectrolyte complexes (PECs) under release of the counterions. The properties of PECs depend on a number of factors, primarily the molecular weights and densities of ionizable groups of the two polyelectrolytes, the polyelectrolyte concentrations upon mixing, the mixing ratio, and the pH and ionic strength of the surrounding medium.

PECs have many current and potential applications, including the encapsulation of sensitive ingredients in food products (de Kruif *et al.*, 2004), the delivery of drugs (Liu *et al.*, 2008b) and genes (Midoux *et al.*, 2008), the entrapment and delivery of proteins and immobilization of enzymes (Cooper *et al.*, 2005), and the encapsulation of cells (Bhatia *et al.*, 2005). One polyelectrolyte that has been extensively studied for use in future PEC applications is chitosan, a cationic polysaccharide. Chitosan is a linear copolymer of β(1–4)-linked 2-amino-2-deoxy-D-glucopyranose (GlcN) and 2-acetamido-2-deoxy-D-glucopyranose residues. In acidic media, the amino groups of the GlcN residues are dissociated and bear a positive charge. Polyanions that have been studied for the complexation with chitosan include alginate (Cekic *et al.*, 2007; Sarmento *et al.*, 2007b; Sarmento *et al.*, 2007c; Dai *et al.*, 2008; Liu *et al.*, 2008a; Motwani *et al.*, 2008), hyaluronic acid (de la Fuente *et al.*, 2008a; de la Fuente *et al.*, 2008b), xanthan (Chellat *et al.*, 2000a; Chellat *et al.*, 2000b), pectin (Wong and Nurjaya, 2008), poly-γ-glutamic acid (Dai *et al.*, 2007; Hajdu *et al.*, 2008), carboxymethyl cellulose (Zhang *et al.*, 2001; Gomez-Burgaz *et al.*, 2008), κ-carrageenan (Piyakulawat *et al.*, 2007), chondroitin sulfate (Sui *et al.*, 2008), heparin (Liu *et al.*, 2007), chitosan sulfate (Berth *et al.*, 2002), and dextran sulfate (Schatz *et al.*, 2004a; Schatz *et al.*, 2004b; Sarmento *et al.*, 2006; Chen *et al.*, 2007; Drogoz *et al.*, 2007; Sarmento *et al.*, 2007a; Drogoz *et al.*, 2008).

Here we report a new type of PEC between chitosan and anionic, rod-like nanoparticles. The anionic nanoparticles are composed of cellulose, a linear polysaccharide of β(1–4)-linked D-glucopyranose residues, structurally very similar to

chitosan. Cellulose exists in nature in form of highly crystalline fibrils with nanoscale cross-sectional dimensions. Rod-like nanoparticles of cellulose, often termed cellulose nanocrystals, were discovered in 1949 by Bengt Rånby (1949), a Swedish scientist, and attracted interest in the 1990s for their ability to form chiral-nematic liquid crystalline phases (Revol *et al.*, 1992; Revol *et al.*, 1994). Cellulose nanocrystals are generally prepared by hydrolysis of a purified cellulose starting material with either hydrochloric or sulfuric acid (Araki *et al.*, 1998; Fleming *et al.*, 2001). The use of sulfuric acid results in the partial esterification of the surface hydroxyl groups and introduction of sulfate groups. At neutral and basic pH values, the sulfate groups are dissociated and bear a negative charge. As a consequence, cellulose nanocrystals prepared with sulfuric acid are anionic in nature.

The objectives of this study were to investigate the formation of PECs between chitosan and cellulose nanocrystals, with a focus on the effect of the polyelectrolyte concentration and mixing sequence, and to determine the properties of the resulting PEC particles.

3.3. EXPERIMENTAL SECTION

3.3.1. Materials

Chitosan ("medium molecular weight", Fluka BioChemika) was purchased from Sigma-Aldrich and purified as follows. Typically, 1 g of chitosan was dissolved overnight in 250 mL 0.1 N HCl and the solution was filtered through a series of Millipore polyvinylidene fluoride (PVDF) syringe filters (pore sizes 1, 0.45, and 0.22 μm). Next, chitosan was precipitated by addition of 1 N NaOH until the solution pH reached 9–10. The purified chitosan was collected by centrifugation (4900 rpm for 15 min at 4 °C), washed three times with deionized water, and freeze-dried overnight.

Cellulose, in the form of dissolving-grade softwood sulfite pulp (Temalfa 93 A-A), was kindly provided by Tembec, Inc. H_2SO_4 (>95%), HCl (0.1 N, certified), NaOH (0.1 N and 1 N, certified), and NaCl (certified) were purchased from Fisher Scientific. The water used in the experiments was deionized water from a Millipore Direct-Q 5 Ultrapure Water System (resistivity at 25 °C: 18.2 MΩ·cm).

3.3.2. Preparation of Chitosan Solutions

Chitosan solutions for the complexation experiments and chitosan characterization procedures were prepared from a stock solution of ~0.1% (w/v) by dilution with deionized water. For preparation of the stock solution, purified chitosan was dried in an oven at 105 °C for 2 h. Then, 0.1 g of the oven-dried, purified chitosan was dissolved in 100 mL 0.1 N HCl. The exact concentration of the stock solution was determined in triplicate by thermogravimetric analysis (TGA). To this end, 30 μL of the stock suspension was heated under nitrogen in a TA Instruments Q5000 TGA to 120 °C, at a heating rate of 20 °C/min, and held isothermal for 10 min. The concentration was determined from the initial suspension volume and the residual weight. If needed, the pH and ionic strength of the dilute chitosan solutions were adjusted with 0.1 N HCl or 0.1 N NaOH and NaCl, respectively.

3.3.3. Characterization of Chitosan

3.3.3.1. Molecular Weight

The molecular weight of the purified chitosan was calculated from the intrinsic viscosity, obtained from a serious of viscosity measurements at different concentrations (2.5–200 mg/mL). Measurements were performed at 30 °C with an Ubbelohde capillary viscometer with an inner capillary diameter of 0.53 mm. In this method, extrapolation of a plot of reduced viscosity, η/c, versus c to $c = 0$ yields the intrinsic viscosity, $[\eta]$, from which the molecular weight, M, can be calculated using the Mark–Houwink equation:

$$[\eta] = KM^{a} \qquad [3.1]$$

The Mark–Houwink parameters, K and a, for chitosan were obtained from the literature (Tsaih and Chen, 1999).

3.3.3.2. Degree of Deacetylation

The degree of deacetylation (DD) of the chitosan sample was determined by ^{1}H NMR spectroscopy according to ASTM standard F2260–03 (ASTM, 2003). Specifically, 10 mg of purified and oven-dried chitosan was dissolved in a mixture of 1.96 mL D_2O and 0.04 mL DCl. Approximately 1 mL of the solution was transferred to an NMR tube (diameter = 5 mm). ^{1}H NMR spectra were acquired on a Variance Mercury 400 MHz NMR spectrometer at 90 ± 1 °C. The DD was calculated using eq 3.2 (Lavertu *et al.*, 2003):

$$\mathrm{DD} = \left[\frac{\mathrm{H1D}}{\left(\mathrm{H1D} + \mathrm{HAc}/3\right)}\right] \times 100\% \qquad [3.2]$$

where H1D is the integral of the H1 GlcN peak and HAc is the integral of the peak corresponding to the three protons of the GlcNAc acetyl group.

3.3.3.3. Hydrodynamic Diameter and Electrophoretic Mobility

The z-average hydrodynamic diameter (cumulants mean) and electrophoretic mobility of chitosan were measured with a Malvern Zetasizer Nano ZS using Malvern DTS1060 folded capillary cells and a 0.001% (w/v) chitosan solution without further modification of the pH or ionic strength. Measurements were performed in triplicate at 25 °C.

3.3.3.4. Amino Group Density

The amino group density of the purified chitosan was measured in triplicate by conductometric titration using a Mettler Toledo SevenMulti S47 pH/conductivity meter with an InLab 730 conductivity probe. A standard NaOH solution (0.1 N) was added in drop-wise under nitrogen and stirring to 25 mL of a 0.1% (w/v) chitosan solution, having an ionic strength of 50 mM. At every 10th drop, the conductivity of the chitosan solution was recorded. The amino group density was calculated from the titrant volume between the two equivalence points.

3.3.4. Synthesis of Cellulose Nanocrystals

Dissolving-grade softwood sulfite pulp was ground in a Thomas Wiley Mini-Mill (Thomas Scientific, Swedesboro, NJ) to pass a 60-mesh screen. Fifty grams of pulp was treated under stirring with a mechanical stirrer with 500 mL 64 wt % H_2SO_4 at 45 °C for 45 min. The hydrolysis was stopped by 10-fold dilution of the reaction medium with deionized water. The cellulose nanocrystals were collected by centrifugation for 15 min at 4900 rpm under cooling (4 °C) and redispersed in deionized water after discarding the supernatant. For removal of the remaining acid, the nanocrystals were dialyzed against deionized water using regenerated cellulose dialysis tubing (Spectra/Por4, Spectrum Laboratories, MWCO 12–14 kDa) until the pH of the dialysis water stayed constant. The obtained suspension was sonicated under ice-bath cooling for 15 min at 40% output with an ultrasonic processor (GE 505, Sonics & Material, Inc. USA). Finally, the suspension

was filtered through a 0.45 μm and then 0.22 μm PVDF syringe filter. The concentration of the filtered cellulose nanocrystal stock suspension, determined in triplicate from the weight difference of a 5 mL aliquot before and after drying for 2 h in an oven at 80 °C, was generally in the range of 0.6–0.9% (w/v).

3.3.5. Preparation of Cellulose Nanocrystal Suspensions

Dilute cellulose nanocrystal suspensions for the complexation experiments and cellulose nanocrystal characterization procedures were prepared from the filtered stock suspension by dilution with deionized water. If needed, the pH and ionic strength of the dilute cellulose nanocrystal suspensions were adjusted with 0.1 N HCl or 0.1 N NaOH and NaCl, respectively.

3.3.6. Characterization of Cellulose Nanocrystals

3.3.6.1. Particle Morphology

The morphology of the resulting cellulose nanocrystals was characterized by atomic force microscopy (AFM). A 10 μL drop of a 0.001% (w/v) cellulose nanocrystal suspension was spin coated at 2000 rpm with a Laurell Technologies WS-400B-6NPP/LITE spin coater onto a freshly cleaved mica disc (V1 mica, 9.9 mm, Ted Pella). The mica disc was then mounted onto a standard microscope slide using epoxy adhesive. AFM images were recorded in AC mode in air with an Asylum Research MFP-3D Bio-AFM using standard silicon probes (OLYMPUS-AC160TS, nominal tip radius: <10 nm, nominal force: 42 N/m).

3.3.6.2. Hydrodynamic Diameter and Electrophoretic Mobility

The z-average hydrodynamic diameter (cumulants mean) and electrophoretic mobility of the cellulose nanocrystals were measured with a Malvern Zetasizer Nano ZS using Malvern DTS1060 folded capillary cells and a 0.02% (w/v) cellulose nanocrystal

suspension without further modification of the pH or ionic strength. Measurements were performed in triplicate at 25 °C.

3.3.6.3. Sulfate Group Density

The sulfate group density of the cellulose nanocrystals was measured in triplicate by conductometric titration using a Mettler Toledo SevenMulti S47 pH/conductivity meter with an InLab 730 conductivity probe. Titrations were carried out with 25 mL aliquots of the filtered stock suspension. The ionic strength of the titrand was adjusted to 0.02 M through addition of NaCl. The titrant, 0.02 N NaOH, prepared by dilution of 0.1 N NaOH with deionized water, was added under nitrogen gas with stirring in 0.5 mL increments. After each addition, the conductivity of the titrand was recorded. The sulfate group density was calculated from the titrant volume at the equivalence point.

3.3.7. Turbidimetric Titration

Turbidimetric titrations were performed using a 0.001% (w/v) chitosan solution and a dilute cellulose nanocrystal suspension (0.02% (w/v), unless stated otherwise), both having a pH of 2.6 and an ionic strength of 1 mM. The ionic strength and pH values were chosen based on preliminary screening experiments. The effect of pH and ionic strength on the formation and properties of the complex are discussed in Chapter 4. In a turbidimetric titration experiment, the cellulose nanocrystal suspension was added drop-wise under vigorous stirring with a magnetic bar to the chitosan solution or vice versa. The transmittance of the reaction mixture was monitored with a probe colorimeter (PC 950, Brinkman, USA) with a 1 cm optical cell (2 cm path length), operating at a wavelength of 420 nm. Turbidity values were calculated as 100 – transmittance (%). Prior to the each titration, the probe colorimeter was zeroed in deionized water. Each experiment was performed in triplicate.

3.3.8. Characterization of PEC Particles

3.3.8.1. Chemical Structure

The chemical structure of the PEC particles was analyzed by Fourier transform infrared (FTIR) spectroscopy. FTIR spectra were recorded from KBr pellets with a resolution of 4 cm^{-1} and a number of scans of 128 using a Thermo Nicolet Nexus 470 ESP FTIR spectrometer. KBr pellets were prepared by grinding 98 mg of dry KBr with 2 mg of sample and compressing the mixture between the ends of two stainless steel bolts inserted from opposite ends into a deep stainless steel nut, which served as the sample holder. The KBr pellet was dried in an oven prior to the measurement.

3.3.8.2. Particle Morphology

The morphology of the PEC particles was analyzed by field emission scanning electron microscopy (FE-SEM). Images were recorded with a LEO 1550 FE-SEM using an accelerating voltage of 1 kV and a working distance of 4–5 mm. Particles for SEM imaging were prepared at different amino/sulfate group molar ratios (N/S ratios) by mixing under vigorous stirring with a magnetic bar the appropriate amounts of a 0.001% (w/v) chitosan solution and a 0.02% (w/v) cellulose nanocrystal suspension, both having a pH of 2.6 and an ionic strength of 1 mM. For SEM sample preparation, a 10 μL drop of the PEC particle suspension was deposited onto Ni–Cu conductive tape (Ted Pella) mounted onto a standard SEM stub (Ted Pella) and allowed to dry under ambient conditions. Prior to imaging, the SEM samples were coated with a thin (6 nm) layer of carbon.

3.3.8.3. Hydrodynamic Diameter and Electrophoretic Mobility

The z-average hydrodynamic diameter (cumulants mean) and electrophoretic mobility of the PEC particles were measured with a Malvern Zetasizer Nano ZS using Malvern DTS1060 folded capillary cells. The PEC particle suspensions, obtained as

described above, were used directly without further dilution or filtration. Measurements were performed in triplicate at 25 °C.

3.4. RESULTS AND DISCUSSION

3.4.1. Properties of the Individual Components

The molecular weight and DD of chitosan were $3.1 \cdot 10^6$ g/mol and 88%, respectively, yielding a degree of polymerization of $\sim 18 \cdot 10^3$. Assuming a monomer length of 0.517 nm, based on the crystal lattice unit cell dimensions of hydrated chitosan (Okuyama *et al.*, 2000), we calculated an average contour length of ~9.5 μm. For comparison, the cellulose nanocrystals had a length on the order of a few tens to a few hundred nanometers as shown in Figure 3.1. The average length ratio of the two PEC components was estimated to about 70:1 (chitosan molecule/cellulose nanocrystal). Dynamic light scattering experiments yielded z-average hydrodynamic diameters of 265 and 104 nm for chitosan and cellulose nanocrystals, respectively. It should be noted, however, that especially for rod-like species the hydrodynamic diameter does not represent the actual size of the particles or molecules but simply represents a size measure for comparison.

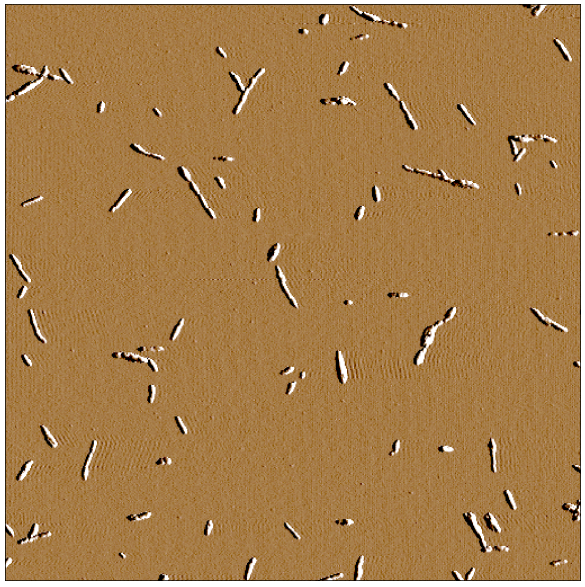

Figure 3.1. AFM amplitude image of cellulose nanocrystals (scan size: 5 μm × 5 μm).

The amino group density of chitosan and the sulfate group density of the cellulose nanocrystals were determined by conductometric titration. Figure 3.2 shows typical conductometric titration curves.

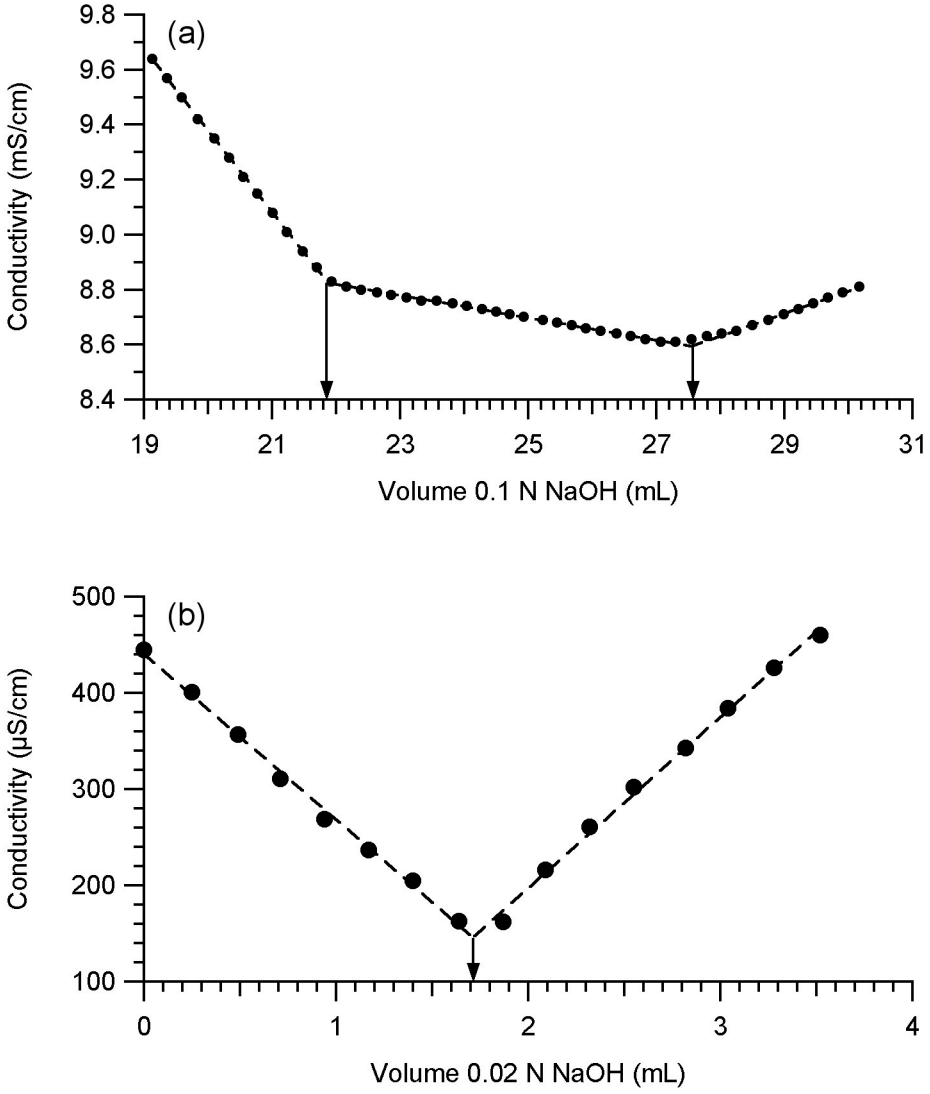

Figure 3.2. Conductometric titration curves for the determination of the amino group density of chitosan (a) and the sulfate group density of the cellulose nanocrystals (b).

The titration curve for chitosan (Figure 3.2(a)) had three sections. The initial linear decrease in conductivity was due to the neutralization of HCl and the lower mobility and molar conductivity of Na^+ with respect to H^+. At the first equivalence point, the decrease in conductivity slowed down. The middle section of the conductivity curve corresponded to the titration of the chitosan amino groups. At the second equivalence point, the conductivity started to increase upon further NaOH addition due to an increasing excess of sodium and hydroxyl ions. The titration curve for the cellulose nanocrystals (Figure 3.2(b)) had two branches corresponding to the neutralization of the partially dissociated surface sulfate groups ($–SO_3H$ and $–SO_3^- H^+$) and excess NaOH, respectively. The amino group density of chitosan was 5.83 mol/kg and the sulfate group density of the cellulose nanocrystals was 0.18 mol/kg. In other words, the amino group density of chitosan was 33 times higher than the sulfate group density of the cellulose nanocrystals. Thus, there was a strong mismatch in the densities of ionizable groups of the two PEC components.

3.4.2. Polyelectrolyte Complex Formation

3.4.2.1. Effect of Cellulose Nanocrystal Concentration

When a cellulose nanocrystal suspension was added drop-wise to a chitosan solution of the same pH and ionic strength, the reaction mixture immediately became opaque due to the formation of an insoluble complex. Figure 3.3 shows turbidimetric titration curves for the titration of a 0.001% (w/v) chitosan solution with cellulose nanocrystal suspensions of different concentration. The chitosan solution was completely transparent. Upon drop-wise addition of the cellulose nanocrystal suspension, the turbidity increased linearly for cellulose nanocrystal concentrations up to 0.02% (w/v) and the increase was more pronounced at higher concentrations. At cellulose nanocrystal concentrations above 0.02% (w/v), the increase in turbidity started to be asymptotic rather than linear.

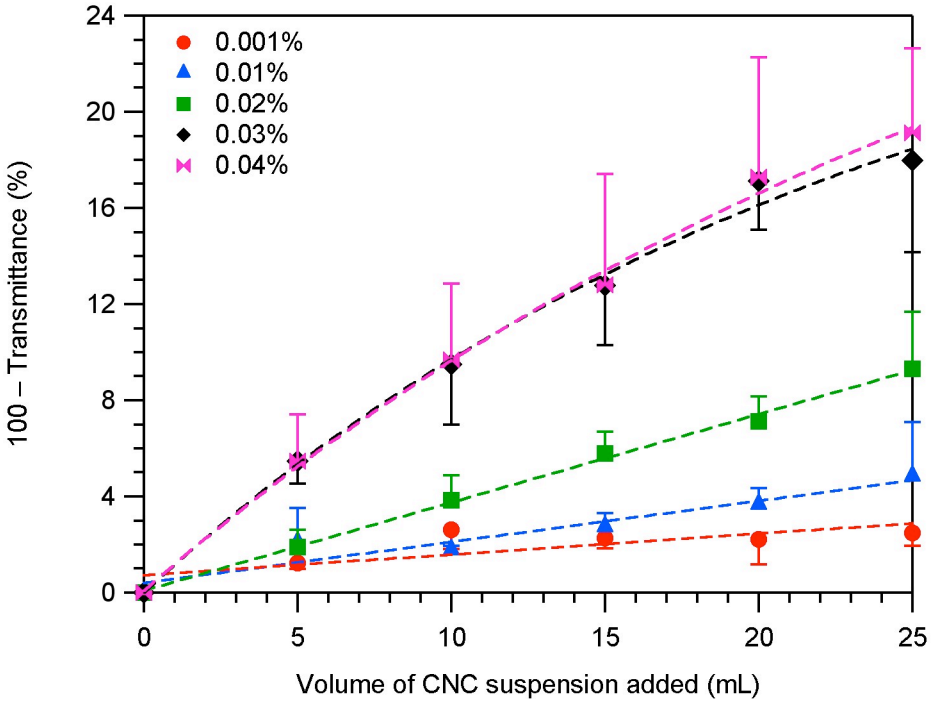

Figure 3.3. Turbidimetric titration curves for titrations of a 0.001% (w/v) chitosan solution with cellulose nanocrystal suspensions of different concentration. (The titrand volume was 25 mL. Data points are means of three measurements. Error bars represent one standard deviation.)

At cellulose nanocrystal concentrations above 0.02% (w/v), flocculation occurred relatively early during the titration, resulting in sedimentation of the complex. Large flocs interfered with the turbidity measurements and caused strong fluctuations in the turbidity data (large error bars). The lowest cellulose nanocrystal concentrations (0.001 and 0.01% (w/v)) gave turbidity values only slightly above the detection limit of the instrument (~2%), which is why we chose an intermediate cellulose nanocrystal concentration (0.02% (w/v)) for subsequent experiments.

Our results are in accordance with those of Dautzenberg *et al.* (1993), who observed higher levels of aggregation at higher polyelectrolyte concentrations for PEC formation between sodium poly(styrene sulfonate) and poly(diallyldimethylammonium chloride).

Two mechanisms for flocculation can be distinguished in colloidal systems that contain both particles and polymer molecules: bridging flocculation and depletion flocculation (Jenkins and Snowden, 1996). Bridging flocculation occurs when a polymer molecule adsorbs simultaneously onto two different particles, thus tying these particles together. Depletion flocculation occurs when adsorption of the polymer molecules onto the surface of the particles is unfavorable. In this case, the decrease in conformational entropy of the polymer molecules is not compensated by an adsorption energy and, consequently, prevents the molecules from approaching the particle surface. For dilute polymer solutions, the thickness of the depletion zone is commonly equated with the polymer's radius of gyration. Above a critical polymer concentration, particle aggregation is spontaneous because it causes overlapping of the depletion zones of adjacent particles and, thus, an increase in the volume that is available to the polymer molecules. The magnitude of the depletion attraction can be controlled through the polymer's molecular weight and concentration. However, aggregation due to depletion flocculation is weak, relative to that due to bridging flocculation, and reversible.

Potential interactions between chitosan and cellulose nanocrystals include attractive Coulomb interactions, van der Waals interactions, and hydrogen bonding. Thus, it is likely, that chitosan molecules adsorb onto the surface of cellulose nanocrystals. Considering the estimated contour length of the chitosan molecules of ~9.5 μm, bridging flocculation might have been the reason for the observed increase in turbidity. Another possible result of mixing the two components could be covering of the cellulose nanocrystal surface by chitosan molecules, which would likely cause overcompensation of the negative surface charge of the cellulose nanocrystals because of the much higher amino group density of chitosan, compared to the sulfate group density of the cellulose nanocrystals. Depending on the type and magnitude of interactions between the chitosan-covered cellulose nanocrystals as well as the chitosan concentration, depletion flocculation might occur. However, because of the low flexibility of chitosan molecules, with reported persistence lengths of 6–22 nm (Terbojevich *et al.*, 1991; Brugnerotto *et al.*, 2001a; Brugnerotto *et al.*, 2001b; Berth and Dautzenberg, 2002; Mazeau and Rinaudo, 2004; Schatz *et al.*, 2004b; Rinaudo, 2008), covering of an individual cellulose

nanocrystal, having a diameter of approximately 5 nm, by a chitosan molecule is less likely than bridging of several cellulose nanocrystals by the chitosan molecule. Furthermore, when the chitosan–cellulose nanocrystal aggregates were isolated by centrifugation and redispersed in deionized water by vortexing, the aggregates did not disintegrate, indicating that aggregation was irreversible and more likely due to strong electrostatic interactions, rather than depletion attraction. Thus, we attributed the observed flocculation to bridging flocculation.

3.4.2.2. Effect of Mixing Sequence

The turbidity profile upon incremental mixing of a chitosan solution with a cellulose nanocrystal suspension depended on the mixing sequence. Figure 3.4 shows the titration curves for the titration of a chitosan solution with a cellulose nanocrystal suspension (type 1) and the reverse direction (type 2).

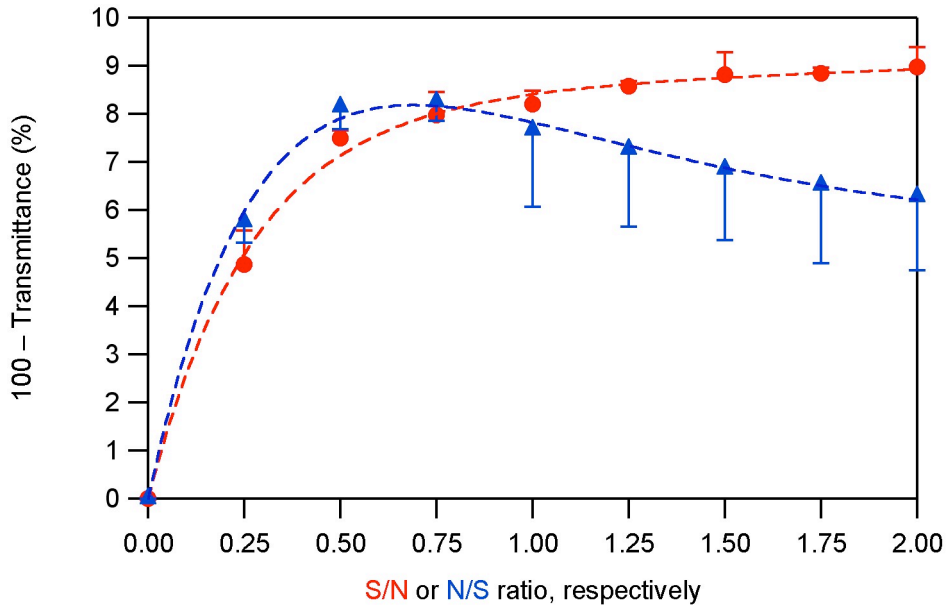

Figure 3.4. Turbidimetric titration curves for the titration of a chitosan solution with a cellulose nanocrystal suspension (type 1, ●) and the reverse direction (type 2, ●). (Data points are means of three measurements. Error bars represent one standard deviation.)

In type 1 titrations, the turbidity increased rapidly initially up to a sulfate/amino group molar ratio (S/N ratio) of about 0.5. Upon further increase of the S/N ratio, the turbidity leveled off and asymptotically approached a maximum turbidity level. In type 2 titrations, the turbidity also increased rapidly initially up to an amino/sulfate group molar ratio (N/S ratio) of about 0.5. The initial increase in turbidity was similar to that observed in type 1 titrations. However, upon further increase of the N/S ratio, the turbidity decreased.

Shybaila *et al.* (2008) made a similar observation in a study of the complexation of chitosan and chitosan sulfate acetate (CSA). Turbidity levels reached a plateau in titrations of a chitosan solution with a CSA solution and decreased after reaching a maximum in titrations of the reverse direction. The decrease in turbidity was related to the presence of a low-molecular-weight electrolyte (CH_3COONa). In the absence of electrolyte, the turbidity stayed constant after reaching the maximum, i.e. exhibited a plateau. The ionic strength in our titration was 1 mM. The fact that the decrease in turbidity was only observed in the presence of electrolyte suggests that it was based on charge screening effects.

As will be shown in Chapter 4, at pH 2.6, which was the pH of the turbidimetric titrations, the degree of ionization of the cellulose nanocrystals was 0.5, i.e. only 50% of the sulfate groups were dissociated and carried a negative charge. Therefore, an N/S ratio of 0.5 represents a NH_3^+/SO_3^- charge ratio of unity. It is commonly accepted that PECs exhibit maximum aggregation at a stoichiometric charge ratio because the net charge of the PECs is zero. At non-stoichiometric charge ratios, PEC particles bear a non-zero net charge and are therefore charge stabilized. Aggregation of the chitosan–cellulose nanocrystal PECs due to a stoichiometric charge ratio would explain the turbidity maximum at an N/S ratio of 0.5 in type 2 titrations. Upon further increase of the N/S ratio, charge overcompensation by incorporation of additional chitosan molecules into the PECs would lead to a net positive charge and charge stabilization of the PECs, reversing PEC aggregation. The incorporation of additional chitosan molecules into the PECs might have been facilitated by the NaCl (1 mM) because of the ability of the Na^+ and Cl^- ions to reduce the attraction forces between the PEC components through charge

screening. The presence of low-molecular-weight electrolytes during PEC formation is known to enable structural rearrangements (Bakeev *et al.*, 1988).

In type 1 titrations, charge stoichiometry corresponded to an S/N ratio of 2, which coincided with the turbidity maximum. The rapid increase in turbidity at low S/N ratios was probably related to the particulate nature of one of the PEC components. Upon addition of cellulose nanocrystals to a chitosan solution, the chitosan molecules likely caused bridging flocculation. The net charge of these flocs would be positive because of an excess of ammonium groups. Upon further increase of the S/N ratio, the net charge of the PEC particles would decrease.

To confirm this interpretation, we monitored the size and net charge of PEC particles during type 1 and type 2 titrations. The titrations for this analysis were performed differently from those of Figure 3.4. As a result, the ranges for the S/N and N/S ratios are different. Table 3.1 lists the hydrodynamic diameters and electrophoretic mobilities of PEC particles obtained at different mixing ratios and sequences.

Table 3.1. PEC particle properties at different mixing ratios and sequences[a]

Volume ratio	Cellulose/chitosan mass ratio	S/N ratio	N/S ratio	Hydrodynamic diameter (nm)	Electrophoretic mobility (μm·cm/V·s)
Titration of a 0.001% chitosan solution with a 0.02% cellulose nanocrystal suspension (type 1)[b]					
0.0	0	0	∞	265 ± 14	4.0 ± 0.1
0.2	4	0.12	8.28	347 ± 6	2.9 ± 0.2
0.4	8	0.24	4.14	411 ± 22	3.6 ± 0.1
0.6	12	0.36	2.76	472 ± 17	3.4 ± 0.1
0.8	16	0.48	2.07	969 ± 81	3.4 ± 0.0
1.0	20	0.60	1.66	–[c]	2.5 ± 0.0
Titration of a 0.02% cellulose nanocrystal suspension with a 0.001% chitosan solution (type 2)[b]					
0.0	∞	∞	0	104 ± 4	-2.8 ± 0.2
0.2	100	3.02	0.33	154 ± 12	-2.7 ± 0.0
0.4	50	1.51	0.66	410 ± 91	-2.4 ± 0.1
0.6	33	1.01	0.99	–[c]	-1.2 ± 0.0
0.8	25	0.75	1.33	–[c]	1.0 ± 0.1
1.0	20	0.60	1.66	–[c]	2.7 ± 0.1

[a] reaction conditions: pH 2.6, ionic strength 1 mM

[b] all concentrations are % (w/v)

[c] scattering data unsuitable for size determination

At all volume ratios greater than 0, the cellulose/chitosan mass ratio was greater than 1, meaning that the mass of cellulose nanocrystals present in the reaction mixture was always greater than that of chitosan. The cellulose/chitosan mass ratio ranged from 4 to 100. In type 1 titrations, the hydrodynamic diameter of the PEC particles increased from 347 nm at an S/N ratio of 0.12 to 969 nm at an S/N ratio of 0.48. At an S/N ratio of 0.6, the reaction mixture yielded scattering data unsuitable for size determination of the aggregates, probably due to large or non-uniform floc sizes. In type 2 titrations, the hydrodynamic diameter increased more gradually, having values of only 154 nm at an N/S ratio of 0.33 and 410 nm at 0.66. At N/S ratios of 0.99 on higher, the reaction mixtures yielded scattering data unsuitable for size determination of the aggregates.

During type 1 titrations, the electrophoretic mobility of the PEC particles was positive, indicating an excess of ammonium groups, and decreased slightly toward the end. During type 2 titrations, the electrophoretic mobility of the PEC particles was initially negative, indicating an excess of sulfate groups, and increased with increasing N/S ratio. The electrophoretic mobility of the particles became positive at an N/S ratio of 1.33. It is important to note, that the composition of the PEC particles, in terms of cellulose/chitosan mass ratio, and S/N or N/S ratio, most likely differed from that of the reaction mixture. For example, the negative electrophoretic mobility value obtained in type 2 titrations at an N/S ratio in the reaction mixture of 0.99 (estimated to correspond to an NH_3^+/SO_3^- ratio of 2) indicated an excess of ionized sulfate groups in the PEC particles. Consequently, the reaction mixture must have contained unreacted chitosan.

The proposed mechanisms of chitosan–cellulose nanocrystal complexation for the two mixing sequences are schematically shown in Figure 3.5. In type 1 titrations, the short, rigid cellulose nanocrystals are added incrementally to the long, flexible chitosan molecules (Figure 3.5(a)). The added cellulose nanocrystals bind to the chitosan molecules and partially compensate the positive charge along the chitosan chain, allowing the chains to take on a more tightly coiled conformation. Upon further addition of cellulose nanocrystals, more charges will be compensated and the charge ratio will eventually reach unity. At this charge ratio, the net charge of the PECs is close to zero and the PECs may aggregate. If more cellulose nanocrystals were added at this point,

additional cellulose nanocrystals would be incorporated in the PECs, resulting in charge overcompensation and a net negative charge. PEC aggregation would be suppressed through repulsive forces between the negatively charged PECs. Unbound cellulose nanocrystals would be present in the reaction mixture.

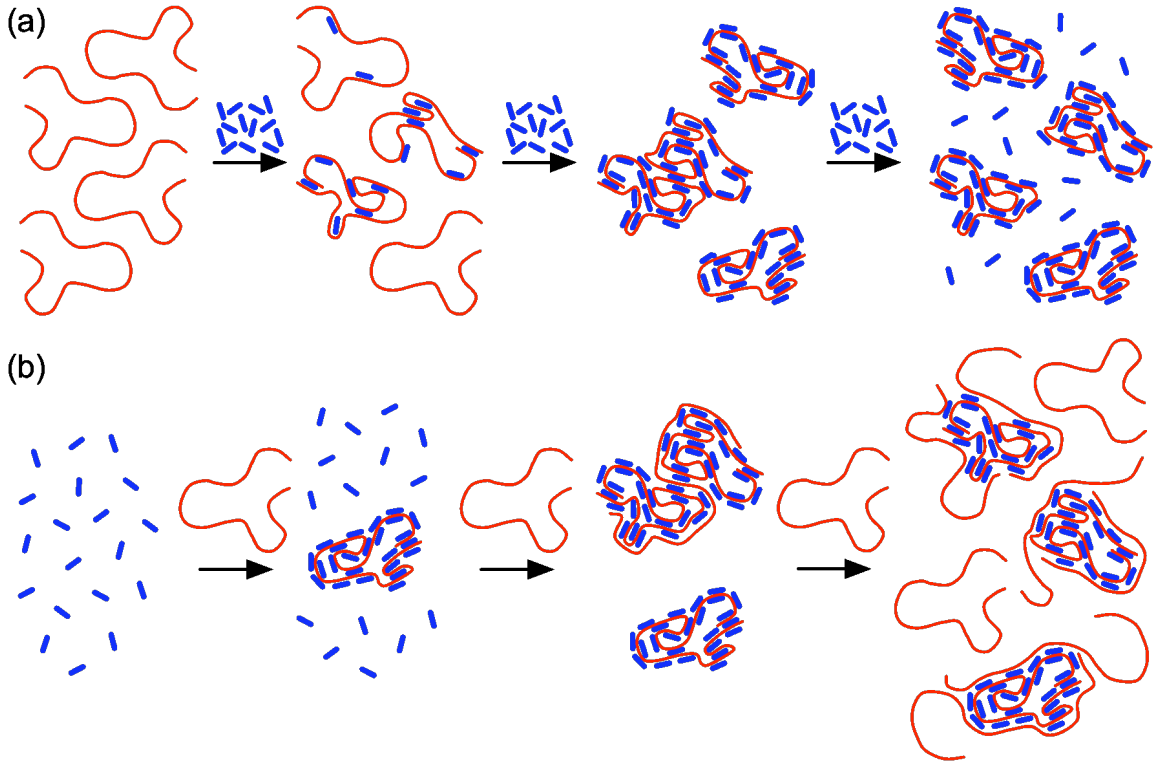

Figure 3.5. Proposed mechanisms of chitosan–cellulose nanocrystal complexation: (a) titration of a chitosan solution with a cellulose nanocrystal suspension (type 1), (b) titration of a cellulose nanocrystal suspension with a chitosan solution (type 2).

In type 2 titrations, the long, more flexible chitosan molecules are added incrementally to the short, rigid cellulose nanocrystals (Figure 3.5(b)). Upon addition to the cellulose nanocrystal suspension, the chitosan molecules rapidly bind a large number of cellulose nanocrystals and form dense PEC particles with an excess of negatively charged sulfate groups (negative electrophoretic mobility, see Table 3.1). Upon further addition of chitosan molecules, all cellulose nanocrystals present in the mixture

eventually become bound. At a charge ratio of unity, the net charge of the PECs is close to zero and the PECs may aggregate. Further addition of chitosan molecules results in charge overcompensation by incorporation of additional chitosan molecules into the PECs (positive electrophoretic mobility, see Table 3.1) and the presence of unbound chitosan molecules in the mixture. In acidic aqueous media, loose ends of chitosan molecules are likely to protrude from the PEC particle surface.

3.4.3. Characterization of PEC Particles

3.4.3.1. Chemical Structure

The chemical structure of the PEC particles was analyzed by FTIR spectroscopy. Figure 3.6 shows the FTIR spectra of chitosan (Figure 3.6(a)), cellulose nanocrystals (Figure 3.6(b)), and of PEC particles formed by mixing equal volumes of a 0.01% (w/v) chitosan solution and a 0.01% (w/v) cellulose nanocrystal suspension. The FT-IR spectra of chitosan (Figure 3.6(a)) and cellulose nanocrystals (Figure 3.6(b)) were nearly identical because of the similarity of the molecular structures of chitosan and cellulose. In the spectrum of the cellulose nanocrystals, the broad absorption band between 3600 and 3000 cm^{-1} was related to OH stretching vibrations (Hinterstoisser and Salmén, 1999). The absorption bands between 3000 and 2800 cm^{-1} and 1500 and 1250 cm^{-1} stemmed from the CH and CH_2 stretching and bending vibrations, respectively (Marchessault and Liang, 1960). The bands in the fingerprint region have been assigned to the antisymmetric bridge C–O–C stretching vibration (Nikonenko *et al.*, 2000; Nikonenko *et al.*, 2005), and the CO stretching vibrations at C–2, C–3, and C–6 (Maréchal and Chanzy, 2000). And lastly, the band between 800 and 450 cm^{-1} originated in the OH out-of-plane bending vibrations (Kondo and Sawatari, 1996; Oh *et al.*, 2005). The FT-IR spectrum of chitosan had additional absorption bands between 1700 and 1500 cm^{-1}, assigned to the carbonyl stretching vibrations (amide I band) and NH bending vibrations (amide II band) (Duarte *et al.*, 2002).

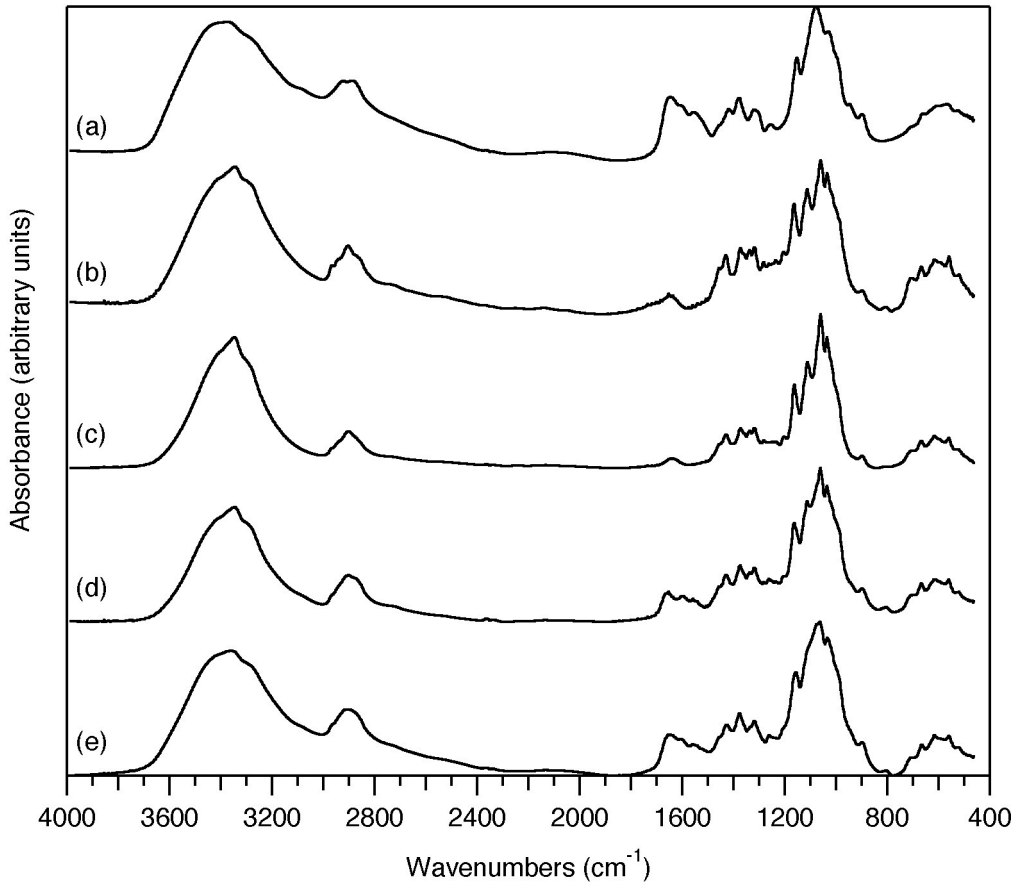

Figure 3.6. FT-IR spectra of (a) chitosan, (b) cellulose nanocrystals, (c) PEC complex particles, (d) PEC complex particles collected after adjusting the pH to 10, and (e) a 50:50 physical blend of chitosan and cellulose nanocrystals.

The FTIR spectrum of the PEC particles (spectrum (c)) was identical to that of the cellulose nanocrystals (spectrum (b)) and did not show the characteristic absorption bands of chitosan. The absence of chitosan absorption bands from the spectrum of the PEC particles confirmed that the particles consisted primarily of cellulose nanocrystals and that chitosan was the minor component.

The PEC particles used to obtain spectrum (c) had been isolated from the reaction mixture by centrifugation, washed three times with deionized water, and freeze-dried. The low chitosan content of the PEC particles indicated that part of the chitosan in the reaction mixture had remained in solution during complex formation and been discarded with the supernatant. To test this hypothesis, we repeated the complexation experiment

but raised the pH of the reaction mixture with 1 N NaOH to about 10 before centrifugation. Raising the pH caused the chitosan that had remained in solution to precipitate and be present in the sediment after centrifugation. Spectrum (d) in Figure 3.6 is the FTIR spectrum obtained from the washed and freeze-dried sediment of this experiment. The characteristic absorption bands of chitosan are clearly visible, corroborating our hypothesis that during complex formation a large fraction of chitosan remains in solution. Spectrum (e) is an FTIR spectrum of a 50:50 physical blend of chitosan and cellulose nanocrystals, recorded for comparison.

To quantify the chitosan content of the binary FTIR samples, we analyzed the FTIR spectra further (Figure 3.7). The largest difference between the absorbances of chitosan and cellulose nanocrystals (spectra (a) and (b) in Figure 3.7, respectively) was observed at a wavelength of 1581 cm^{-1}. At this wavelength, chitosan showed carbonyl and NH-related absorption, whereas absorption by cellulose was minimal. The absorbance at 1375 cm^{-1}, related to CH_2 bending vibrations (Kondo and Sawatari, 1996), was used as an internal reference. The ratios of the absorbances at 1581 and 1375 cm^{-1} (A_{1581}/A_{1375}) for chitosan and cellulose as well as the three binary FTIR samples are listed in Table 3.2.

Table 3.2. Ratios of FTIR absorbances at 1581 and 1375 cm^{-1} (A_{1581}/A_{1375}) for chitosan and cellulose as well as the three binary FTIR samples and calculated chitosan contents

Sample	A_{1581}/A_{1375}	Chitosan content (%)
Chitosan	0.76	100
Cellulose nanocrystals	0.09	0
PEC complex particles formed by mixing equal volumes of a 0.01% (w/v) chitosan solution and a 0.01% (w/v) cellulose nanocrystal suspension	0.08	0
PEC complex particles collected after adjusting the pH to 10	0.40	46
50:50 physical blend of chitosan and cellulose nanocrystals	0.49	60

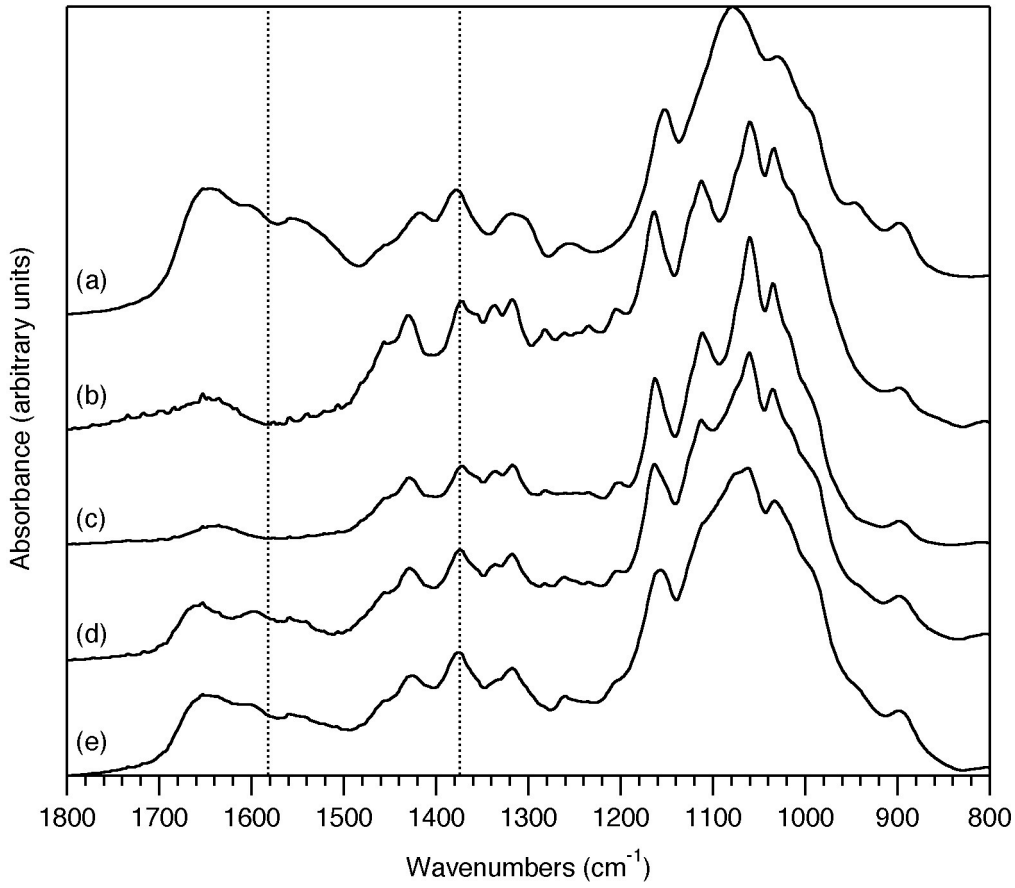

Figure 3.7. Quantitative analysis of FTIR spectra (same as in Figure 3.6). The ratios of the absorbances at 1581 and 1375 cm^{-1} (A_{1581}/A_{1375}) was used for quantification of the chitosan content.

Assuming that this ratio is unaffected by the process of mixing the two components, it can be used to estimate the composition of the mixtures. The calculated chitosan contents of the three binary FTIR samples are listed in Table 3.2. The values confirm that the chitosan content of PEC particles formed by mixing equal volumes of a 0.01% (w/v) chitosan solution and a 0.01% (w/v) cellulose nanocrystal suspension was very low. Increasing the pH to 10 before centrifugation resulted in a chitosan content close to 50%, suggesting that most of the chitosan remained in solution during complex formation. The high chitosan content of the '50:50' physical blend of 60% indicates either a low accuracy of the analysis method or insufficient mixing during sample preparation.

3.4.3.2. Particle Morphology

The morphology of the PEC particles was analyzed by FE-SEM. Figure 3.8 shows SEM images of PEC particles formed by addition of a 0.001% (w/v) chitosan solution to a 0.02% (w/v) cellulose nanocrystal suspension at different N/S ratios in the reaction mixture. At N/S ratios below 1 (Figure 3.8(a)-(c)), the PEC particles were non-spherical and had more or less well-defined edges. The shape of the particles seemed to become better defined as the N/S ratio in the reaction mixture approached 1. At N/S ratios of 0.66 and 0.99, many particles appeared to have a somewhat symmetric hexagonal shape with three long and three short sides. Some particles had four long sides and two short ones, approaching a rhombus in shape (see also Figure 3.9(a)).

At N/S ratios above 1, the shape of the PEC particles became more and more spherical with increasing N/S ratio in the reaction mixture. The reason for the non-spherical shape of the PEC particles at the N/S ratios 0.66 and 0.99 is not clear. It is likely to be related to packing constraints due to the rod-like shape of the cellulose nanocrystals. However, the spatial arrangement of the cellulose nanocrystals in the PEC particles is not known.

Figure 3.9 shows two PEC particles at higher magnification. The particle formed at an N/S ratio of 0.66 (Figure 3.9(a)) was covered in cellulose nanocrystals. The rod-like particles were also covering the substrate indicating that at this N/S ratio, unbound cellulose nanocrystals were present in the reaction mixture. The cellulose nanocrystal coating of the PEC particle was in accordance with the observed negative electrophoretic mobility at this N/S ratio (Table 3.1).

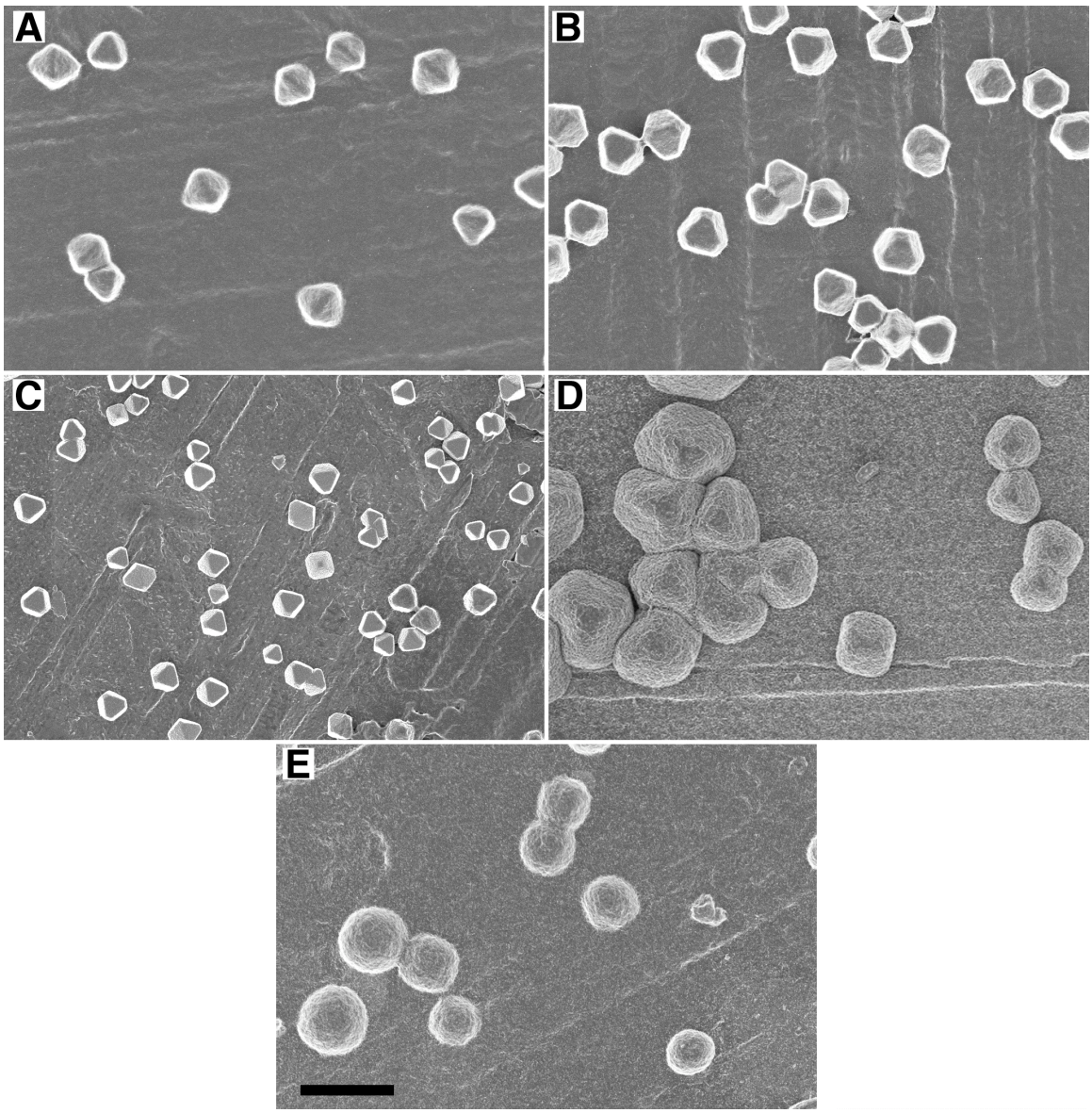

Figure 3.8. FE-SEM images of PEC particles formed by addition of a 0.001% (w/v) chitosan solution to a 0.02% (w/v) cellulose nanocrystal suspension at reaction mixture N/S ratios of (a) 0.33, (b) 0.66, (c) 0.99, (d) 1.33, (e) 1.66. Scale bar: 3 μm (applies to all images).

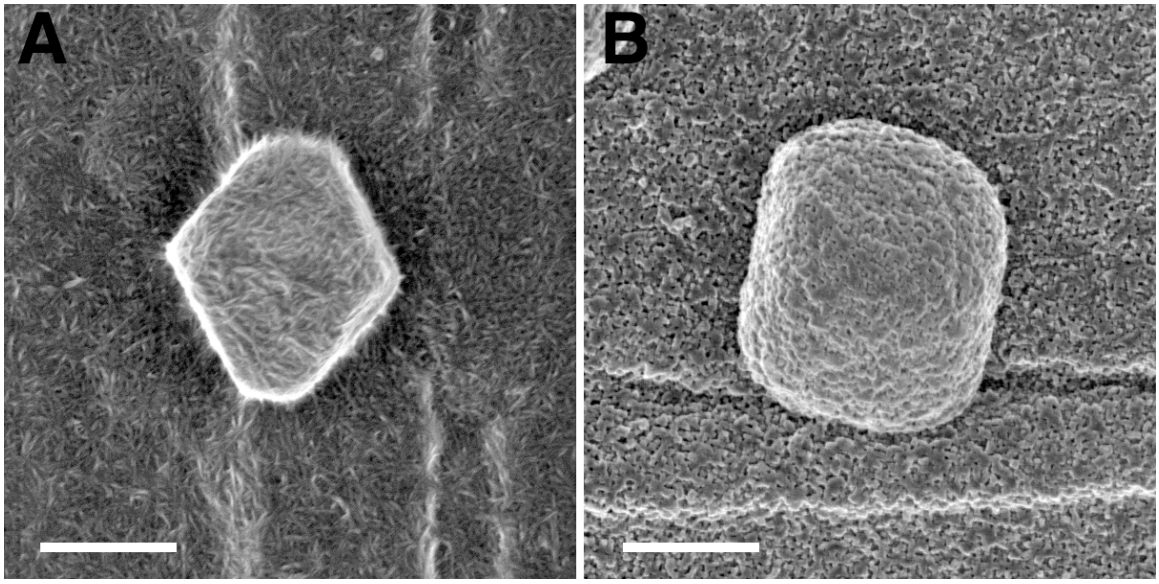

Figure 3.9. Surface morphology of PEC particles at different reaction mixture N/S ratios: (a) 0.66, (b) 1.33. (Cellulose/chitosan mass ratio: (a) 50, (b) 25). Scale bar: 1 μm.

The particle formed at an N/S ratio of 1.33 (Figure 3.9(b)), on the other hand, was coated in chitosan. The chitosan coating of the particle and the substrate indicated that at this N/S ratio, unbound chitosan was present in the reaction mixture. This is somewhat surprising as the cellulose/chitosan mass ratio at this N/S ratio was still 25, i.e. in terms of mass, there was 25 times more cellulose present in the reaction mixture than chitosan. The chitosan coating of the PEC particle was in agreement with the observed positive electrophoretic mobility at this N/S ratio (Table 3.1). The images in Figure 3.9 support the proposed mechanism of chitosan–cellulose nanocrystal complexation during type 2 titrations (Figure 3.5(b)). Figure 3.9(a) and (b) corresponds to the second and fourth stage of the sequence shown in Figure 3.5(b), respectively.

3.5. CONCLUSIONS

The formation and properties of PEC particles from chitosan and cellulose nanocrystals are governed by the strong mismatch in the densities of ionizable groups. Chitosan–cellulose nanocrystal PEC particles are composed primarily of cellulose nanocrystals. Different mixing ratios result in different particle compositions and shapes. Higher chitosan proportions during PEC formation result in spherical particles with a chitosan shell and positive net charge, whereas lower chitosan proportions result in non-spherical particles with a cellulose nanocrystal shell and negative net charge. The concentration of cellulose nanocrystals has a strong effect on PEC formation. Higher cellulose nanocrystal concentrations result in larger or more highly aggregated PEC particles. The effect of the mixing sequence on the formation of PEC particles is governed by the charge stoichiometry at a given mixing ratio.

Acknowledgement

This material is based upon work supported in part by the USDA/CSREES under Grant No. 2005-35504-16088, the National Science Foundation under Grant No. CHE-0724126, and the Institute for Critical Technology and Applied Science at Virginia Tech. Additional support from Omnova, Inc. and Tembec, Inc. is also acknowledged. Furthermore, HW thanks the staff of the Nanoscale Characterization and Fabrication Laboratory for assistance with the SEM images.

3.6. REFERENCES

Araki, J., M. Wada, S. Kuga and T. Okano (1998). "Flow properties of microcrystalline cellulose suspension prepared by acid treatment of native cellulose." Colloids and Surfaces, A: Physicochemical and Engineering Aspects **142**(1): 75–82.

ASTM (2003). "Standard test method for determining degree of deacetylation in chitosan salts by proton nuclear magnetic resonance (^{1}H NMR) spectroscopy." Annual book of ASTM standards, Designation: F2260 - 03 **13**(01): 1318–1323.

Bakeev, K. N., V. A. Izumrudov, A. B. Zezin and V. A. Kabanov (1988). "Kinetics and mechanism of reactions of the fromation of polyelectrolytic complexes." Doklady Akademii Nauk SSSR **299**(6): 1405–1408.

Berth, G. and H. Dautzenberg (2002). "The degree of acetylation of chitosans and its effect on the chain conformation in aqueous solution." Carbohydrate Polymers **47**(1): 39–51.

Berth, G., A. Voigt, H. Dautzenberg, E. Donath and H. Mohwald (2002). "Polyelectrolyte complexes and layer-by-layer capsules from chitosan/chitosan sulfate." Biomacromolecules **3**(3): 579–590.

Bhatia, S. R., S. F. Khattak and S. C. Roberts (2005). "Polyelectrolytes for cell encapsulation." Current Opinion in Colloid & Interface Science **10**(1-2): 45–51.

Brugnerotto, J., J. Desbrieres, L. Heux, K. Mazeau and M. Rinaudo (2001a). "Overview on structural characterization of chitosan molecules in relation with their behavior in solution." Macromolecular Symposia **168**(1): 1–20.

Brugnerotto, J., J. Desbrieres, G. Roberts and M. Rinaudo (2001b). "Characterization of chitosan by steric exclusion chromatography." Polymer **42**(25): 9921–9927.

Cekic, N. D., S. D. Savic, J. Milic, M. M. Savic, Z. Jovic and M. Malesevic (2007). "Preparation and characterisation of phenytoin-loaded alginate and alginate-chitosan microparticles." Drug Delivery **14**(8): 483–490.

Chellat, F., M. Tabrizian, S. Dumitriu, E. Chornet, P. Magny, C. H. Rivard and L. Yahia (2000a). "*In vitro* and *in vivo* biocompatibility of chitosan-xanthan polyionic complex." Journal of Biomedical Materials Research **51**(1): 107–116.

Chellat, F., M. Tabrizian, S. Dumitriu, E. Chornet, C.-H. Rivard and L. H. Yahia (2000b). "Study of biodegradation behavior of chitosan-xanthan microspheres in simulated physiological media." Journal of Biomedical Materials Research **53**(5): 592–599.

Chen, Y., V. J. Mohanraj, F. Wang and H. A. E. Benson (2007). "Designing chitosan-dextran sulfate nanoparticles using charge ratios." AAPS PharmSciTech **8**(4): 131–139.

Cooper, C. L., P. L. Dubin, A. B. Kayitmazer and S. Turksen (2005). "Polyelectrolyte-protein complexes." Current Opinion in Colloid & Interface Science **10**(1-2): 52–78.

Dai, Y. N., P. Li, J. P. Zhang, A. O. Wang and Q. Wei (2008). "Swelling characteristics and drug delivery properties of nifedipine-loaded pH sensitive alginate-chitosan hydrogel beads." Journal of Biomedical Materials Research Part B-Applied Biomaterials **86B**(2): 493–500.

Dai, Z. Z., J. B. Yin, S. F. Yan, T. Cao, J. Ma and X. Chen (2007). "Polyelectrolyte complexes based on chitosan and poly(L-glutamic acid)." Polymer International **56**(9): 1122–1127.

Dautzenberg, H., G. Rother and J. Hartmann (1993). Light-scattering studies of polyelectrolyte complex-formation - Effect of polymer concentration. In: Schmitz, K. S., Ed., Macroion characterization: From dilute solution to complex fluids, ACS Symposium Series 548. pp. 210–224. Washington, DC: American Chemical Society.

de Kruif, C. G., F. Weinbreck and R. de Vries (2004). "Complex coacervation of proteins and anionic polysaccharides." Current Opinion in Colloid & Interface Science **9**(5): 340–349.

de la Fuente, M., B. Seijo and M. J. Alonso (2008a). "Design of novel polysaccharidic nanostructures for gene delivery." Nanotechnology **19**(7): 1–9.

de la Fuente, M., B. Seijo and M. J. Alonso (2008b). "Novel hyaluronan-based nanocarriers for transmucosal delivery of macromolecules." Macromolecular Bioscience **8**(5): 441–450.

Drogoz, A., L. David, C. Rochas, A. Domard and T. Delair (2007). "Polyelectrolyte complexes from polysaccharides: Formation and stoichiometry monitoring." Langmuir **23**(22): 10950–10958.

Drogoz, A., S. Munier, B. Verrier, L. David, A. Dornard and T. Delair (2008). "Towards biocompatible vaccine delivery systems: Interactions of colloidal PECs based on polysaccharides with HIV-1 p24 antigen." Biomacromolecules **9**(2): 583–591.

Duarte, M. L., M. C. Ferreira, M. R. Marvao and J. Rocha (2002). "An optimised method to determine the degree of acetylation of chitin and chitosan by FTIR spectroscopy." International Journal of Biological Macromolecules **31**(1-3): 1–8.

Fleming, K., D. G. Gray and S. Matthews (2001). "Cellulose crystallites." Chemistry--A European Journal **7**(9): 1831–1835.

Gomez-Burgaz, M., B. Garcia-Ochoa and S. Torrado-Santiago (2008). "Chitosan-carboxymethylcellulose interpolymer complexes for gastric-specific delivery of clarithromycin." International Journal of Pharmaceutics **359**(1-2): 135–143.

Hajdu, I., M. Bodnar, G. Filipcsei, J. F. Hartmann, L. Daroczi, M. Zrinyi and J. Borbely (2008). "Nanoparticles prepared by self-assembly of chitosan and poly-gamma-glutamic acid." Colloid and Polymer Science **286**(3): 343–350.

Hinterstoisser, B. and L. Salmén (1999). "Two-dimensional step-scan FTIR: A tool to unravel the OH-valency-range of the spectrum of cellulose I." Cellulose **6**(3): 251–263.

Jenkins, P. and M. Snowden (1996). "Depletion flocculation in colloidal dispersions." Advances in Colloid and Interface Science **68**: 57–96.

Kondo, T. and C. Sawatari (1996). "A Fourier transform infra-red spectroscopic analysis of the character of hydrogen bonds in amorphous cellulose." Polymer **37**(3): 393–399.

Lavertu, M., Z. Xia, A. N. Serreqi, M. Berrada, A. Rodrigues, D. Wang, M. D. Buschmann and A. Gupta (2003). "A validated 1H NMR method for the determination of the degree of deacetylation of chitosan." Journal of Pharmaceutical and Biomedical Analysis **32**(6): 1149-1158.

Liu, X. D., W. T. Yu, W. Wang, Y. Xiong, X. J. Ma and Q. A. Yuan (2008a). "Polyelectrolyte microcapsules prepared by alginate and chitosan for biomedical application." Progress in Chemistry **20**(1): 126–139.

Liu, Z. G., Y. P. Jiao, F. Liu and Z. Y. Zhang (2007). "Heparin/chitosan nanoparticle carriers prepared by polyelectrolyte complexation." Journal of Biomedical Materials Research Part A **83A**(3): 806–812.

Liu, Z. H., Y. P. Jiao, Y. F. Wang, C. R. Zhou and Z. Y. Zhang (2008b). "Polysaccharides-based nanoparticles as drug delivery systems." Advanced Drug Delivery Reviews **60**(15): 1650–1662.

Marchessault, R. H. and C. Y. Liang (1960). "Infrared spectra of crystalline polysaccharides. III. Mercerized cellulose." Journal of Polymer Science **43**: 71–84.

Maréchal, Y. and H. Chanzy (2000). "The hydrogen bond network in I-beta cellulose as observed by infrared spectrometry." Journal of Molecular Structure **523**: 183–196.

Mazeau, K. and M. Rinaudo (2004). "The prediction of the characteristics of some polysaccharides from molecular modeling. Comparison with effective behavior." Food Hydrocolloids **18**(6): 885–898.

Midoux, P., G. Breuzard, J. P. Gomez and C. Pichon (2008). "Polymer-based gene delivery: A current review on the uptake and intracellular trafficking of polyplexes." Current Gene Therapy **8**(5): 335–352.

Motwani, S. K., S. Chopra, S. Talegaonkar, K. Kohl, F. J. Ahmad and R. K. Khar (2008). "Chitosan-sodium alginate nanoparticles as submicroscopic reservoirs for ocular delivery: Formulation, optimisation and *in vitro* characterisation." European Journal of Pharmaceutics and Biopharmaceutics **68**(3): 513–525.

Nikonenko, N. A., D. K. Buslov, N. I. Sushko and R. G. Zhbankov (2000). "Investigation of stretching vibrations of glycosidic linkages in disaccharides and polysaccarides with use of IR spectra deconvolution." Biopolymers **57**(4): 257–262.

Nikonenko, N. A., D. K. Buslov, N. I. Sushko and R. G. Zhbankov (2005). "Spectroscopic manifestation of stretching vibrations of glycosidic linkage in polysaccharides." Journal of Molecular Structure **752**(1-3): 20–24.

Oh, S. Y., D. I. Yoo, Y. Shin, H. C. Kim, H. Y. Kim, Y. S. Chung, W. H. Park and J. H. Youk (2005). "Crystalline structure analysis of cellulose treated with sodium hydroxide and carbon dioxide by means of X-ray diffraction and FTIR spectroscopy." Carbohydrate Research **340**(15): 2376–2391.

Okuyama, K., K. Noguchi, M. Kanenari, T. Egawa, K. Osawa and K. Ogawa (2000). "Structural diversity of chitosan and its complexes." Carbohydrate Polymers **41**(3): 237–247.

Piyakulawat, P., N. Praphairaksit, N. Chantarasiri and N. Muangsin (2007). "Preparation and evaluation of chitosan/carrageenan beads for controlled release of sodium diclofenac." AAPS PharmSciTech **8**(4): 120–130.

Rånby, B. G. (1949). "Aqueous colloidal solutions of cellulose micelles." Acta Chemica Scandinavica **3**: 649–650.

Revol, J.-F., L. Godbout, X.-M. Dong, D. G. Gray, H. Chanzy and G. Maret (1994). "Chiral nematic suspensions of cellulose crystallites; phase separation and magnetic field orientation." Liquid Crystals **16**(1): 127–134.

Revol, J. F., H. Bradford, J. Giasson, R. H. Marchessault and D. G. Gray (1992). "Helicoidal self-ordering of cellulose microfibrils in aqueous suspension." International Journal of Biological Macromolecules **14**(3): 170–172.

Rinaudo, M. (2008). "Main properties and current applications of some polysaccharides as biomaterials." Polymer International **57**(3): 397–430.

Sarmento, B., A. Ribeiro, F. Veiga and D. Ferreira (2006). "Development and characterization of new insulin containing polysaccharide nanoparticles." Colloids and Surfaces, B: Biointerfaces **53**(2): 193–202.

Sarmento, B., A. Ribeiro, F. Veiga, D. Ferreira and R. Neufeld (2007a). "Oral bioavailability of insulin contained in polysaccharide nanoparticles." Biomacromolecules **8**(10): 3054–3060.

Sarmento, B., A. Ribeiro, F. Veiga, P. Sampaio, R. Neufeld and D. Ferreira (2007b). "Alginate/chitosan nanoparticles are effective for oral insulin delivery." Pharmaceutical Research **24**(12): 2198–2206.

Sarmento, B., A. J. Ribeiro, F. Veiga, D. C. Ferreira and R. J. Neufeld (2007c). "Insulin-loaded nanoparticles are prepared by alginate ionotropic pre-gelation followed by chitosan polyelectrolyte complexation." Journal of Nanoscience and Nanotechnology **7**(8): 2833–2841.

Schatz, C., A. Domard, C. Viton, C. Pichot and T. Delair (2004a). "Versatile and efficient formation of colloids of biopolymer-based polyelectrolyte complexes." Biomacromolecules **5**(5): 1882–1892.

Schatz, C., J. M. Lucas, C. Viton, A. Domard, C. Pichot and T. Delair (2004b). "Formation and properties of positively charged colloids based on polyelectrolyte complexes of biopolymers." Langmuir **20**(18): 7766–7778.

Shybaila, T. N., T. A. Savitskaya, T. A. Kislyakova, A. I. Albulov and D. D. Grinshpan (2008). "Chitosan-cellulose sulfate acetate complexation in acetic acid solutions." Colloid Journal **70**(5): 661–665.

Sui, W., L. L. Huang, J. Wang and Q. B. Bo (2008). "Preparation and properties of chitosan chondroitin sulfate complex microcapsules." Colloids and Surfaces, B: Biointerfaces **65**(1): 69–73.

Terbojevich, M., A. Cosani, G. Conio, E. Marsano and E. Bianchi (1991). "Chitosan: Chain rigidity and mesophase formation." Carbohydrate Research **209**: 251–260.

Tsaih, M. L. and R. H. Chen (1999). "Molecular weight determination of 83% degree of decetylation chitosan with non-Gaussian and wide range distribution by high-performance size exclusion chromatography and capillary viscometry." Journal of Applied Polymer Science **71**(11): 1905–1913.

Wong, T. W. and S. Nurjaya (2008). "Drug release property of chitosan-pectinate beads and its changes under the influence of microwave." European Journal of Pharmaceutics and Biopharmaceutics **69**(1): 176–188.

Zhang, L., Y. Jin, H. Q. Liu and Y. M. Du (2001). "Structure and control release of chitosan/carboxymethyl cellulose microcapsules." Journal of Applied Polymer Science **82**(3): 584–592.

CHAPTER 4

CHITOSAN–CELLULOSE NANOCRYSTAL POLYELECTROLYTE COMPLEX—PART II: EFFECTS OF PH AND IONIC STRENGTH

4.1. ABSTRACT

This study was conducted to determine the effects of pH and ionic strength on the formation and properties of chitosan–cellulose nanocrystal polyelectrolyte complexes (PECs). The pK_a of the cellulose nanocrystals, determined indirectly by potentiometric titration, was 2.6 and the pK_b of chitosan was 6.4. PEC formation at different pH values and ionic strengths was studied by turbidimetric titration. In titrations of a chitosan solution with a cellulose nanocrystal suspension (type 1), the maximum turbidity was reached at an SO_3^-/NH_3^+ ratio of 0.45 ± 0.12. In titrations of the reverse direction, the turbidity maximum occurred at an NH_3^+/SO_3^- ratio of 1.22 ± 0.13. The turbidity of a PEC particle suspension increased strongly upon lowering the pH from 2.6 and decreased upon raising the pH above 5.5, which was attributed to a swelling and shrinking of the PEC particles, respectively. In type 1 titrations, an increase in ionic strength caused the maximum turbidity to be reached at higher sulfate/amino group molar ratios. The turbidity of a PEC particle suspension decreased upon raising the ionic strength from 0 to 0.5 M, which was attributed to a shrinking of the particles. A decrease in particle size with increasing pH and ionic strength was confirmed by scanning electron microscopy. The effect of pH was based on its influence on the degree of ionization and, thus, charge density of the PEC components. Formation of PEC particles at higher ionic strengths was less kinetically controlled and resulted in particles with closer-to-equilibrium structures.

4.2. INTRODUCTION

Upon mixing, polyelectrolytes of opposite charge form polyelectrolyte complexes (PECs) under release of the counter ions. The properties of PECs depend on a number of factors, primarily the molecular weights and densities of ionizable groups of the two polyelectrolytes, the polyelectrolyte concentrations upon mixing, the mixing ratio, and the pH and ionic strength of the surrounding medium. The effect of pH is primarily related to its effect on the degree of ionization, and thus charge density, of the polyelectrolytes. As the pH approaches or drops below the pK_a of the poly-acid, the acidic groups gradually become protonated and loose their negative charge. Accordingly, as the pH approaches or rises above the pK_b of the poly-base, the basic groups gradually become deprotonated and loose their positive charge.

The effects of charge density on the formation, structure, and composition of PECs have been studied by several groups (Dautzenberg *et al.*, 1982; Koetz *et al.*, 1986; Vishalakshi *et al.*, 1993; Hugerth *et al.*, 1997; Dautzenberg and Jaeger, 2002; Shovsky *et al.*, 2009a; Shovsky *et al.*, 2009b). The results indicate that densely structured PECs are formed when the charge densities of the two polyelectrolytes are similar whereas highly swellable PECs with lower structural densities are formed in the case of a mismatch in the charge densities of the polyelectrolytes (Dautzenberg *et al.*, 1996; Dautzenberg and Jaeger, 2002). These findings are in agreement with the results of numerous studies on the pH-sensitive swelling behavior of PECs (Sakiyama *et al.*, 1993; Chu *et al.*, 1995; Ikeda *et al.*, 1995; Chu *et al.*, 1996; Kumagai *et al.*, 1996; Yao *et al.*, 1997; Sakiyama *et al.*, 1999; Sui *et al.*, 2006).

The effects of ionic strength on the formation and stability of PECs have been studied extensively (Cundall *et al.*, 1979; Izumrudov *et al.*, 1980; Kabanov *et al.*, 1982; Zezin and Kabanov, 1982; Bakeev *et al.*, 1988; Pergushov *et al.*, 1993; Trinh and Schnabel, 1993; Pergushov *et al.*, 1995; Dautzenberg, 1997; Dautzenberg and Karibyants, 1999; Nordmeier and Beyer, 1999; Dragan and Cristea, 2001; Chen *et al.*, 2003; de Vasconcelos *et al.*, 2006; Kovacevic *et al.*, 2007; Vasheghani *et al.*, 2008). Salt effects are based on the ability of the salt ions to screen the Coulomb interactions between the polyelectrolytes. Small amounts of salt, present during the formation of the

PECs, enable rearrangement processes toward a state of thermodynamic equilibrium (Bakeev *et al.*, 1988). Addition of small amounts of salt subsequent to PEC formation causes the PECs to shrink due to charge screening. Higher salt levels may cause rearrangement and flocculation of the PECs through secondary aggregation (Dautzenberg and Karibyants, 1999). Depending on the types of ionizable groups present in the polyelectrolytes, yet higher ionic strengths may lead to the dissociation of the PECs (Izumrudov *et al.*, 1980; Pergushov *et al.*, 1993; Nordmeier and Beyer, 1999).

In Chapter 3, we have reported a new type of PEC consisting of chitosan, a positively charged polysaccharide, and cellulose nanocrystals, negatively charged, rod-like nanoparticles. The formation and properties of these PECs were governed by the strong mismatch in density of the ionizable groups. The size, shape, and net charge of the PEC particles depended strongly on the mixing ratio during PEC formation. This study is a continuation of the previous work with the aim to deepen our understanding of the factors that affect the complexation of chitosan and cellulose nanocrystals. The specific objectives of this study were to determine the effects of the pH and ionic strength of the surrounding medium on the formation and properties of chitosan–cellulose nanocrystal PEC particles.

4.3. MATERIALS AND METHODS

4.3.1. Materials

Chitosan (medium molecular weight, Fluka BioChemika) was purchased from Sigma-Aldrich and purified as follows. Typically, 1 g of chitosan was dissolved overnight in 250 mL 0.1 N HCl and the solution was filtered through a series of Millipore polyvinylidene fluoride (PVDF) syringe filters (pore sizes 1, 0.45, and 0.22 μm). Next, chitosan was precipitated by addition of 1 N NaOH until the solution pH reached 9–10. The purified chitosan was collected by centrifugation (4900 rpm for 15 min at 4 °C), washed three times with deionized water, and freeze-dried overnight. The purified chitosan was characterized as described in Chapter 3. The molecular weight and degree of deacetylation were 3.1×10^6 Dalton and 87.8%, respectively. The amino group density was 5.83 mol/kg.

Cellulose nanocrystals were prepared and characterized as described in Chapter 3. Briefly, 50 g ground (60-mesh) dissolving-grade softwood sulfite pulp (Temalfa 93 A-A), kindly provided by Tembec, Inc., was treated with 500 mL 64 wt % H_2SO_4 at 45 °C for 45 min. The hydrolysis was stopped by 10-fold dilution of the reaction medium with deionized water. The cellulose nanocrystals were collected by centrifugation and dialyzed against deionized water until the pH of the dialysis water stayed constant. The obtained suspension was sonicated under ice-bath cooling and subsequently filtered through a 0.45 μm and then 0.22 μm PVDF syringe filter. The concentration of the filtered cellulose nanocrystal stock suspension was generally in the range of 0.6–0.9% (w/v). The cellulose nanocrystals had a sulfate group density of 0.18 mmol/kg.

H_2SO_4 (>95%), HCl (0.1 N and 5 N, certified), NaOH (0.1 N and 1 N, certified), and NaCl (certified) were purchased from Fisher Scientific. The water used in the experiments was deionized water from a Millipore Direct-Q 5 Ultrapure Water System (resistivity at 25 °C: 18.2 MΩ·cm).

4.3.2. Preparation of Chitosan Solutions

Chitosan solutions for the complexation experiments were prepared from a stock solution of ~0.1% (w/v) by dilution with deionized water. For preparation of the stock solution, purified chitosan was dried in an oven at 105 °C for 2 h. Then, 0.1 g of the oven-dried, purified chitosan was dissolved in 100 mL 0.1 N HCl. The exact concentration of the stock solution was determined in triplicate by thermogravimetric analysis as described in Chapter 3. The pH and ionic strength of the dilute chitosan solutions were adjusted with 0.1 N HCl or 0.1 N NaOH and NaCl, respectively.

4.3.3. Preparation of Cellulose Nanocrystal Suspensions

Dilute cellulose nanocrystal suspensions for the complexation experiments were prepared from the filtered stock suspension by dilution with deionized water. The pH and ionic strength of the dilute cellulose nanocrystal suspensions were adjusted with 0.1 N HCl or 0.1 N NaOH and NaCl, respectively.

4.3.4. Potentiometric Titration

Potentiometric titration curves were measured in triplicate using a Mettler Toledo SevenMulti S47 pH/conductivity meter with an InLab 413 pH electrode. In the case of cellulose nanocrystals, titrations were carried out with 25–50 mL aliquots of the filtered stock suspension, adjusted to an ionic strength of 1 mM through addition of NaCl. In the case of chitosan, the titrand was 100 mL of a 0.1% (w/v) solution of chitosan in 0.025 N HCl with an ionic strength of 0.1 M. The titrant, 0.02 N NaOH, prepared by dilution of 0.1 N NaOH with deionized water, was added under nitrogen and stirring in 0.5 mL increments. After each addition, the pH of the titrand was recorded.

4.3.5. Turbidimetric Titration

Turbidimetric titrations were performed with a 0.001% (w/v) chitosan solution and a 0.02% (w/v) cellulose nanocrystal suspension, both having the same pH and ionic strength. The concentrations were chosen based on the results reported in the preceding chapter. In a turbidimetric titration experiment, the cellulose nanocrystal suspension was added drop-wise under vigorous stirring with a magnetic bar to the chitosan solution or vice versa. The transmittance of the reaction mixture was monitored with a probe colorimeter (PC 950, Brinkman, USA) with a 1 cm optical cell (2 cm path length), operating at a wavelength of 420 nm. Turbidity values were calculated as 100 – transmittance (%). Prior to each titration, the probe colorimeter was zeroed in deionized water. Each experiment was performed in triplicate.

4.3.6. Characterization of PEC Particles

The morphology of the PEC particles was analyzed by field emission scanning electron microscopy (FE-SEM). Images were recorded with a LEO 1550 FE-SEM using an accelerating voltage of 1 kV and a working distance of 4–5 mm. Particles for SEM imaging were prepared at an amino/sulfate group molar ratio (N/S ratio) of unity by mixing under vigorous stirring with a magnetic bar the appropriate amounts of a 0.001% (w/v) chitosan solution and a 0.02% (w/v) cellulose nanocrystal suspension, both having a pH of 2.6 and an ionic strength of 1 mM. The pH and ionic strength of the PEC particle suspensions were subsequently adjusted with 0.1 N HCl or 0.1 N NaOH and 5 M NaCl, respectively, and the particles were allowed to equilibrate for a minimum of 10 min. For SEM sample preparation, a 10 μL drop of the suspension was deposited onto Ni–Cu conductive tape (Ted Pella) mounted onto a standard SEM stub (Ted Pella) and allowed to dry under ambient conditions. For the highly acidic sample (pH 1), a spherical piece of gold foil was used as the substrate instead of the Ni–Cu tape, because with the Ni–Cu tape, $NiCl_2$ formation interfered with the analysis. Prior to imaging, the SEM samples were coated with a thin (6 nm) layer of carbon.

4.4. RESULTS AND DISCUSSION

4.4.1. Effect of pH

The effect of pH on the complexation of chitosan and cellulose nanocrystals was studied by turbidimetric titration. Figure 4.1 shows the turbidimetric titration curves for the titration of a 0.001% (w/v) chitosan solution with a 0.02% (w/v) cellulose nanocrystal suspension (type 1) and the inverse titration (type 2) for different pH values and an ionic strength of 1 mM. In accordance with the results presented in the preceding chapter, in the type 1 titrations, the turbidity of the reaction mixture asymptotically approached a maximum value with increasing sulfate/amino group molar ratio (S/N ratio) (Figure 4.1(a)), whereas the turbidity reached a maximum and then decreased with increasing N/S ratio in type 2 titrations (Figure 4.1(b)). For both methods, an increase in pH from 2.6 to 5.6 resulted in a decrease in maximum turbidity. Furthermore, in type 2 titrations, an increase in pH caused a shift of the turbidity maximum to higher N/S ratios.

The turbidity of a colloidal dispersion is a complicated function of the number density, i.e. the number per unit volume, size, and optical properties of the light-scattering bodies. In the system studied here, the number density and size of the light-scattering PEC particles are inversely related. Furthermore, the optical properties of the PEC particles depend on the optical properties of the two components and the particle composition. The particle composition, in turn, depends on the charge stoichiometry in the reaction mixture, which is governed by the mass ratio of the two components, their ionizable group density, and their degree of ionization, i.e. the fraction of ionizable groups ionized. To better understand the composition of the PEC particles, we determined the degrees of ionization of the two components at the four pH values investigated.

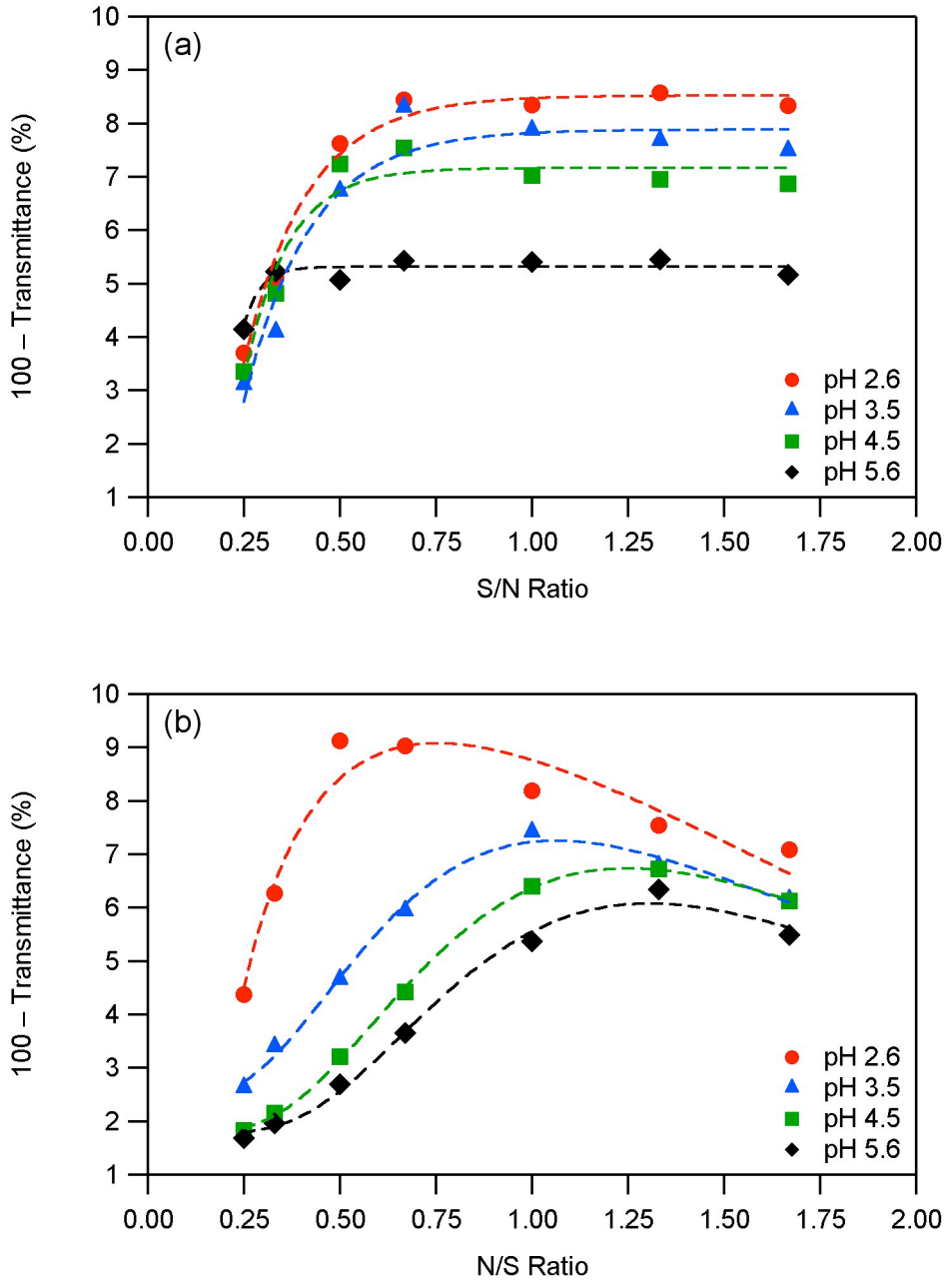

Figure 4.1. Turbidimetric titration curves for (a) the titration of a chitosan solution with a cellulose nanocrystal suspension (type 1) and (b) the reverse direction (type 2) for different pH values and an ionic strength of 1 mM. (Data points are means of three measurements. Error bars are omitted for clarity.)

For basic groups, the degree of ionization, α_b, is related to the pH by

$$pH = pK_b - \log\left(\frac{\alpha_b}{1 - \alpha_b}\right) \quad [4.1]$$

where pK_b is the dissociation constant of the basic groups. For acidic groups, the degree of ionization, α_a, is related to the pH by

$$pH = pK_a + \log\left(\frac{\alpha_a}{1 - \alpha_a}\right) \quad [4.2]$$

where pK_a is the dissociation constant of the acidic groups. The pK_b of chitosan was measured by potentiometric titration. A typical potentiometric titration curve for chitosan is shown in Figure 4.2. The obtained pK_b, given by the pH at the halfway point between the two equivalence points, was 6.40 ± 0.03, in good agreement with the literature (Hejazi and Amiji, 2002).

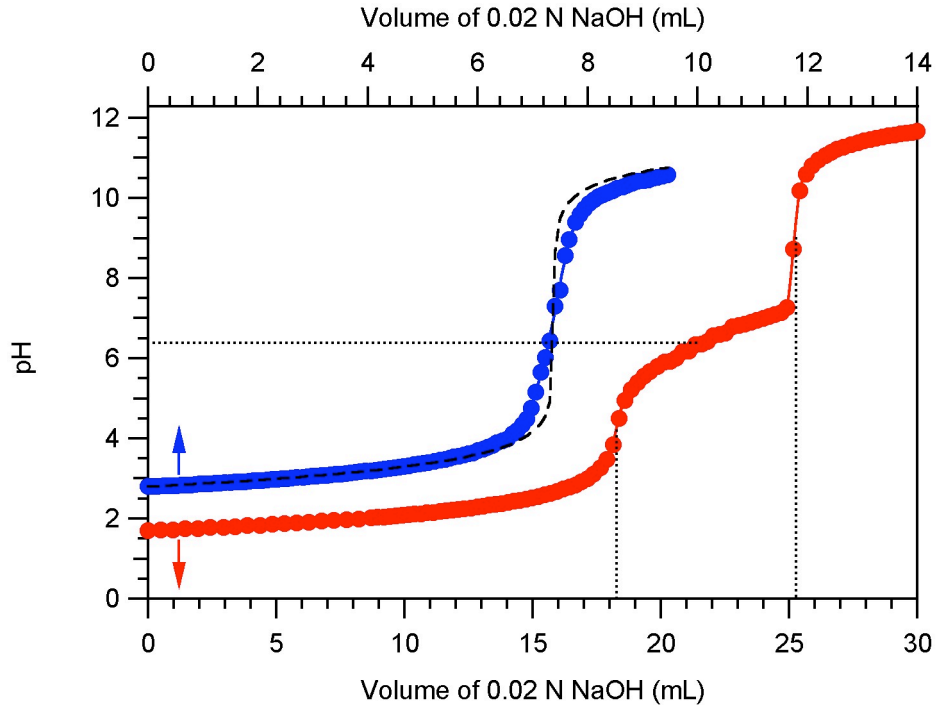

Figure 4.2. Potentiometric titration curves for chitosan (●) and cellulose nanocrystals (●).

Determination of the pK_a of the cellulose nanocrystals was more difficult because of their low sulfate group density (0.18 mol/kg). A titration simulation assuming a pK_a of 2.6 for the sulfate groups showed that a barely measurable equivalence point for the onset of sulfate group dissociation would require 14 g of cellulose nanocrystals suspended in 25 mL 0.1 N HCl to be titrated with 2 N NaOH. In lack of a practical method for measuring the pK_a of the sulfate groups directly, we used the approach of Ikeda et al. (1995) to determine the degree of ionization of the sulfate groups at different pH values from the charge balance. The degree of ionization of the sulfate groups, α_a, for a direct titration of an aqueous cellulose nanocrystal suspension, containing dissolved CO_2, with NaOH can be expressed as

$$\alpha_a = \frac{[H^+] + \frac{C \cdot V}{V_0 + V} - \frac{K_W}{[H^+]} - \frac{\alpha_{CO_2} \cdot C_{CO_2} \cdot V_0}{V_0 + V}}{\frac{C_a \cdot V_0}{V_0 + V}} \qquad [4.3]$$

where $[H^+]$ is the concentration of hydrogen ions; C, the concentration of the titrant; V, the volume of the titrant added; V_0, the initial volume of the titrand; K_W, the ionic product of water; C_a, the initial concentration of sulfate groups, C_{CO_2}, the initial concentration of dissolved CO_2; and α_{CO_2}, the fraction of CO_2 molecules present as HCO_3^-. α_{CO_2} is given by $(([H^+]/K_{a,CO_2})+1)^{-1}$, where K_{a,CO_2} is the dissociation constant for the reaction $CO_2 + H_2O \rightleftharpoons HCO_3^- + H^+$, taken as 6.352 (Harned and Scholes, 1941). The reaction $HCO_3^- \rightleftharpoons CO_3^{2-} + H^+$ has been disregarded because it occurs at pH levels outside the relevant range.

A typical potentiometric titration curve for cellulose nanocrystals is shown in Figure 4.2. The equivalence point corresponds to the completion of the dissociation of sulfate groups. The dashed line indicates the hypothetical shape of the titration curve in the absence of dissolved CO_2. Figure 4.3 shows the degree of ionization values obtained with eq 4.3 from the titration data. The plotted values assume a dissolved CO_2 concentration of 4% of the total initial concentration of anion forming species. The dashed line in Figure 4.3 shows the degree of ionization curve obtained with eq. 4.2. The best fit with the measured data was obtained for a pK_a of 2.6.

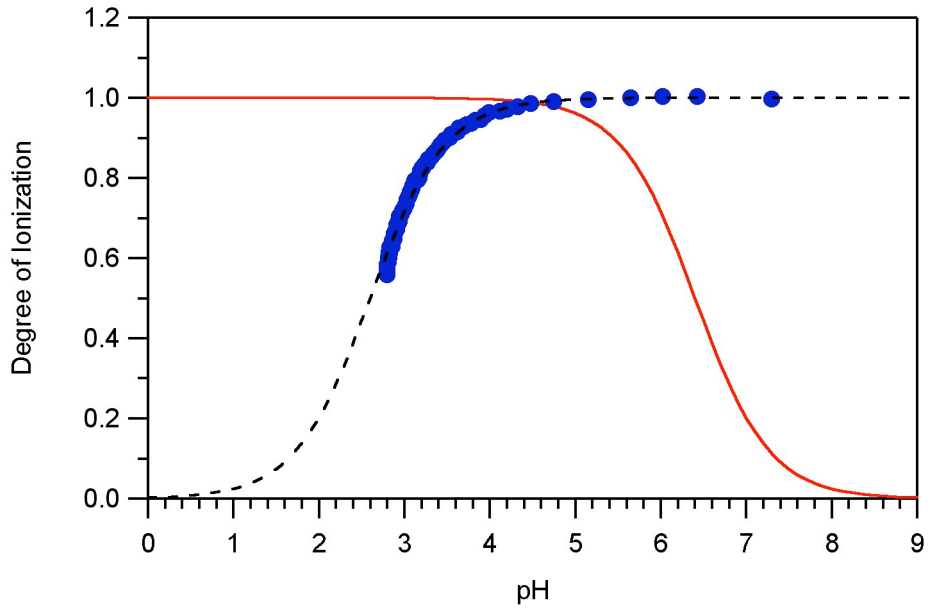

Figure 4.3. Degree of ionization as a function of pH for chitosan (α_b) and cellulose nanocrystals (α_a): — α_b for pK_b = 6.4 (measured), ● experimental α_a values, – – α_a for pK_a = 2.6 (best fit).

Also shown in Figure 4.3 is the degree of ionization curve for chitosan obtained with eq. 4.1 and the measured pK_b of 6.40. It is apparent in Figure 4.3 that the pH range in which both components are completely ionized is narrow and centered at 4.5. At higher pH values, chitosan is incompletely ionized, and at lower pH values, the cellulose nanocrystals loose their charge. The degrees of ionization of the two components for the investigated pH values are listed in Table 4.1. As seen in Table 4.1, with increasing pH, the degree of ionization of the amino groups decreased and that of the sulfate groups increased, causing a decrease in NH_3^+/SO_3^- charge ratio at any given N/S ratio. Consequently, at higher pH values, an NH_3^+/SO_3^- charge ratio of unity required a higher N/S ratio. As the NH_3^+/SO_3^- charge ratio increased, the cellulose/chitosan mass ratio for an NH_3^+/SO_3^- charge ratio of unity decreased from 66 at a pH of 2.6 to 28 at a pH of 5.6.

Table 4.1. Degrees of ionization of the chitosan amino groups, α_b, and the cellulose nanocrystal sulfate groups, α_a; NH_3^+/SO_3^- charge ratio in the reaction mixture at an N/S ratio of unity; and cellulose/chitosan mass ratio in the reaction mixture at an NH_3^+/SO_3^- ratio of unity, at the four pH values investigated

pH	α_b	α_a	NH_3^+/SO_3^- at N/S = 1	cellulose/chitosan mass ratio at NH_3^+/SO_3^- = 1
2.6	1.00	0.50	2.00	66
3.5	1.00	0.89	1.12	37
4.5	0.99	0.99	1.00	33
5.6	0.86	1.00	0.86	28

The decrease in maximum turbidity in the turbidimetric titration curves (Figure 4.1) with increasing pH was therefore attributed to the decrease in NH_3^+/SO_3^- charge ratio of the two components, requiring fewer cellulose nanocrystals at higher pH values to compensate the charge of chitosan. The decrease in NH_3^+/SO_3^- charge ratio with increasing pH was also considered the reason for the shift of the turbidity maximum to higher N/S ratios in the type 2 titrations. The curve maxima at pH 2.6, 3.5, 4.5, and 5.6 occurred at N/S ratios of 0.7, 1.0, 1.2, and 1.3, respectively, corresponding to an NH_3^+/SO_3^- charge ratio of 1.22 ± 0.13. In the type 1 titrations (Figure 4.1(a)), the maximum turbidity levels at pH 2.6, 3.5, 4.5, and 5.6 were reached at S/N ratios of 0.3, 0.5, 0.7, and 0.7, corresponding to an SO_3^-/NH_3^+ charge ratio of 0.45 ± 0.12.

To further elucidate the effect of pH on chitosan–cellulose nanocrystal complexes, we studied the turbidity of a reaction mixture with an N/S ratio of unity as a function of pH. The initial pH and ionic strength of the reaction mixture were 2.6 and 1 mM, respectively. The turbidity of the reaction mixture was monitored upon addition of 0.1 N NaOH or 5 N HCl. Figure 4.4 shows the changes in turbidity of the reaction mixture with increasing or decreasing pH, with respect to the starting pH of 2.6.

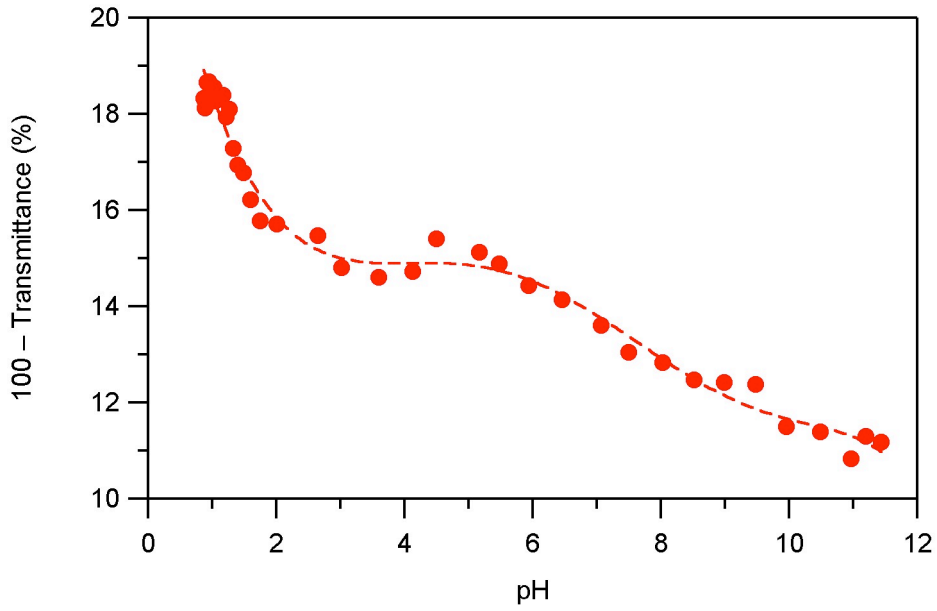

Figure 4.4. Turbidity of a PEC particle suspension of an ionic strength of 1 mM and an N/S ratio of unity as a function of pH.

Lowering of the reaction mixture's pH from 2.6 to 0.9 caused a strong increase in turbidity. According to Figure 4.3, the decrease in pH from 2.6 to 0.9 resulted in a decrease in the degree of ionization of the cellulose nanocrystals from 0.50 to 0.02 whereas the degree of ionization of chitosan stayed constant and had a value of unity. The observed increase in turbidity was attributed to an increase in the size of the PEC particles with decreasing SO_3^-/NH_3^+ charge ratio, as more and more cellulose nanocrystals were needed to compensate the charge of a given number of ammonium groups. In addition, the chitosan chains may partially uncoil as some of the ammonium groups along the chitosan backbone loose their counter ion (SO_3^-). Raising the reaction mixture's pH from 2.6 to 11.4 caused initially no change in turbidity and then a decrease above a pH value of about 5.5. At pH 5.5, the cellulose nanocrystals had a degree of ionization of unity and chitosan had a degree of ionization of 0.89. The degree of ionization of chitosan reached a value of zero at a pH of about 9. The observed decrease in turbidity was attributed to a decrease in the size of the PEC particles. As the chitosan degree of ionization decreased, the PEC particles may have partially dissociated and rearranged into smaller particles with a higher chitosan/cellulose mass ratio. Furthermore,

the decrease in chitosan charge density may have caused the chitosan molecules to form tighter coils and precipitate. The observed decrease in PEC particle size with increasing pH above 5.5 was in agreement with the results of López-León *et al.* (2005) who observed a decrease in mean particle diameter for a pH increase from 4 to 7 in suspensions of chitosan–tripolyphosphate nanoparticles.

The morphology of chitosan–cellulose nanocrystal PEC particles equilibrated at different pH values were analyzed by FE-SEM. Figure 4.5 shows SEM images of particles equilibrated at a pH of 1.0, 4.5, 6.5, 7.5, and 9.0. At all pH values, the particles were roughly spherical in shape. The SEM images confirmed a decrease in particle size with increasing pH.

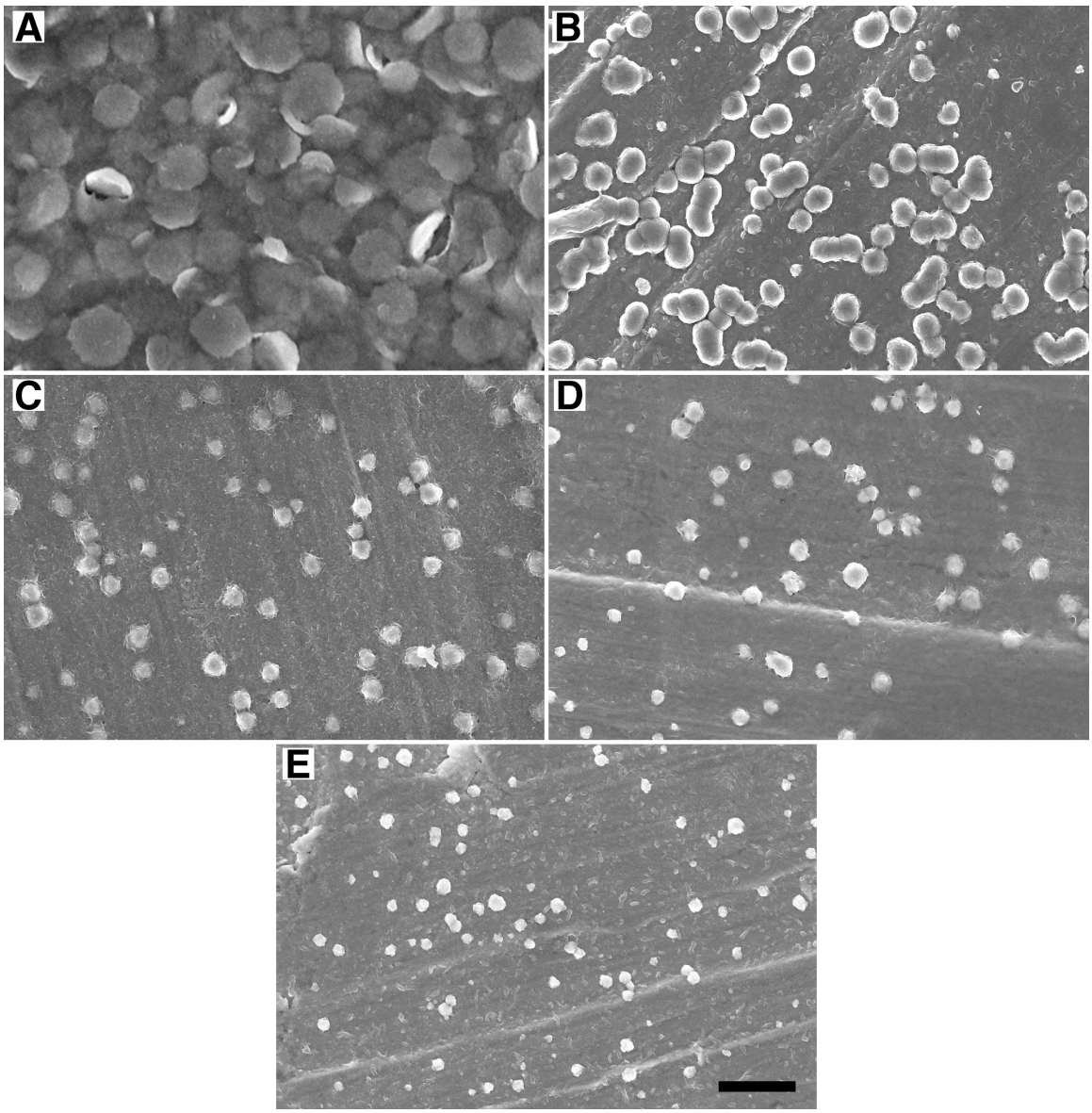

Figure 4.5. FE-SEM images of PEC particles equilibrated at different pH values: (a) 1.0, (b) 4.5, (c) 6.5, (d) 7.5, (e) 9.0. Scale bar: 1 μm (applies to all images).

4.4.2. Effect of Ionic Strength

Figure 4.6 shows the turbidimetric titration curves for the addition of a 0.02% (w/v) cellulose nanocrystal suspension to a 0.001% (w/v) chitosan solution for a pH of 2.6 and different ionic strengths. The maximum turbidity observed in the presence of electrolyte

was slightly lower than that observed in the absence of electrolyte. Furthermore, in the absence of electrolyte, the maximum turbidity was reached at an S/N ratio of 0.5, whereas at ionic strengths of 0.1 M and 0.4 M, the maximum turbidity was reached at S/N ratios of 0.75 and unity, respectively. In other words, at S/N ratios below unity a higher ionic strength resulted in a lower turbidity. As mentioned earlier, small amounts of salt, present during the formation of PECs, have been shown to enable rearrangement processes toward a state of thermodynamic equilibrium (Bakeev *et al.*, 1988). The lower turbidity values observed at higher ionic strengths might therefore indicate smaller PEC particles with closer-to-equilibrium structures.

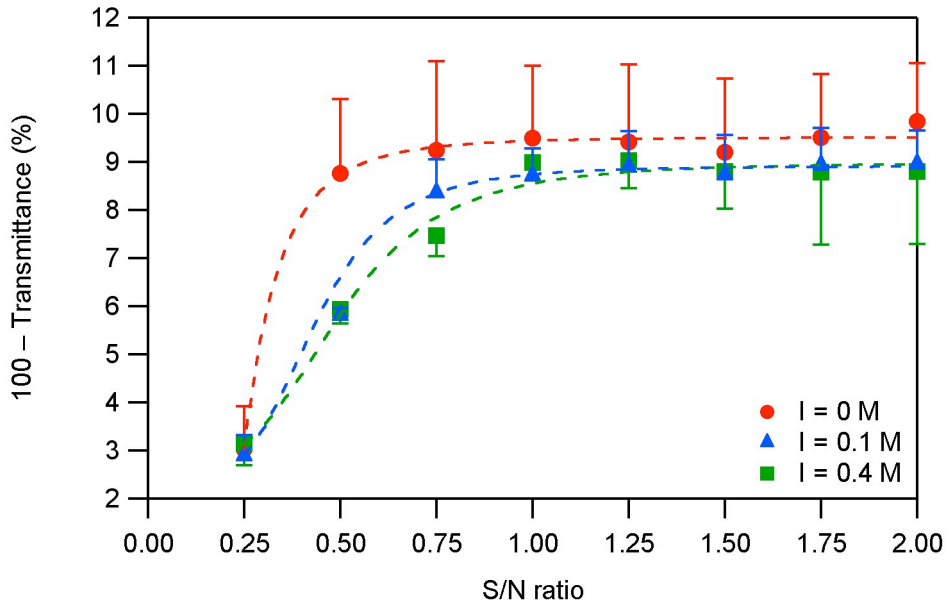

Figure 4.6. Turbidimetric titration curves for the addition of a cellulose nanocrystal suspension to a chitosan solution for different ionic strengths and a pH of 2.6. (Data points are means of three measurements. Error bars represent one standard deviation.)

Figure 4.7 shows the turbidity of a reaction mixture with an N/S ratio of unity as a function of ionic strength. The initial pH and ionic strength of the reaction mixture were 2.6 and 1 mM, respectively. The ionic strength of six aliquots of the reaction mixture was adjusted to different values through addition of 5 M NaCl and the turbidity of each

aliquot was determined after a short equilibration period (3 min). The turbidity decreased with increasing ionic strength up to an ionic strength of 0.1 M. Upon further increase of the ionic strength, the turbidity leveled off and asymptotically approached a minimum turbidity level.

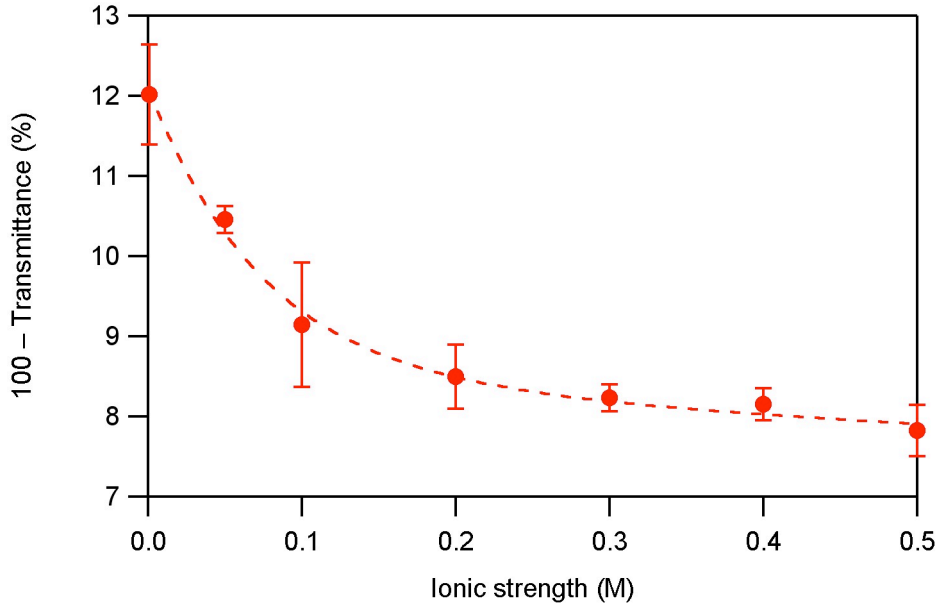

Figure 4.7. Turbidity of a PEC particle suspension of pH 2.6 and a reaction mixture N/S ratio of unity as a function of ionic strength. (Data points are means of three measurements. Error bars represent ± one standard deviation.)

The observed changes in turbidity with ionic strength are in accordance with the observed maximum turbidity levels in the turbidimetric titrations (Figure 4.6). The maximum turbidity in the titrations decreased with an increase in ionic strength from 0 to 0.1 M and stayed constant with an increase from 0.1 to 0.4 M. As shown above, at a pH of 2.6, only 50% of the sulfate groups on the cellulose nanocrystals are charged. Consequently, an N/S ratio of unity represents an NH_3^+/SO_3^-charge ratio of 2 and therefore an excess of chitosan ammonium groups. A low-molecular-weight electrolyte will partially screen the excess charge and enable the chitosan molecules to take on a more tightly coiled conformation, resulting in a shrinking of the particles.

The size and morphology of chitosan–cellulose nanocrystal PEC particles equilibrated at different ionic strengths were analyzed by FE-SEM. Figure 4.8 shows SEM images of particles equilibrated at an ionic strength of 0.001, 0.005, 0.1, and 0.5 M. The SEM images confirm that the particle size decreased with increasing ionic strength and that the decrease was more pronounced at lower ionic strengths.

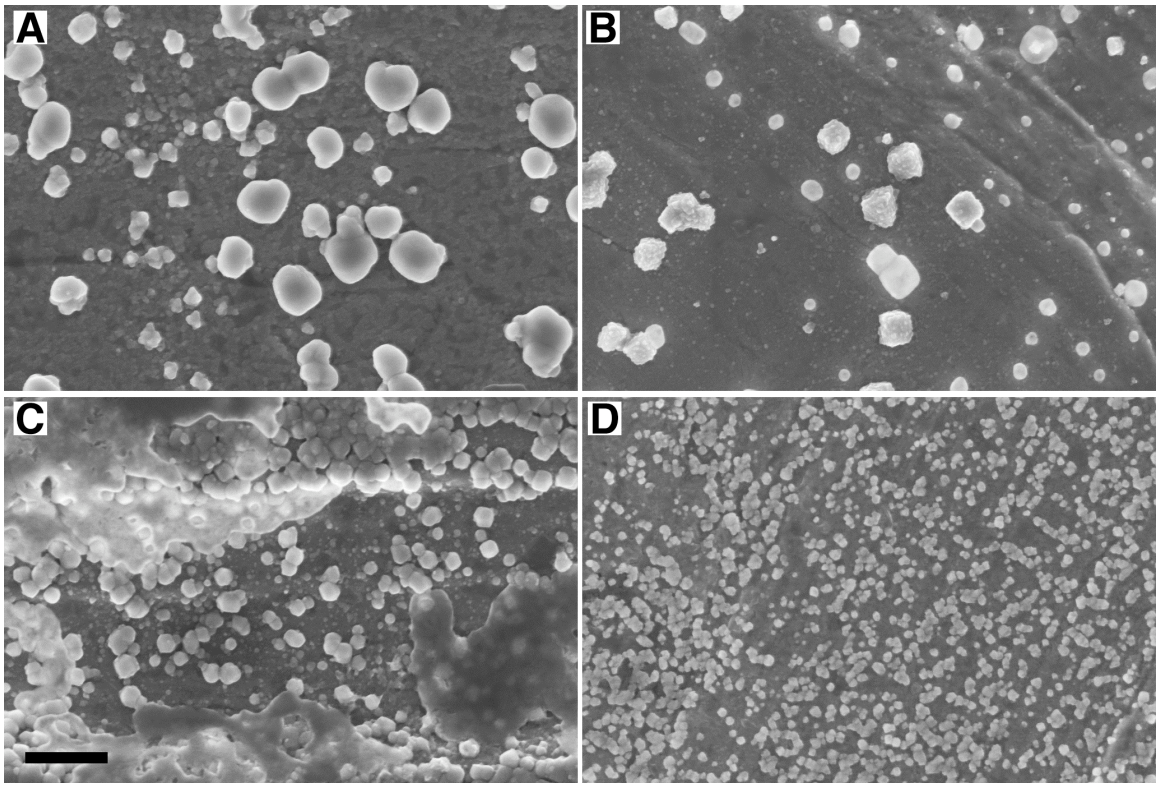

Figure 4.8. FE-SEM images of PEC particles equilibrated at different ionic strengths: (a) 1 mM, (b) 5 mM, (c) 100 mM, (d) 500 mM. Scale bar: 500 nm (applies to all images).

4.5. CONCLUSIONS

The pH strongly affects the formation and properties of chitosan–cellulose nanocrystal PEC particles. The effect of the pH is based on its influence on the degree of ionization and, thus, charge density of the PEC components. A decrease in pH below a certain value causes swelling of the PEC particles due to a decrease in the charge density of the cellulose nanocrystals. An increase in pH above a certain value causes shrinking of the PEC particles due to a decrease in the charge density of chitosan. At levels within the range of this study, the ionic strength has a minor effect on the formation and properties of chitosan–cellulose nanocrystal PEC particles. An increase in ionic strength causes shrinking of the PEC particles due to charge screening. Formation of PEC particles at higher ionic strengths is less kinetically controlled and results in particles with closer-to-equilibrium structures.

Acknowledgement

This material is based upon work supported in part by the USDA/CSREES under Grant No. 2005-35504-16088, the National Science Foundation under Grant No. CHE-0724126, and the Institute for Critical Technology and Applied Science at Virginia Tech. Additional support from Omnova, Inc. and Tembec, Inc. is also acknowledged. Furthermore, HW thanks the staff of the Nanoscale Characterization and Fabrication Laboratory for assistance with the SEM images.

4.6. REFERENCES

Bakeev, K. N., V. A. Izumrudov, A. B. Zezin and V. A. Kabanov (1988). "Kinetics and mechanism of reactions of the fromation of polyelectrolytic complexes." Doklady Akademii Nauk SSSR **299**(6): 1405–1408.

Chen, J. H., J. A. Heitmann and M. A. Hubbe (2003). "Dependency of polyelectrolyte complex stoichiometry on the order of addition. 1. Effect of salt concentration during streaming current titrations with strong poly-acid and polybase." Colloids and Surfaces, A: Physicochemical and Engineering Aspects **223**(1-3): 215–230.

Chu, C. H., H. Kumagai, T. Sakiyama, S. Ikeda and K. Nakamura (1996). "Development of a model for analyzing the swelling rate of ionic gels on the basis of the diffusion of mobile ions: Application to the pH-sensitive swelling of a polyelectrolyte complex gel prepared from xanthan and chitosan." Bioscience Biotechnology and Biochemistry **60**(10): 1627–1632.

Chu, C. H., T. Sakiyama and T. Yano (1995). "pH-sensitive swelling of a polyelectrolyte complex gel prepared from xanthan and chitosan." Bioscience Biotechnology and Biochemistry **59**(4): 717–719.

Cundall, R. B., J. B. Lawton, D. Murray and G. O. Phillips (1979). "Polyelectrolyte complexes. 1. Effect of pH and ionic-strength on the stoichiometry of model polycation-polyanion complexes." Makromolekulare Chemie-Macromolecular Chemistry and Physics **180**(12): 2913–2922.

Dautzenberg, H. (1997). "Polyelectrolyte complex formation in highly aggregating systems. 1. Effect of salt: polyelectrolyte complex formation in the presence of NaCl." Macromolecules **30**(25): 7810–7815.

Dautzenberg, H., J. Hartmann, S. Grunewald and F. Brand (1996). "Stoichiometry and structure of polyelectrolyte complex particles in diluted solution." Berichte der Bunsen-Gesellschaft fuer Physikalische Chemie **100**(6): 1024–1032.

Dautzenberg, H. and W. Jaeger (2002). "Effect of charge density on the formation and salt stability of polyelectrolyte complexes." Macromolecular Chemistry and Physics **203**(14): 2095–2102.

Dautzenberg, H. and N. Karibyants (1999). "Polyelectrolyte complex formation in highly aggregating systems. Effect of salt: Response to subsequent addition of NaCl." Macromolecular Chemistry and Physics **200**(1): 118–125.

Dautzenberg, H., K. J. Linow and B. Philipp (1982). "The formation of water-soluble polysalts (simplexes) of anionic and cationic co-polymers of acrylamide. 2. Effect of charge-density and conversion on the structure of the simplexes." Acta Polymerica **33**(11): 619–625.

de Vasconcelos, C. L., P. M. Bezerril, D. E. S. dos Santos, T. N. C. Dantas, M. R. Pereira and J. L. C. Fonseca (2006). "Effect of molecular weight and ionic strength on the formation of polyelectrolyte complexes based on poly(methacrylic acid) and chitosan." Biomacromolecules **7**(4): 1245–1252.

Dragan, S. and M. Cristea (2001). "Influence of low-molecular-weight salts on the formation of polyelectrolyte complexes based on polycations with quaternary ammonium salt groups in the main chain and poly(sodium acrylate)." European Polymer Journal **37**(8): 1571–1575.

Harned, H. S. and S. R. Scholes, Jr. (1941). "The ionization constant of HCO_3^- from 0º to 50º." Journal of the American Chemical Society **63**: 1706–1709.

Hejazi, R. and M. Amiji (2002). Chitosan-based delivery system: Physicochemical properties and pharmaceutical applications. In: Dumitriu, S., Ed., Polymeric Biomaterials. 2nd ed., pp. 213–238. New York: Macel Dekker.

Hugerth, A., N. Caram-Lelham and L. O. Sundelöf (1997). "The effect of charge density and conformation on the polyelectrolyte complex formation between carrageenan and chitosan." Carbohydrate Polymers **34**(3): 149–156.

Ikeda, S., H. Kumagai, T. Sakiyama, C. H. Chu and K. Nakamura (1995). "Method for analyzing pH-sensitive swelling of amphoteric hydrogels - Application to a

polyelectrolyte complex gel prepared from xanthan and chitosan." Bioscience Biotechnology and Biochemistry **59**(8): 1422–1427.

Izumrudov, V. A., O. A. Kharenko, A. V. Kharenko, Z. G. Gulyaeva, V. A. Kasaikin, A. B. Zezin and V. A. Kabanov (1980). "Behavior of nonstoichiometric poly-electrolyte complexes in aqueous salt solutions." Vysokomolekulyarnye Soedineniya Seriya A **22**(3): 692–699.

Kabanov, V. A., A. B. Zezin, V. B. Rogacheva and S. V. Ryzhikov (1982). "Disproportionation of nonstoichiometric poly-electrolyte complexes in water-salt solutions." Doklady Akademii Nauk SSSR **267**(4): 862–865.

Koetz, J., K. J. Linow, B. Philipp, P. H. Li and O. Vogl (1986). "Effects of charge-density and structure of side-chain branching on the composition of polyanion polycation complexes." Polymer **27**(10): 1574–1580.

Kovacevic, D., S. Borkovic and J. Pozar (2007). "The influence of ionic strength, electrolyte type and preparation procedure on formation of weak polyelectrolyte complexes." Colloids and Surfaces, A: Physicochemical and Engineering Aspects **302**(1-3): 107–112.

Kumagai, H., C. H. Chu, T. Sakiyama, S. Ikeda and K. Nakamura (1996). "Analysis of the pH-sensitive swelling rate of a polyelectrolyte complex gel prepared from xanthan and chitosan by the collective diffusion model." Bioscience Biotechnology and Biochemistry **60**(10): 1623–1626.

López-León, T., E. L. S. Carvalho, B. Seijo, J. L. Ortega-Vinuesa and D. Bastos-González (2005). "Physicochemical characterization of chitosan nanoparticles: electrokinetic and stability behavior." Journal of Colloid and Interface Science **283** 344–351.

Nordmeier, E. and P. Beyer (1999). "Nonstoichiometric polyelectrolyte complexes: A mathematical model and some experimental results." Journal of Polymer Science, Part B: Polymer Physics **37**(4): 335–348.

Pergushov, D. V., V. A. Izumrudov, A. B. Zezin and V. A. Kabanov (1993). "Effect of low-molecular-mass salts on the behavior of water-soluble nonstoichiometric polyelectrolyte complexes." Vysokomolekulyarnye Soedineniya Seriya A & Seriya B **35**(7): A844–A849.

Pergushov, D. V., V. A. Izumrudov, A. B. Zezin and V. A. Kabanov (1995). "Stability of interpolyelectrolyte complexes in aqueous saline solutions - Effect of the degree of polymerization of polyions." Vysokomolekulyarnye Soedineniya Seriya A & Seriya B **37**(10): 1739–1746.

Sakiyama, T., C. H. Chu, T. Fujii and T. Yano (1993). "Preparation of a polyelectrolyte complex gel from chitosan and kappa-carrageenan and its pH-sensitive swelling." Journal of Applied Polymer Science **50**(11): 2021–2025.

Sakiyama, T., H. Takata, M. Kikuchi and K. Nakanishi (1999). "Polyelectrolyte complex gel with high pH-sensitivity prepared from dextran sulfate and chitosan." Journal of Applied Polymer Science **73**(11): 2227–2233.

Shovsky, A., I. Varga, R. Makuska and P. M. Claesson (2009a). "Formation and stability of water-soluble, molecular polyelectrolyte complexes: Effects of charge density, mixing ratio, and polyelectrolyte concentration." Langmuir **25**(11): 6113–6121.

Shovsky, A. V., I. Varga, R. Makuska and P. M. Claesson (2009b). "Formation and stability of soluble stochiometric polyelectrolyte complexes: Effects of charge density and polyelectrolyte concentration." Journal of Dispersion Science and Technology **30**(6): 980–988.

Sui, Z. J., J. A. Jaber and J. B. Schlenoff (2006). "Polyelectrolyte complexes with pH-tunable solubility." Macromolecules **39**(23): 8145–8152.

Trinh, C. K. and W. Schnabel (1993). "Ionic-strength dependence of the stability of polyelectrolyte complexes - Its importance for the isolation of multiply-charge polymers." Angewandte Makromolekulare Chemie **212**(1): 167–179.

Vasheghani, B. F., F. H. Rajabi, M. H. Ahmadi and F. Mashhadi (2008). "Investigation on thermodynamic parameters and stability of some polyelectrolyte complexes with respect to ionic strength of the medium." Polymer Bulletin **61**(2): 247–255.

Vishalakshi, B., S. Ghosh and V. Kalpagam (1993). "The effects of charge-density and concentration on the composition of polyelectrolyte complexes." Polymer **34**(15): 3270–3275.

Yao, K. D., H. L. Tu, F. Cheng, J. W. Zhang and J. Liu (1997). "pH-sensitivity of the swelling of a chitosan-pectin polyelectrolyte complex." Angewandte Makromolekulare Chemie **245**(1): 63–72.

Zezin, A. B. and V. A. Kabanov (1982). "A new class of complex watersoluble polyelectrolytes." Russian Chemical Reviews **51**(9): 833–855.

CHAPTER 5

CHITOSAN–CELLULOSE NANOCRYSTAL POLYELECTROLYTE COMPLEX—PART III: EFFECTS OF CHITOSAN MOLECULAR WEIGHT AND DEGREE OF DEACETYLATION

5.1. ABSTRACT

This study was conducted to determine the effects of chitosan molecular weight and degree of deacetylation (DD) on the formation and properties of chitosan–cellulose nanocrystal polyelectrolyte complexes (PECs). Chitosan samples with three different molecular weights (81, $3 \cdot 10^3$, $6 \cdot 10^3$ kDa) and four different DDs (77, 80, 85, 89%) were used. The effects on PEC formation were determined by turbidimetric titration. An effect of the molecular weight of chitosan was not observed in turbidimetric titrations. Turbidity levels were higher for chitosans with higher DDs. PEC particles from chitosans with different molecular weights were characterized by scanning electron microscopy, dynamic light scattering, and laser Doppler electrophoresis. PECs from high-molecular-weight chitosan were more spherical and those from medium-molecular-weight chitosan had a slightly larger hydrodynamic diameter than PECs from the respective other two chitosans. The molecular weight of chitosan was concluded to have no effect on the formation of chitosan–cellulose nanocrystal PEC particles and only a minor effect on the shape and size of the particles. The effect of chitosan DD on the formation and properties of chitosan–cellulose nanocrystal PEC particles was attributed to its correlation with charge density.

5.2. INTRODUCTION

Chitosan is one of very few known polysaccharides that bear exclusively positive charges. A positive charge in polysaccharides is generally related to the amino group of 2-amino-2-deoxy-D-glucopyranosyl (GlcN) residues, which is protonated in acidic aqueous media. In addition to these residues, chitosan contains 2-acetamido-2-deoxy-D-glucopyranosyl (GlcNAc) residues, which under most conditions bear no charge. The proportions of GlcN and GlcNAc residues in a chitosan sample depend on the processing conditions during manufacture or preparation, involving the chemical or enzymatic deacetylation of the parent polysaccharide chitin. The fraction of GlcN residues in a chitosan sample is termed the degree of deacetylation (DD), generally expressed in percent. The polycationic nature and availability of chitosan render it attractive for applications involving ionic interactions. For such applications, the DD is a crucial parameter as it is related to the charge density along the polymer chain.

An area of intense research, into which chitosan has been absorbed, is the area of polyelectrolyte complexes (PECs). PECs are intermolecular complexes of oppositely charged polyelectrolytes based on attractive Coulomb interactions (Thünemann *et al.*, 2004). The interest in PECs is motivated by their numerous current and potential applications, such as the encapsulation of sensitive ingredients in food products (de Kruif *et al.*, 2004), the delivery of drugs (Liu *et al.*, 2008) and genes (Midoux *et al.*, 2008), the entrapment and delivery of proteins and immobilization of enzymes (Cooper *et al.*, 2005), and the encapsulation of cells (Bhatia *et al.*, 2005). The properties of PECs depend on a number of factors, primarily the molecular weights and densities of ionizable groups of the two polyelectrolytes, the polyelectrolyte concentrations upon mixing, the mixing ratio, and the pH and ionic strength of the surrounding medium.

The effect of molecular weight on the properties of PECs is incompletely understood. Several groups have reported the composition of PECs to be independent of the molecular weight of the polyelectrolytes (Vishalakshi *et al.*, 1993; Becherán-Marón *et al.*, 2004). Dautzenberg (2001) and his collaborators have observed no effect of the molecular weight of sodium poly(styrene sulfate) on the structural parameters of its PECs with poly(diallyldimethylammonium chloride). De Vasconcelos *et al.* (2006), on the

other hand, have reported an increase and shift in the turbidity maximum in turbidimetric titrations of poly(methacrylic acid) (PMMA) with chitosan toward a higher chitosan/PMMA mass ratio with increasing molecular weight of PMMA. The authors concluded that PECs from PMMA of higher molecular weight were more water-soluble and larger than PECs from PMMA of lower molecular weight.

The effect of the density of ionizable groups, generally equated with the charge density, on the properties of PECs is much better understood as it has been more widely studied (Dautzenberg *et al.*, 1982; Koetz *et al.*, 1986; Vishalakshi *et al.*, 1993; Hugerth *et al.*, 1997; Dautzenberg and Jaeger, 2002; Shovsky *et al.*, 2009a; Shovsky *et al.*, 2009b). The results of these studies indicate that densely structured PECs are formed when the charge densities of the two polyelectrolytes are similar whereas highly swellable PECs with lower structural densities are formed in the case of a mismatch in the charge densities of the polyelectrolytes (Dautzenberg *et al.*, 1996; Dautzenberg and Jaeger, 2002).

In the preceding chapters, we have reported a new type of PEC between chitosan and cellulose nanocrystals, anionic, rod-like nanoparticles. The formation and properties of these PECs were governed by the strong mismatch in density of the ionizable groups. A decrease in pH of the surrounding medium was found to amplify the mismatch and cause PEC particle swelling whereas an increase in pH resulted in particle shrinking. Moreover, an increase in ionic strength caused a slight decrease in particles size, which was attributed to charge screening. This study is a continuation of the previous work with the aim to deepen our understanding of the factors that affect the complexation of chitosan and cellulose nanocrystals. The specific objectives of this study were to determine the effects of the molecular weight and DD of chitosan on the formation and properties of chitosan–cellulose nanocrystal PEC particles.

5.3. MATERIALS AND METHODS

5.3.1. Materials

High, medium, and low molecular weight chitosan (Fluka BioChemika) was purchased from Sigma-Aldrich and purified as follows. Typically, 1 g of chitosan was dissolved overnight in 250 mL 0.1 N HCl and the solution was filtered through a series of Millipore polyvinylidene fluoride (PVDF) syringe filters (pore sizes 1, 0.45, and 0.22 μm). Next, chitosan was precipitated by addition of 1 N NaOH until the solution pH reached 9–10. The purified chitosan was collected by centrifugation (4900 rpm for 15 min at 4 °C), washed three times with deionized water, and freeze-dried overnight. The purified chitosans were characterized as described in Chapter 3. The characteristics of the three types of chitosan are listed in Table 5.1.

Table 5.1. Characteristics of the high, medium, and low-molecular-weight chitosan

Chitosan	Molecular weight [a] (kDa)	DD[b] (%)	Hydrodynamic diameter[c] (nm)	Electrophoretic mobility[d] (μm·cm/V·s)	Amino group density[e] (mol/kg)
High Mw[f]	$6 \cdot 10^3$	87	319 ± 18	2.6 ± 0.2	6.1
Medium Mw[f]	$3 \cdot 10^3$	88	265 ± 14	3.2 ± 0.1	5.8
Low Mw[f]	81	88	238 ± 52	1.7 ± 0.9	5.3

[a] Calculated from the intrinsic viscosity
[b] Determined by ^{1}H NMR
[c] Determined by dynamic light scattering
[d] Measured with a Malvern Zetasizer Nano ZS 90
[e] Determined by conductometric titration
[f] molecular weight

Cellulose nanocrystals were prepared and characterized as described in Chapter 3. Briefly, 50 g ground (60-mesh) dissolving-grade softwood sulfite pulp (Temalfa 93 A-A), kindly provided by Tembec, Inc., was treated with 500 mL 64 wt % H_2SO_4 at 45 °C for 45 min. The hydrolysis was stopped by 10-fold dilution of the reaction medium with deionized water. The cellulose nanocrystals were collected by centrifugation and dialyzed against deionized water until the pH of the dialysis water stayed constant. The obtained

suspension was sonicated under ice-bath cooling and subsequently filtered through a 0.45 1 μm and then 0.22 μm PVDF syringe filter. The concentration of the filtered cellulose nanocrystal stock suspension was generally in the range of 0.6–0.9% (w/v). The results reported here stem from two different batches of cellulose nanocrystals. The second batch (Batch 2) was prepared with a hydrolysis time of 60 min instead of 45 min, resulting in slightly different properties, compared to the first batch (Batch 1). The nanocrystals were characterized as described in Chapter 3. Table 5.2 lists the characteristics of the cellulose nanocrystals from the two batches.

Table 5.2. Characteristics of the cellulose nanocrystals from the two batches

Cellulose nanocrystal sample	Hydrodynamic diameter[a] (nm)	Electrophoretic mobility[b] (μm·cm/V·s)	Sulfate group density[b] (mol/kg)
Batch 1	104 ± 4	-2.8 ± 0.2	0.18
Batch 2	68 ± 5	-3.1 ± 0.4	0.33

[a] Determined by dynamic light scattering

[b] Determined by conductometric titration

Beta-(1,4)-2-acetamido-2-deoxy-D-glucose (chitin) was purchased from ACROS, New Jersey, USA. H_2SO_4 (>95%), HCl (0.1 N, certified), NaOH (0.1 N and 1.0 N, certified), and NaCl (certified) were purchased from Fisher Scientific. 50% NaOH was ACS reagent grade and purchased from Ricca Chemical Company, Texas, USA. The water used in the experiments was deionized water from a Millipore Direct-Q 5 Ultrapure Water System (resistivity at 25 °C: 18.2 MΩ·cm).

5.3.2. Preparation of Chitosan Samples with Different DDs

Chitosan samples with different DDs were prepared by deacetylation of chitin according to literature procedures (Mima *et al.*, 1983; No and Meyers, 1995). In detail, 20 g chitin was heated for 1 h under nitrogen and stirring in 400 mL 47% NaOH at 110 °C. The reaction mixture was allowed to cool to 80 °C and the reaction product was washed with deionized water and dried in an oven at 105 °C for 2 h. Approximately 5 g

of the reaction product was set aside and the rest was subjected again to the procedure above. This process was repeated twice more to yield a total of four samples with different DDs. Finally, the chitosan samples were purified as described above by dissolution, filtration, precipitation, washing, and freeze-drying.

5.3.3. Characterization of Chitosan Samples with Different DDs

5.3.3.1. Molecular weight

The molecular weights of the four prepared chitosan samples were determined with the viscosity method using the Mark–Houwink equation ($[\eta] = KM^a$) as described in Chapter 3. The values used for the Mark–Houwink parameters, K and a, obtained from the literature (Wang *et al.*, 1991), were $K = 1.64 \times 10^{-30} \times \mathrm{DD}^{14}$, and $a = -1.02 \times 10^{-2} \times \mathrm{DD} + 1.82$.

5.3.3.2. Degree of Deacetylation

The DDs of the four samples were determined by FTIR spectroscopy according to the method by Baxter *et al.* (1992). The method is based on the intensity ratio of the amide I band at 1650 cm^{-1} and the hydroxyl band at 3450 cm^{-1}. KBr pellets were prepared by grinding 98 mg of dry KBr with 2 mg of sample and compressing the mixture between the ends of two stainless steel bolts inserted from opposite ends into a deep stainless steel nut, which served as the sample holder. The KBr pellet was dried in an oven prior to the measurement. FTIR spectra were recorded from KBr pellets with a resolution of 4 cm^{-1} and a number of scans of 128 using a Thermo Nicolet Nexus 470 FTIR spectrometer.

5.3.4. Preparation of Chitosan Solutions

Chitosan solutions for the complexation experiments were prepared from a stock solution of ~0.1% (w/v) by dilution with deionized water. For preparation of the stock solution, purified chitosan was dried in an oven at 105 °C for 2 h. Then, 0.1 g of the

oven-dried, purified chitosan was dissolved in 100 mL 0.1 N HCl. The exact concentration of the stock solution was determined in triplicate by thermogravimetric analysis as described in Chapter 3. Prior to the complexaton experiments, the pH and ionic strength of the chitosan solutions were adjusted with 0.1 N HCl or 0.1 N NaOH and NaCl, respectively.

5.3.5. Preparation of Cellulose Nanocrystal Suspensions

Dilute cellulose nanocrystal suspensions for the complexation experiments were prepared from the filtered stock suspension by dilution with deionized water. Prior to the complexation experiments, the pH and ionic strength of the cellulose nanocrystal suspensions were adjusted with 0.1 N HCl or 0.1 N NaOH and NaCl, respectively.

5.3.6. Turbidimetric Titrations

Turbidimetric titrations were performed with a 0.001% (w/v) chitosan solution and a 0.02% (w/v) cellulose nanocrystal suspension, both having a pH of 2.6 and an ionic strength of 1 mM. The concentrations, pH, and ionic strength were chosen based on the results reported in Chapters 3 and 4. In a turbidimetric titration experiment, the cellulose nanocrystal suspension was added drop-wise under vigorous stirring with a magnetic bar to the chitosan solution or vice versa. The transmittance of the reaction mixture was monitored with a probe colorimeter (PC 950, Brinkman, USA) with a 1 cm optical cell (2 cm path length), operating at a wavelength of 420 nm. Turbidity values were calculated as 100 – transmittance (%). Prior to each titration, the probe colorimeter was zeroed in deionized water. Each experiment was performed in triplicate.

5.3.7. Characterization of PEC Particles

5.3.7.1. Morphology

The morphology of chitosan–cellulose nanocrystal PEC particles was analyzed by field emission scanning electron microscopy (FE-SEM). Images were recorded with a LEO 1550 FE-SEM using an accelerating voltage of 5 kV and a working distance of 4 mm. Particles for SEM imaging were prepared at an amino/sulfate group molar ratio (N/S ratio) of unity by mixing under vigorous stirring with a magnetic bar the appropriate amounts of a 0.001% (w/v) chitosan solution and a 0.02% (w/v) cellulose nanocrystal suspension, both having a pH of 3.4 and an ionic strength of 1 mM. For SEM sample preparation, a 10 μL drop of the PEC particle suspension was deposited onto Ni–Cu conductive tape (Ted Pella) mounted onto a standard SEM stub (Ted Pella) and allowed to dry under ambient conditions. Prior to imaging, the SEM samples were coated with a thin (6 nm) layer of carbon.

5.3.7.2. Hydrodynamic diameter and electrophoretic mobility

The z-average hydrodynamic diameter and electrophoretic mobility of chitosan–cellulose nanocrystal PEC particles were measured with a Malvern Zetasizer Nano ZS90 using Malvern DTS1060 folded capillary cells. Particles for this analysis were prepared at an sulfate/amino group molar ratio (S/N ratio) of 0.3 by mixing under rapid stirring with a small magnetic bar the appropriate amounts of a 0.001% (w/v) chitosan solution and a 0.02% (w/v) cellulose nanocrystal suspension, both having a pH of 2.6 and an ionic strength of 1 mM. The resulting PEC particle suspensions were used directly without further dilution or filtration. Measurements were performed in triplicate at 25 °C.

5.3.8. Statistical Data Analysis

The turbidity data from the turbidimetric titrations were analyzed using one-way analysis of variance (ANOVA) with a 95% confidence interval ($\alpha = 0.05$) and Tukey's

HSD (Honestly Significant Difference) test. Statistical analysis of the data was carried out with the SAS software JMP 7.0.

5.4. RESULTS AND DISCUSSION

5.4.1. Effect of Chitosan Molecular Weight

The complexation of cellulose nanocrystals with chitosans of different molecular weight was studied by turbidimetric titration. The titration curves for the titration of a chitosan solution with a cellulose nanocrystal suspension from both Batch 1 and 2 are shown in Figure 5.1. In all titrations, upon addition of the cellulose nanocrystal suspension to the chitosan solution, the turbidity increased rapidly initially and then leveled off or decreased slightly at higher S/N ratios. In the titrations using cellulose nanocrystals from Batch 1 (Figure 5.1(a)), the maximum turbidity was reached at lower S/N ratios than in the titrations using cellulose nanocrystals from Batch 2 (Figure 5.1(b)). The difference was attributable to the higher cellulose/chitosan mass ratio required for charge stoichiometry in the case of the cellulose nanocrystals with lower sulfate group density. The turbidimetric titrations were carried out at a pH of 2.6. As shown in Chapter 4, at this pH the cellulose nanocrystals had a degree of ionization of 0.5, i.e. only 50% of the available sulfate groups were deprotonated and negatively charged. Charge stoichiometry, or an NH_3^+/SO_3^- ratio of unity, required a cellulose/chitosan mass ratio of about 66:1 for the cellulose nanocrystals from Batch 1 and of about 35:1 for the cellulose nanocrystals from Batch 2. As a result, PEC particles prepared with cellulose nanocrystals from Batch 1 probably contained more cellulose nanocrystals and were bulkier than PEC particles prepared with cellulose nanocrystals from Batch 2. The initial formation of bulkier PEC particles in the case of cellulose nanocrystals from Batch 1 might be the reason for the observed faster increase in turbidity.

The titration curves for different molecular weights of chitosan differed slightly. Because of the large standard deviations of the measured turbidity values (error bars in Figure 5.1), the significance of the observed differences in the titration curves was assessed by one-way ANOVA of the turbidity data. The ANOVA test results are listed in Table 5.3.

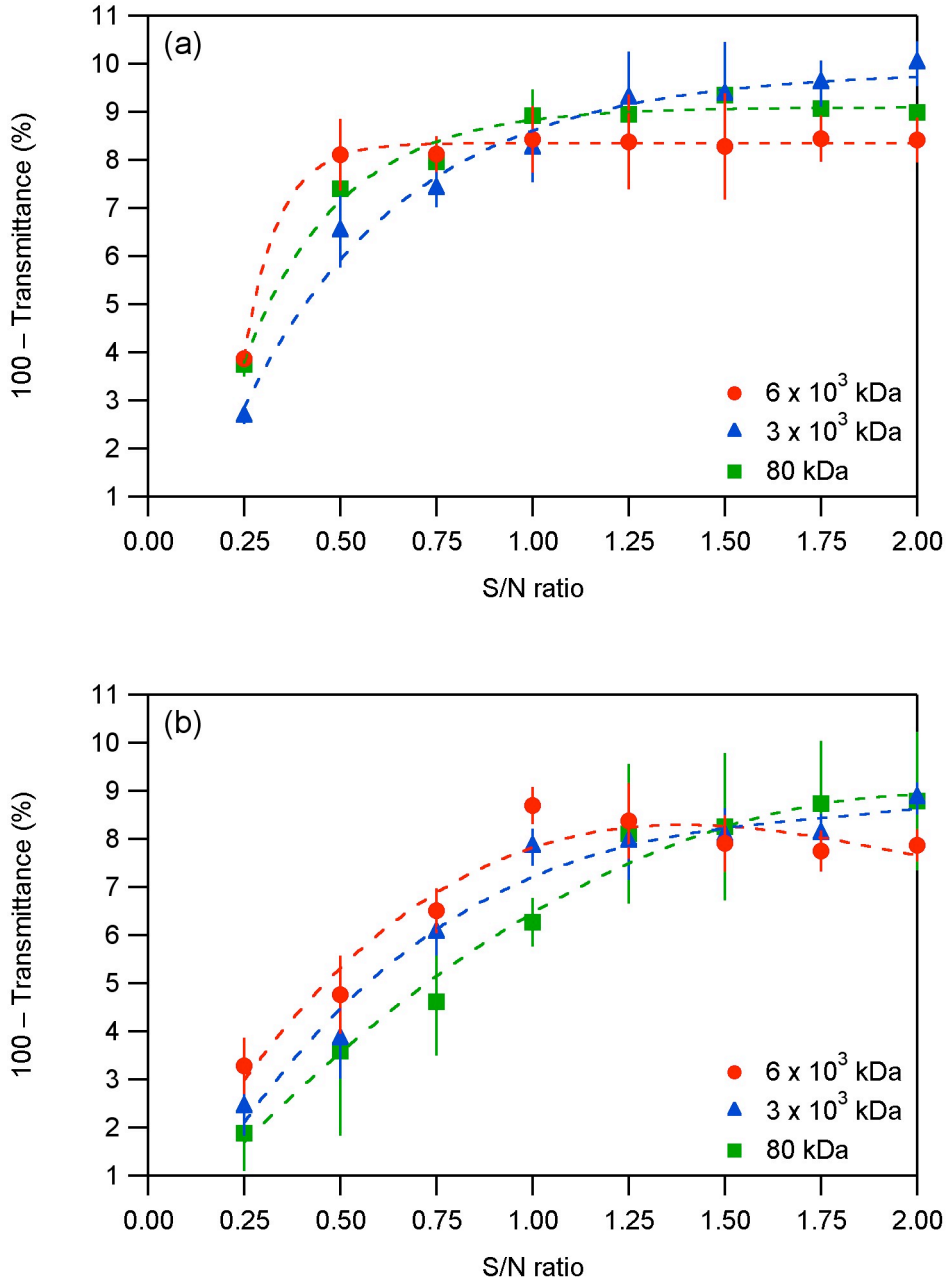

Figure 5.1. Turbidimetric titration curves for the addition of a cellulose nanocrystal suspension to a chitosan solution for different molecular weight chitosans and cellulose nanocrystals from (a) Batch 1 and (b) Batch 2. (Data points are means of three measurements. Error bars represent ± one standard deviation.)

Table 5.3. One-way ANOVA test results ($\alpha = 0.05$) for the effect of molecular weight of the commercial chitosan samples on the turbidity

Source of cellulose nanocrystals	DF	F Ratio	Prob > F
Batch 1	2	0.1250	0.8827
Batch 2	2	0.4208	0.6580

Statistical analysis of the turbidity data revealed that there was no significant difference between the data from different molecular weight chitosans. Thus, an effect of the molecular weight of chitosan was not observed in the turbidimetric titrations experiments.

The effect of the molecular weight of chitosan on the morphology of chitosan–cellulose nanocrystal PEC particles was studied by SEM. Figure 5.2 shows FE-SEM images of PEC particles prepared with different molecular weight chitosans. The particles from high-molecular-weight chitosan appeared to be more spherical than the particles from medium and low-molecular-weight chitosan. This finding is in accordance with the results of Ko *et al.* (2002), who reported more spherical particle shapes at higher molecular weights for tripolyphosphate-crosslinked chitosan microparticles.

Table 5.4 lists the hydrodynamic diameters and electrophoretic mobilities of chitosan–cellulose nanocrystal PEC particles from different molecular weight chitosans. The particles were formed at an N/S ratio of 0.3 to yield sizes within the analytical range. The particles from medium-molecular-weight chitosan were slightly larger than those from high and low-molecular weight chitosan. PEC particles from the latter two types were of comparable size. The slightly larger size of the PEC particles from medium-molecular-weight chitosan might indicate and optimum length ratio of the PEC components. The estimated length ratios (contour length of the chitosan molecules/length of the cellulose nanocrystals) were 140, 70, and 2:1 for the high, medium, and low-molecular weight chitosan respectively. The electrophoretic mobilities of the PEC particles were positive for all chitosan types, indicating a non-stoichiometric composition and excess of ammonium groups in the particles.

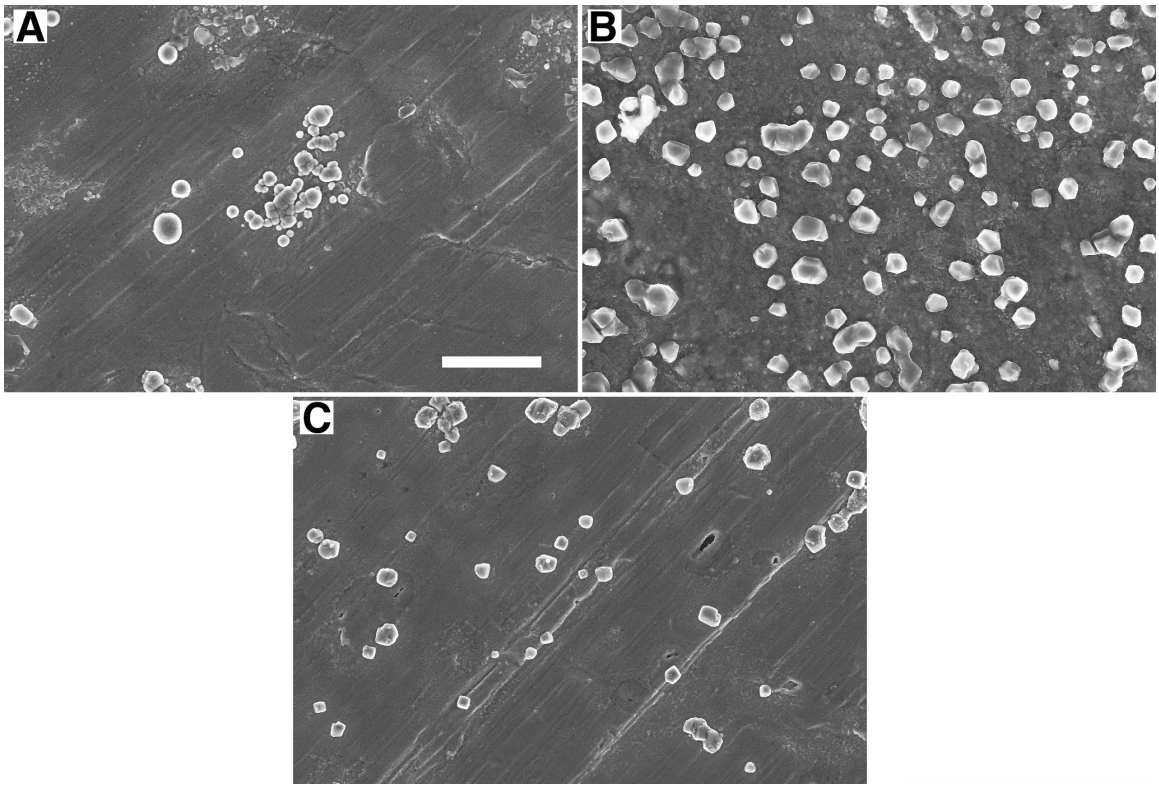

Figure 5.2. FE-SEM images of PEC particles formed by addition of a cellulose nanocrystal suspension to a chitosan solution for different chitosan molecular weights: (a) $6 \cdot 10^3$ kDa, (b) $3 \cdot 10^3$ kDa, (c) 80 kDa. Scale bar: 3 μm (applies to all images).

Table 5.4. Hydrodynamic diameter and electrophoretic mobility of PEC particles from different molecular weight chitosans

Sample	Hydrodynamic diameter (nm)	Electrophoretic mobility (μm·cm/V·s)
PEC with high-molecular-weight chitosan	373 ± 9	3.0 ± 0.1
PEC with medium-molecular-weight chitosan	539 ± 32	3.4 ± 0.1
PEC with low-molecular-weight chitosan	363 ± 37	2.9 ± 0.2

Our results are in accordance with those studies that have found the molecular weight to have not effect on the parameters of PECs (Vishalakshi *et al.*, 1993; Dautzenberg, 2001; Becherán-Marón *et al.*, 2004).

5.4.2. Effect of Chitosan Degree of Deacetylation

The effect of the DD of chitosan on chitosan–cellulose nanocrystal PEC particles was studied by turbidimetric titration using chitosan samples prepared by a chitin deacetylation procedure. The characteristics of these chitosan samples are listed in Table 5.5. The data in Table 5.5 shows that the deacetylation procedure caused a decrease in the molecular weight in addition to an increase in the DD.

Table 5.5. Characteristics of the chitosan samples prepared in-house by chitin deacetylation

Number of deacetylation cycles	Molecular weight [a] (kDa)	DD[b] (%)
1	1.7	77
2	1.9	80
3	1.4	85
4	1.0	89

[a] Calculated from intrinsic viscosity

[b] Determined by FTIR spectroscopy

The turbidimetric titrations curves for titrations of cellulose nanocrystal suspensions from Batch 1 with chitosan solutions of different DD are shown in Figure 5.3. Upon addition of the chitosan solution to the cellulose nanocrystal suspension, the turbidity increased rapidly initially and then leveled off. At higher volumes of chitosan solution added, the turbidity decreased slightly in accordance with the results reported in Chapter 3 for the effect of mixing sequence.

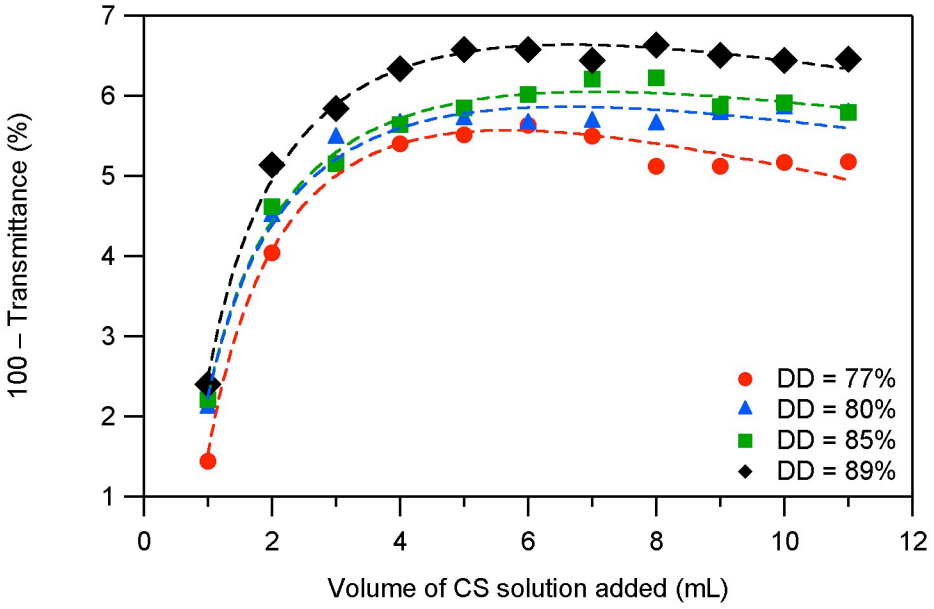

Figure 5.3. Turbidimetric titration curves for the addition of a chitosan solution to a cellulose nanocrystal suspension for chitosans with different DDs. (Data points are means of three measurements. Error bars are omitted for clarity.)

At any given volume of chitosan solution added, the turbidity increased with increasing DD. To establish whether the observed effect was related to the sample differences in DD or molecular weight, we analyzed the turbidity data by one-way ANOVA. The ANOVA test results are shown in Table 5.6.

Table 5.6. One-way ANOVA test results ($\alpha = 0.05$) for the effects of DD and molecular weight of the deacetylated chitin samples on the turbidity

Effect	DF	F Ratio	Prob > F
Molecular weight	2	1.7644	0.2497
DD	3	8.7221	<.0001*

Analysis of the data by one-way ANOVA showed that the molecular weight did not have a significant effect on the turbidity and that the differences in the turbidity curves were due to the differences in DD. Post hoc comparisons using the Tukey HSD test

(Table 5.7) indicated that the turbidity levels for a DD of 80 and 77% were significantly lower than for a DD of 89 and 85%.

Table 5.7. Significance levels and least squares means (Tukey HSD, $\alpha = 0.05$) for the effect of DD of the deacetylated chitin samples on the turbidity

Number of deacetylation cycles	Level (DD %)	Significance[a]	Least Squares Mean
1	77	A	4.871285
2	80	A	5.270278
3	85	B	5.422639
4	89	B	5.975972

[a] Levels not connected by same letter are significantly different

A lower DD signifies a lower charge density resulting in a closer match in the charge densities of the two components since the charge density of the cellulose nanocrystals was much lower than that of chitosan. According to a study by Dautzenberg and Jaeger (2002), PECs have a denser structure when the charge densities of the two polyelectrolytes are similar and a less dense structure when there is a mismatch in the charge densities. In light of these findings, the lower turbidity levels for the lower DD chitosans could be attributed to a higher structural density of the PEC particles. An alternative explanation could be that a higher charge density of chitosan requires a larger number of cellulose nanocrystals for charge compensation. Thus, PEC particles from chitosans with higher DDs might contain a larger number of cellulose nanocrystals and therefore be larger than PEC particles from chitosans with lower DDs.

5.5. CONCLUSIONS

The molecular weight of chitosan has no effect on the formation of chitosan–cellulose nanocrystal PEC particles and only a minor effect on the shape and size of the particles. The effect of chitosan DD on the formation and properties of chitosan–cellulose nanocrystal PEC particles is based on its correlation with charge density. Chitosans with higher DDs form larger PEC particles because the higher charge density requires a larger number of cellulose nanocrystal for charge compensation.

Acknowledgement

This material is based upon work supported in part by the USDA/CSREES under Grant No. 2005-35504-16088, the National Science Foundation under Grant No. CHE-0724126, and the Institute for Critical Technology and Applied Science at Virginia Tech. Additional support from Omnova, Inc. and Tembec, Inc. is also acknowledged. Furthermore, HW thanks the staff of the Nanoscale Characterization and Fabrication Laboratory for assistance with the SEM images.

5.6. REFERENCES

Baxter, A., M. Dillon, K. D. Anthony Taylor and G. A. F. Roberts (1992). "Improved method for i.r. determination of the degree of N-acetylation of chitosan." International Journal of Biological Macromolecules **14**(3): 166–169.

Becherán-Marón, L., C. Peniche and W. Argüelles-Monal (2004). "Study of the interpolyelectrolyte reaction between chitosan and alginate: influence of alginate composition and chitosan molecular weight." International Journal of Biological Macromolecules **34**(1-2): 127–133.

Bhatia, S. R., S. F. Khattak and S. C. Roberts (2005). "Polyelectrolytes for cell encapsulation." Current Opinion in Colloid & Interface Science **10**(1-2): 45–51.

Cooper, C. L., P. L. Dubin, A. B. Kayitmazer and S. Turksen (2005). "Polyelectrolyte-protein complexes." Current Opinion in Colloid & Interface Science **10**(1-2): 52–78.

Dautzenberg, H. (2001). Polyelectrolyte complex formation in highly aggregating systems: Methodical aspects and general tendencies. In: Radeva, T., Ed., Physical Chemistry of Polyelectrolytes. pp. 743–792. New York: Marcel Dekker.

Dautzenberg, H., J. Hartmann, S. Grunewald and F. Brand (1996). "Stoichiometry and structure of polyelectrolyte complex particles in diluted solution." Berichte der Bunsen-Gesellschaft fuer Physikalische Chemie **100**(6): 1024–1032.

Dautzenberg, H. and W. Jaeger (2002). "Effect of charge density on the formation and salt stability of polyelectrolyte complexes." Macromolecular Chemistry and Physics **203**(14): 2095–2102.

Dautzenberg, H., K. J. Linow and B. Philipp (1982). "The formation of water-soluble polysalts (simplexes) of anionic and cationic co-polymers of acrylamide. 2. Effect of charge-density and conversion on the structure of the simplexes." Acta Polymerica **33**(11): 619–625.

de Kruif, C. G., F. Weinbreck and R. de Vries (2004). "Complex coacervation of proteins and anionic polysaccharides." Current Opinion in Colloid & Interface Science **9**(5): 340–349.

de Vasconcelos, C. L., P. M. Bezerril, D. E. S. dos Santos, T. N. C. Dantas, M. R. Pereira and J. L. C. Fonseca (2006). "Effect of molecular weight and ionic strength on the formation of polyelectrolyte complexes based on poly(methacrylic acid) and chitosan." Biomacromolecules **7**(4): 1245–1252.

Hugerth, A., N. Caram-Lelham and L. O. Sundelöf (1997). "The effect of charge density and conformation on the polyelectrolyte complex formation between carrageenan and chitosan." Carbohydrate Polymers **34**(3): 149–156.

Ko, J. A., H. J. Park, S. J. Hwang, J. B. Park and J. S. Lee (2002). "Preparation and characterization of chitosan microparticles intended for controlled drug delivery." International Journal of Pharmaceutics **249**(1-2): 165–174.

Koetz, J., K. J. Linow, B. Philipp, P. H. Li and O. Vogl (1986). "Effects of charge-density and structure of side-chain branching on the composition of polyanion polycation complexes." Polymer **27**(10): 1574–1580.

Liu, Z. H., Y. P. Jiao, Y. F. Wang, C. R. Zhou and Z. Y. Zhang (2008). "Polysaccharides-based nanoparticles as drug delivery systems." Advanced Drug Delivery Reviews **60**(15): 1650–1662.

Midoux, P., G. Breuzard, J. P. Gomez and C. Pichon (2008). "Polymer-based gene delivery: A current review on the uptake and intracellular trafficking of polyplexes." Current Gene Therapy **8**(5): 335–352.

Mima, S., M. Miya, R. Iwamoto and S. Yoshikawa (1983). "Highly deacetylated chitosan and its properties." Journal of Applied Polymer Science **28**(6): 1909–1917.

No, H. K. and S. P. Meyers (1995). "Preparation and characterization of chitin and chitosan- A review." Journal of Aquatic Food Product Technology **4**(2): 27–52.

Shovsky, A., I. Varga, R. Makuska and P. M. Claesson (2009a). "Formation and stability of water-soluble, molecular polyelectrolyte complexes: Effects of charge density, mixing ratio, and polyelectrolyte concentration." Langmuir **25**(11): 6113–6121.

Shovsky, A. V., I. Varga, R. Makuska and P. M. Claesson (2009b). "Formation and stability of soluble stochiometric polyelectrolyte complexes: Effects of charge density and polyelectrolyte concentration." Journal of Dispersion Science and Technology **30**(6): 980–988.

Thünemann, A. F., M. Müller, H. Dautzenberg, J. F. O. Joanny and H. Löwen (2004). Polyelectrolyte complexes. In: Schmidt, M., Ed., Polyelectrolytes with defined molecular architecture II. pp. 113–171. Berlin: Springer-Verlag.

Vishalakshi, B., S. Ghosh and V. Kalpagam (1993). "The effects of charge-density and concentration on the composition of polyelectrolyte complexes." Polymer **34**(15): 3270–3275.

Wang, W., S. Bo, S. Li and W. Qin (1991). "Determination of the Mark-Houwink equation for chitosans with different degrees of deacetylation." International Journal of Biological Macromolecules **13**(5): 281–285.

CHAPTER 6

CHITOSAN–CELLULOSE NANOCRYSTAL POLYELECTROLYTE COMPLEX—PART IV: *IN VITRO* DRUG RELEASE PROPERTIES

6.1. ABSTRACT

Polyelectrolyte complexes (PECs) between chitosan, a mucoadhesive, permeability-enhancing polysaccharide, and cellulose nanocrystals, rod-like cellulose nanoparticles with sulfate groups on their surface, have potential applications in oral drug delivery. The purpose of this research was to determine the *in vitro* drug release properties of chitosan–cellulose nanocrystal PEC particles, using caffeine and ibuprofen as model drugs. Drug-loaded PEC particles were characterized by FTIR spectroscopy and scanning electron microscopy. The drug-loaded PEC particles were spherical in shape and had diameters of a few hundred nanometers to a few micrometers. Release of caffeine from the PEC particles at a pH of 3.4 and an ionic strength of 1 mM was rapid and uncontrolled. Ibuprofen-loaded PEC particles showed no release in simulated gastric fluid and rapid release in simulated intestinal fluid. Complexation of ionized ibuprofen by chitosan was potentially the reason for the incomplete release observed in simulated intestinal fluid. Chitosan–cellulose nanocrystal PEC particles provided no control over the release rates of caffeine and ibuprofen and did not noticeably enhance the solubility of ibuprofen in simulated gastric fluid. Further evaluation studies should focus on the expected mucoadhesive and permeability-enhancing properties.

6.2. INTRODUCTION

In oral drug delivery, multi-particulate dosage forms have several advantages over single-unit formulations. They distribute more uniformly in the gastrointestinal (GI) tract, resulting in more uniform drug release and a reduced risk of local irritation. Moreover, their larger surface area-to-volume ratio provides a larger interface for partitioning and release of the drug. One of the main challenges of oral drug delivery is the limited and variable GI transit time of the drug formulation. Particles smaller than 10 μm in diameter are assumed to have the advantage of entering the intestinal mucosa, resulting in longer residence times in the intestine and close contact between the drug formulation and the site of absorption (Galindo-Rodriguez *et al.*, 2005). The ability of submicron particles to provide extended release of the encapsulated drug, enhance its absorption and, thus, bioavailability has been demonstrated in several *in vivo* studies (Dunn and Hollister, 1995; Callender *et al.*, 1999; Arangoa *et al.*, 2001; Jiao *et al.*, 2002; Wang *et al.*, 2004). However, a study by Kreuter *et al.* (1989), involving mice, reported a low retention of only 5% of orally administered nanoparticles 24 h after administration.

One possible means of controlling the residence time of drug formulations in the small intestine is to incorporate materials into the formulation that engage in nonspecific or specific interactions with the mucosal membrane, thus temporarily immobilizing the drug formulation in the small intestine. In addition to prolonging the transit time through the small intestine, mucoadhesive drug formulations release the drug near the site of absorption, limiting the drugs exposure to digestive enzymes. A mucoadhesive material that has received substantial attention in oral drug delivery is chitosan, a linear polysaccharide of β(1–4)-linked 2-amino-2-deoxy-D-glucopyranose and 2-acetamido-2-deoxy-D-glucopyranose residues. The mucoadhesive properties of chitosan-coated nanoparticles have been attributed to attractive electrostatic interactions between the negatively charged intestinal mucosa and the positively charge nanoparticles as well as physical entanglements between the chitosan molecules and mucus components (Kawashima *et al.*, 2000). In addition, chitosan has been shown to open up the tight junctions in the intestinal epithelium (Illum *et al.*, 1994; Kotze *et al.*, 1997; Schipper *et al.*, 1997; Junginger and Verhoef, 1998). Chitosan is therefore considered a GI

paracellular permeability enhancer, i.e. a compound that increases the flux of poorly absorbed drugs through the intestinal epithelium by modulating the paracellular pathway.

Nanoparticulate chitosan matrices have shown promise in the oral delivery of both hydrophilic and hydrophobic drugs (El-Shabouri, 2002; Pan *et al.*, 2002; Ma *et al.*, 2005). Several methods for the preparation of multi-particulate chitosan drug delivery systems have been explored. Because chitosan is soluble in the acidic environment of the stomach, it has to be crosslinked for chitosan-based particles to maintain integrity. Chemical crosslinking methods often involve organic solvents or toxic crosslinking agents, such as glutaraldehyde (Wei *et al.*, 2008), which could be detrimental if released in the GI tract. Ionic crosslinking with low molecular weight, negatively charged multivalent ions, in particular tripolyphosphate, is generally preferred because of the mild conditions during particle preparation and the absence of toxic substances (Agnihotri *et al.*, 2004). Alternatively, ionic crosslinking with negatively charged polyelectrolytes has been investigated for the formation of chitosan-containing micro- and nanoparticles for oral drug delivery. To this end, many natural and synthetic polyanions have been studied, including alginate (Cekic *et al.*, 2007; Sarmento *et al.*, 2007b; Sarmento *et al.*, 2007c; Dai *et al.*, 2008; Liu *et al.*, 2008; Motwani *et al.*, 2008), hyaluronic acid (de la Fuente *et al.*, 2008a; de la Fuente *et al.*, 2008b), xanthan (Chellat *et al.*, 2000a; Chellat *et al.*, 2000b), pectin (Wong and Nurjaya, 2008), poly-γ-glutamic acid (Dai *et al.*, 2007; Hajdu *et al.*, 2008), carboxymethyl cellulose (Zhang *et al.*, 2001; Gomez-Burgaz *et al.*, 2008), κ-carrageenan (Piyakulawat *et al.*, 2007), chondroitin sulfate (Sui *et al.*, 2008), heparin (Liu *et al.*, 2007), chitosan sulfate (Berth *et al.*, 2002), and dextran sulfate (Schatz *et al.*, 2004a; Schatz *et al.*, 2004b; Sarmento *et al.*, 2006; Chen *et al.*, 2007; Drogoz *et al.*, 2007; Sarmento *et al.*, 2007a; Drogoz *et al.*, 2008).

In the preceding chapters, we have reported a new type of polyelectrolyte complex (PEC) between chitosan and cellulose nanocrystals, rod-like cellulose nanoparticles with a small number of sulfate groups on the surface. The motivation for the research was two-fold. First, the study of ionic complexes between a polyelectrolyte and a rod-like nanoparticle might yield new insights into charge-based self-assembly processes. Second, ionic complexes of chitosan and cellulose might show promise for oral drug delivery

applications. Though it has not been experimentally proven, the safety of cellulose nanocrystals with regard to oral consumption is likely, given the following facts: Cellulose, in the form of micron-scale particles has been used as a pharmaceutical excipient since 1966 (Steele *et al.*, 2003). Microparticulate cellulose has GRAS (generally recognized as safe) status with the U.S. Food and Drug Administration. An *in vivo* study has revealed no physical or chemical breakdown of micron and sub-micron cellulose particles in humans upon ingestion (Tusing *et al.*, 1964). And finally, a study on the GI absorption of sodium cellulose sulfate in cats has shown that cellulose sulfate is neither hydrolyzed nor absorbed from the duodenal loops and that GI absorption upon administration by mouth is insignificant (Morrow *et al.*, 1952). These facts suggest that cellulose nanocrystals would neither be absorbed nor digested when administered orally. Chitosan is generally considered safe for oral administration (Agnihotri *et al.*, 2004).

Our previous studies have shown that the formation and properties of chitosan–cellulose nanocrystal PECs are governed by the strong mismatch in the densities of ionizable groups. The molecular weight and degree of deacetylation of chitosan as well as the ionic strength of the surrounding medium have had a minor effect. The PECs had diameters of several hundred nanometers to several micrometers, depending on the preparation conditions, and showed strong swelling at pH values below 2, due to protonation of the sulfate groups of the cellulose nanocrystals, and shrinking at pH values above 6, due to deprotonation of the chitosan amino groups. This study is a continuation of the previous work with the aim to evaluate the potential of chitosan–cellulose nanocrystal PECs in oral drug delivery applications. The specific objectives of this study were to determine the drug release properties of the PECs. Caffeine and ibuprofen were chosen as a highly soluble, non-ionizable and a poorly soluble, ionizable model drug, respectively. The molecular structures of caffeine and ibuprofen are shown in Figure 6.1.

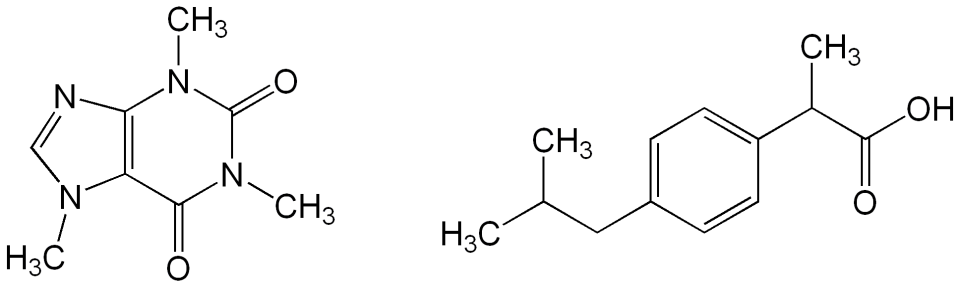

(a) (b)

Figure 6.1. Molecular structures of caffeine (a) and ibuprofen (b).

Caffeine is a heterocyclic aromatic molecule with a pK_a of its conjugate acid of around 0.7 (Katsu *et al.*, 2008). The caffeine molecule is therefore neutral at most pH values. The solubility of caffeine in aqueous media is around 22 mg/mL (Al-Maaieh and Flanagan, 2002). Ibuprofen is an aromatic carboxylic acid, the pK_a of which has been reported to lie in the range 4.4–5.3 (Shaw *et al.*, 2005; Domanska *et al.*, 2009). Its solubility in aqueous media is strongly dependent on pH and has been reported as 0.058 mg/mL in the pH range 1–4 and 0.938 mg/mL at a nominal pH of 7 (actual pH of 5.55) (Shaw *et al.*, 2005).

6.3. MATERIALS AND METHODS

6.3.1. Materials

Chitosan (medium molecular weight, Fluka BioChemika) was purchased from Sigma-Aldrich and purified as follows. Typically, 1 g of chitosan was dissolved overnight in 250 mL 0.1 N HCl and the solution was filtered through a series of Millipore polyvinylidene fluoride (PVDF) syringe filters (pore sizes 1, 0.45, and 0.22 μm). Next, chitosan was precipitated by addition of 1 N NaOH until the solution pH reached 9–10. The purified chitosan was collected by centrifugation (4900 rpm for 15 min at 4 °C), washed three times with deionized water, and freeze-dried overnight. The purified chitosan was characterized as described in Chapter 3. The molecular weight and degree of deacetylation were 3.1×10^6 Dalton and 87.8%, respectively. The amino group density was 5830 mmol/kg.

Cellulose nanocrystals were prepared and characterized as described in Chapter 3. Briefly, 50 g ground (60-mesh) dissolving-grade softwood sulfite pulp (Temalfa 93 A-A), kindly provided by Tembec, Inc., was treated with 500 mL 64 wt % H_2SO_4 at 45 °C for 45 min. The hydrolysis was stopped by 10-fold dilution of the reaction medium with deionized water. The cellulose nanocrystals were collected by centrifugation and dialyzed against deionized water until the pH of the dialysis water stayed constant. The obtained suspension was sonicated under ice-bath cooling and subsequently filtered through a 0.45 μm and then 0.22 μm PVDF syringe filter. The concentration of the filtered cellulose nanocrystal stock suspension was generally in the range of 0.6–0.9% (w/v). The cellulose nanocrystals had a sulfate group density of 333 mmol/kg.

Caffeine (99.7 %) was purchased from Alfa Aesar. Ibuprofen (99%, Acros Organics), H_2SO_4 (> 95%), HCl (0.1 N, certified), NaOH (0.1 N and 1.0 N, certified), NaCl (certified), and phosphate buffered saline (ACS reagent grade) were purchased from Fisher Scientific. Simulated gastric fluid (ACS reagent grade) was purchased from Ricca Chemical Company. The water used in the experiments was deionized water from a Millipore Direct-Q 5 Ultrapure Water System (resistivity at 25 °C: 18.2 MΩ·cm).

6.3.2. Preparation of Chitosan Solutions

Chitosan solutions were prepared from a stock solution of ~0.1% (w/v) by dilution with deionized water. For preparation of the stock solution, purified chitosan was dried in an oven at 105 °C for 2 h. Then, 0.1 g of the oven-dried, purified chitosan was dissolved in 100 mL 0.1 N HCl. The exact concentration of the stock solution was determined in triplicate by thermogravimetric analysis as described in Chapter 3. The pH and ionic strength of the final solutions were adjusted with 0.1 N HCl or 0.1 N NaOH and NaCl, respectively.

6.3.3. Preparation of Cellulose Nanocrystal Suspensions

Dilute cellulose nanocrystal suspensions were prepared from the filtered stock suspension by dilution with deionized water. The pH and ionic strength were adjusted with 0.1 N HCl or 0.1 N NaOH and NaCl, respectively.

6.3.4. UV–vis Spectroscopy

Solution concentrations of caffeine and ibuprofen were determined by UV–vis spectroscopy using a Thermo Scientific Evolution 300 UV–vis spectrophotometer and 1 cm light-path-length quartz cuvettes. UV–vis spectra of solutions were recorded at solution concentrations between 10 and 100 μM using a bandwidth of 1.0 nm, intelliscan scan speed, and 3 scan cycles. Caffeine concentrations were measured at a wavelength of 273 nm and ibuprofen concentrations at 222 nm.

6.3.5. Drug Loading Procedures

6.3.5.1. Caffeine Loading

Caffeine loading experiments were performed with a 0.001% (w/v) chitosan solution and a 0.02% (w/v) cellulose nanocrystal suspension, both having a pH of 3.4 and

ionic strength of 1 mM. The volumes of the chitosan solution and cellulose nanocrystal suspension to be added to one another were chosen to yield a sulfate/amino group molar ratio of unity. Two different drug loading methods were evaluated. In Method 1, a certain amount of caffeine was dissolved in the chitosan solution and the cellulose nanocrystal suspension was subsequently added drop-wise and under stirring (500 rpm), resulting in the formation of caffeine-loaded PECs. In Method 2, caffeine was dissolved in the cellulose nanocrystal suspension and the chitosan solution was added. The amount of caffeine was chosen based on the final volume of the PEC suspension to yield a caffeine concentration of 2 mg/mL. After stirring at 250 rpm for 24 h, the loaded PEC particles were collected by centrifugation for 15 min at 4400 rpm and 4 °C. The supernatant was decanted and the loaded PEC particles were resuspended by vortexing in deionized water, freeze-dried over night, and oven-dried at 80 °C for 2 h. The drug loading and loading efficiency were calculated using eqs 6.1 and 6.2, respectively.

$$\text{drug loading (\%)} = \frac{m_A - m_B}{m_{PEC}} \times 100\% \qquad [6.1]$$

$$\text{loading efficiency (\%)} = \frac{m_A - m_B}{m_A} \times 100\% \qquad [6.2]$$

where m_A is the mass of drug initially present, m_B is the mass of drug present in the supernatant, and m_{PEC} is the mass of unloaded PEC particles, taken to be the combined mass of chitosan and cellulose nanocrystals before complexation. The drug concentration in the supernatant, for calculation of m_B, was determined spectrophotometrically.

In a modified loading method, denoted hereafter with -d, the loaded PEC particles were freeze-dried directly from the caffeine solution, omitting the centrifugation and resuspension steps. All experiments were performed in triplicate.

6.3.5.2. Ibuprofen Loading

Because of the low solubility of ibuprofen in acidic aqueous media (~ 0.06 mg/mL at pH 1–4 (Shaw *et al.*, 2005)), loading of ibuprofen into PEC particles was carried out in

a mixed solvent system. The solvent system consisted of ethanol and deionized water at a volume ratio of 80:20. The pH and ionic strength were adjusted through addition of 0.1 N HCl and NaCl to 4.6 and 1 mM, respectively. Ibuprofen was dissolved in the solvent system at a concentration of 2 mg/mL. PEC particles for ibuprofen loading were prepared by mixing a 0.001% (w/v) chitosan solution with a 0.02% (w/v) cellulose nanocrystal suspension, both having a pH and ionic strength of 2.6 and 1 mM, respectively, at a sulfate/amino group molar ratio of 1:1. The PEC particles were collected by centrifugation, washed three times with deionized water, and freeze dried. For ibuprofen loading, 20 mg of PEC particles, were added to 25 mL of the ibuprofen solution and stirred at 200 rpm for 24 h. The loaded PEC particles were collected by centrifugation for 15 min at 4400 rpm and 4 °C. The supernatant was decanted and the loaded PEC particles were resuspended in deionized water, freeze-dried over night, and oven-dried at 80 °C for 2 h. The drug loading and loading efficiency were calculated as described above. All experiments were performed in triplicate.

6.3.6. *In Vitro* Drug Release Procedures

6.3.6.1. Caffeine Release

Caffeine release experiments were carried out at room temperature at a pH of 3.4 and an ionic strength of 1 mM. Ten milligrams of caffeine-loaded PEC particles were dispersed in 25 mL of dissolution medium in regenerated cellulose dialysis tubing of a given length (Spectrum Spectra/Por 4, molecular weight cut-off of 12–14 kDa). The dialysis tubing was immersed in 250 mL of dissolution medium, stirred at 500 rpm with a magnetic bar. At predetermined times during the release experiment, a 5 mL aliquot was withdrawn from the external dissolution medium and an equal volume of fresh dissolution medium was added so that the total volume of the dissolution medium stayed constant (275 mL). The caffeine concentration in the aliquot was determined spectrophotometrically after suitable dilution. The mass of caffeine released from the loaded PEC particles, m_t, at a given sampling time, t, denoting the number of times an aliquot has been withdrawn, was calculated from

$$m_t = VC_tM + \sum_{0}^{t-1} v_t C_t M \qquad [6.3]$$

where V is the total volume of dissolution medium, C_t is the drug concentration in the aliquot at sampling time t, M is the molar mass of the drug, and v_t is the aliquot volume at sampling time t. The mass released was expressed as a percentage of the total mass initially present in the loaded PEC particles. All experiments were performed in triplicate.

6.3.6.2. Ibuprofen Release

Ibuprofen release experiments were carried out in simulated gastric fluid (pH 1.2) and simulated intestinal fluid (phosphate buffered saline, pH 7.4) at 37 °C. Five to twenty milligram of ibuprofen-loaded PEC particles were dispersed in 50 mL of dissolution medium. The dissolution medium was stirred at 250 rpm with a magnetic bar during the experiment. At predetermined times, a 1–3 mL aliquot was withdrawn and centrifuged at 13,200 rpm for 5 min. The sediment was redispersed in an equal volume of fresh dissolution medium and returned to the vessel. The ibuprofen concentration in the supernatant was determined spectrophotometrically after suitable dilution. The mass of ibuprofen released from the loaded PEC particles at a given sampling time was calculated using eq 6.1 and expressed as a percentage of the total mass initially present in the loaded PEC particles. All experiments were performed in triplicate.

6.3.7. Characterization of Drug-Loaded PEC Particles

6.3.7.1. FTIR Spectroscopy

FTIR spectra were recorded from KBr pellets with a resolution of 4 cm^{-1} and a number of scans of 128 using a Thermo Nicolet Nexus 470 ESP FTIR spectrometer. KBr pellets were prepared by grinding 98 mg of dry KBr with 2 mg of sample and compressing the mixture between the ends of two stainless steel bolts inserted from opposite ends into a deep stainless steel nut, which served as the sample holder. The KBr pellet was dried in an oven prior to the measurement.

6.3.7.2. Scanning Electron Microscopy

Scanning electron microscopy (SEM) images were recorded with a LEO 1550 field-emission SEM using an accelerating voltage of 5 kV and a working distance of 5 mm. For sample preparation, a 10 μL drop of the drug solution from the loading experiments, containing the loaded PEC particles, was deposited onto Ni–Cu conductive tape (Ted Pella) mounted onto a standard SEM stub (Ted Pella) and allowed to dry under ambient conditions. Prior to imaging, the SEM samples were coated with a thin (6 nm) layer of carbon.

6.4. RESULTS AND DISCUSSION

6.4.1. UV–Vis Spectra of the Model Drugs

The UV–Vis spectrum of caffeine in aqueous solution at a pH of 3.4 and ionic strength of 1 mM is shown in Figure 6.2. The spectrum showed two absorption maxima, one at a wavelength of 203 nm and one at 273 nm, in accordance with previous reports (Li *et al.*, 1990; Lopez-Martinez *et al.*, 2003; Belay *et al.*, 2008; Yamauchi *et al.*, 2008). We chose the absorption intensity at 273 nm for the determination of caffeine solution concentrations. The molar extinction coefficient of caffeine at 273 nm under these solution conditions was measured to $8.82 \cdot 10^3$ $M^{-1} \cdot cm^{-1}$. The coefficient of determination (R^2 value) for the linear regression of the absorbance values, measured at concentrations in the range 10–90 μM, was 0.99995. Our value for the molar extinction coefficient of caffeine was somewhat lower than the previously reported values of $9.74 \cdot 10^3$ $M^{-1} \cdot cm^{-1}$ (Veselkov *et al.*, 2000), $9.85 \cdot 10^3$ $M^{-1} \cdot cm^{-1}$ (Li *et al.*, 1990), and $9.81 \cdot 10^3$ $M^{-1} \cdot cm^{-1}$ (Yamauchi *et al.*, 2008). The difference could be due to differences in the choice of solvent and solution pH.

The UV–Vis spectra of ibuprofen dissolved in simulated gastric and intestinal fluid are shown in Figure 6.3. The spectra showed a broad absorption peak with a maximum around 205 nm. The absorption intensity of ibuprofen in simulated gastric fluid (pH 1.2) was slight higher than that in simulated intestinal fluid (pH 7.4). The spectra obtained from the ibuprofen sample used in this study differed from those reported in the literature (Krzek *et al.*, 2005; Du *et al.*, 2006). The main absorption peak of ibuprofen has been reported to occur at 222 nm. The differences in appearance of the spectra reported here and those previously reported could be due to experimental differences with respect to solvent and ibuprofen concentration. The absorption intensity at 222 nm is frequently chosen for the determination of ibuprofen concentrations (Sochor *et al.*, 1994; Sochor *et al.*, 1995; Save *et al.*, 1997; Liu and Fang, 1998; Krzek *et al.*, 2005). Here, we evaluated both this wavelength (222 nm) and that of maximum absorption intensity (205 nm) and observed no significant difference. Therefore, only the values for 222 nm are reported.

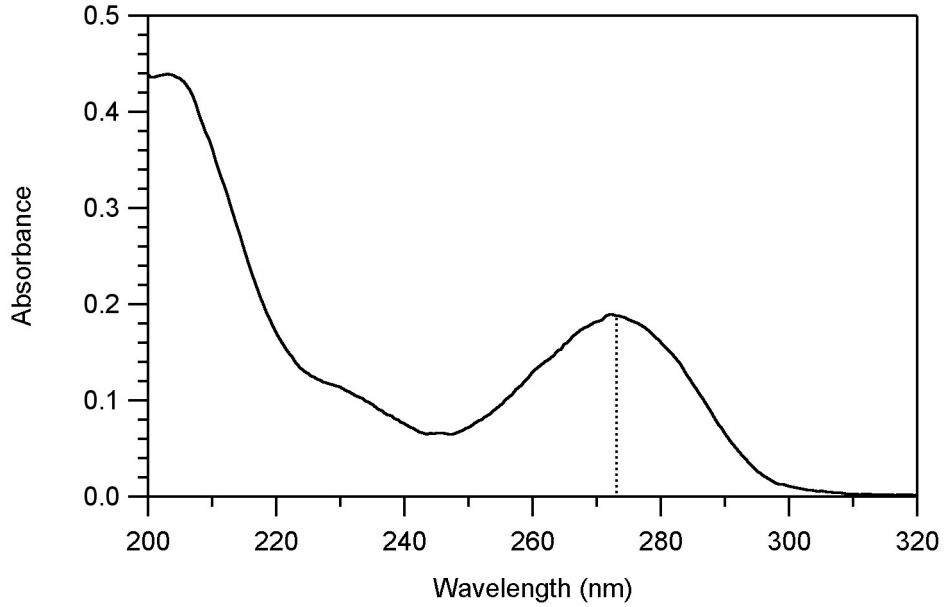

Figure 6.2. UV–vis spectrum of caffeine in water at a concentration of $2 \cdot 10^{-5}$ M, a pH of 3.4, and an ionic strength of 1 mM. (The dotted line marks the wavelength that was used for quantification.)

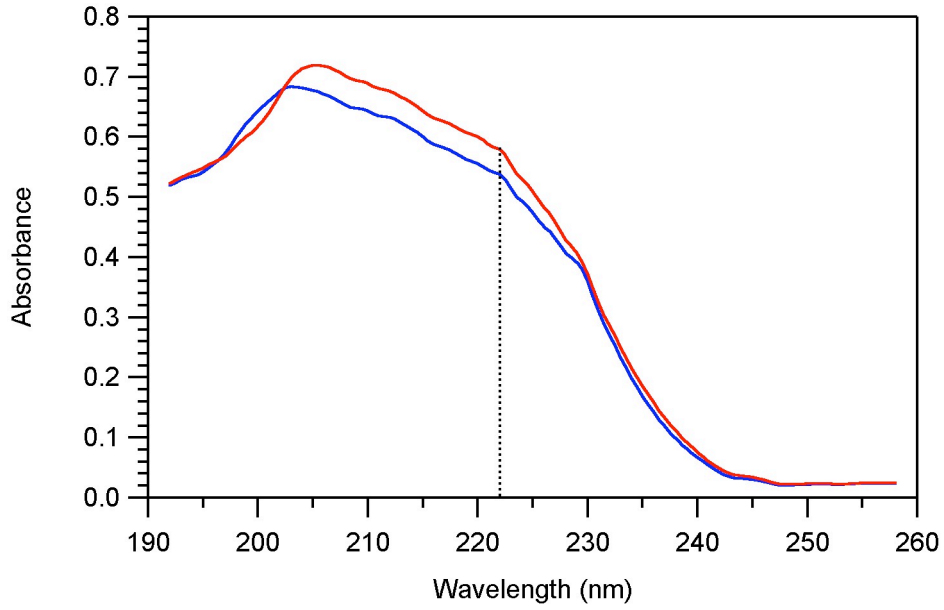

Figure 6.3. UV–vis spectra of ibuprofen in simulated gastric fluid (—) and simulated intestinal fluid (—) at a concentration of 10^{-4} M. (The dotted line marks the wavelength that was used for quantification.)

The molar extinction coefficients of ibuprofen at 222 nm in simulated gastric and intestinal fluid were measured to $5.60 \cdot 10^3$ and $6.63 \cdot 10^3$ $M^{-1} \cdot cm^{-1}$, respectively. The coefficients of determination for the linear regression of the absorbance values, measured at concentrations in the range 30–100 μM, were 0.99932 and 0.99813 for simulated gastric and intestinal fluid, respectively. Our values for the molar extinction coefficient of ibuprofen were significantly lower than the previously reported value of $1.27 \cdot 10^4$ $M^{-1} \cdot cm^{-1}$ (Du *et al.*, 2006). The reasons for this difference are probably related to those for the differences in appearance of the absorption spectra.

6.4.2. Characterization of Drug-Loaded PEC particles

6.4.2.1. FT-IR Spectroscopy

The drug-loaded PEC particles were characterized by FT-IR spectroscopy. The FT-IR spectra for the PEC particles before and after loading and those of caffeine and ibuprofen are shown in Figure 6.4. As discussed in Chapter 3, the PEC particles consisted primarily of cellulose nanocrystals and contained only very little chitosan. Thus, the FT-IR spectrum of the PEC particles (Figure 6.4(a)) showed only the characteristic absorption bands of cellulose. The broad absorption band between 3600 and 3000 cm^{-1} is related to OH stretching vibrations (Hinterstoisser and Salmén, 1999). The absorption bands between 3000 and 2800 cm^{-1} and 1500 and 1250 cm^{-1} stem from the CH and CH_2 stretching and bending vibrations, respectively (Marchessault and Liang, 1960). The bands in the fingerprint region have been assigned to the antisymmetric bridge C–O–C stretching vibration (Nikonenko *et al.*, 2000; Nikonenko *et al.*, 2005) and the CO stretching vibrations at C–2, C–3, and C–6 (Maréchal and Chanzy, 2000). And the band between 800 and 450 cm^{-1} originates in the OH out-of-plane bending vibrations (Kondo and Sawatari, 1996; Oh *et al.*, 2005).

Spectrum (b) in Figure 6.4 is the FT-IR spectrum of caffeine. The most prominent feature of the caffeine spectrum are the absorption bands at 1700 and 1660 cm^{-1}, assigned to the stretching vibrations of the two caffeine carbonyl groups (Kesimli *et al.*, 2003).

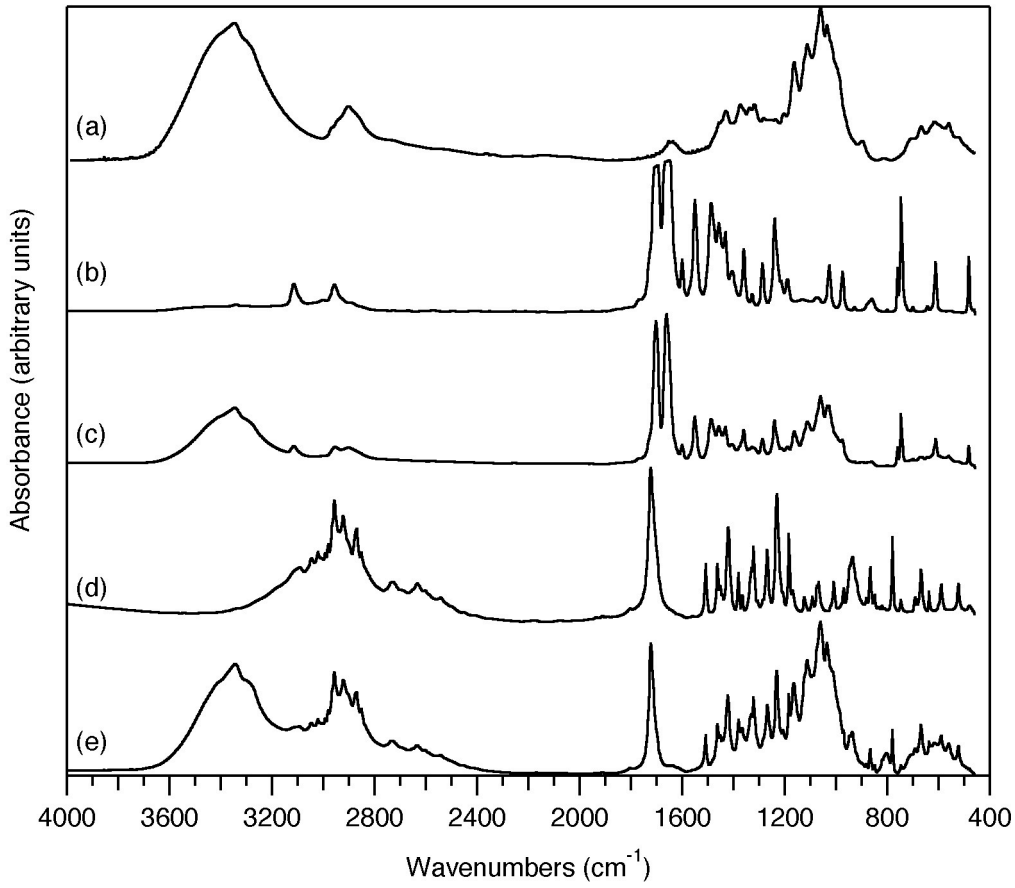

Figure 6.4. FT-IR spectra of (a) chitosan–cellulose nanocrystal PEC particles, (b) caffeine, (c) caffeine-loaded PEC particles, (d) ibuprofen, (e) ibuprofen-loaded PEC particles.

The FT-IR spectrum of the caffeine-loaded PEC particles (Figure 6.4(c)), prepared by Method 1-d, clearly showed the caffeine absorption bands, indicating a high caffeine content in the sample. Spectrum (d) is the FT-IR spectrum of ibuprofen. The most prominent feature of the ibuprofen spectrum is the absorption band at 1722 cm^{-1}, originating from the stretching vibration of the ibuprofen carbonyl group (Matkovic *et al.*, 2005). The FT-IR absorption bands of ibuprofen were clearly visible in the spectrum of the ibuprofen-loaded PEC particles (Figure 6.4(f)), confirming the presence of ibuprofen in the loaded particles. The relative intensity of the ibuprofen bands with respect to the bands of the PEC particles was lower than that of the caffeine bands in

spectrum (c), suggesting a lower drug loading for the ibuprofen-loaded PEC particles compared to the caffeine-loaded particles, loaded with Method 1-d.

6.4.2.2. Scanning Electron Microscopy

Figure 6.5 shows FE-SEM images of the drug-loaded PEC particles. The morphology of the particles was roughly spherical in both cases. Both images were recorded with the same microscope settings and at the same magnification. A comparison of the images revealed that the ibuprofen-loaded PEC particles were much smaller than the caffeine-loaded particles. Most caffeine-loaded particles in Figure 6.5(a) had diameters in the range 300–1000 nm. The diameters of most ibuprofen-loaded particles were below 200 nm. We attributed the difference to the limited solubility of chitosan in the ethanol/water solvent system used for ibuprofen loading, as reported in the literature (Sano *et al.*, 1999). Upon immersion of the PEC particles, freeze-dried from deionized water, into the ethanol-containing ibuprofen solution, the particles probably took on a more compact structure to minimize unfavorable solvent interactions.

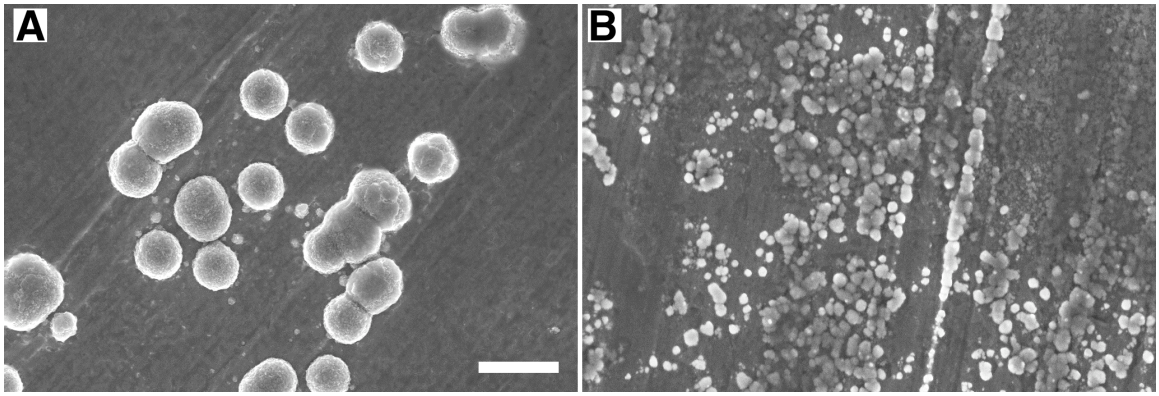

Figure 6.5. FE-SEM images of drug-loaded PEC particles: (a) Caffeine-loaded particles prepared by Method 1, (b) ibuprofen-loaded particles. Scale bar: 1 μm (applies to both images).

6.4.3. Drug Loading and Loading Efficiency

The drug loadings and loading efficiencies for caffeine and ibuprofen are listed in Table 6.1. The values obtained with Method 1 did not differ significantly from those obtained with Method 2, indicating that the polyelectrolyte mixing sequence during loading did not play a role. The values for Methods 1-d and 2-d (PEC particles freeze-dried directly from the caffeine solution) were given by the experimental conditions. It was assumed that all of the caffeine initially present was present after freeze-drying in the loaded PEC particles. The experimental conditions for ibuprofen loading were quite different from those used for caffeine loading. During caffeine loading, the amount of caffeine initially present was 20 times the combined amount of chitosan and cellulose nanocrystals. During ibuprofen loading, the amount of ibuprofen initially present was only 2.4 times the amount of unloaded PEC particles. The difference in experimental conditions explains the much lower loading efficiencies obtained for caffeine (Methods 1 and 2) compared with that obtained for ibuprofen. Interestingly, the drug loadings achieved with caffeine (Methods 1 and 2) were comparable to the drug loading achieved with ibuprofen.

Table 6.1. Loading efficiencies for caffeine and ibuprofen

Drug/Loading Method	Drug Loading (%)	Loading Efficiency (%)
Caffeine		
Method 1	263 ± 52	13.0 ± 2.6
Method 2	227 ± 55	11.2 ± 2.7
Method 1-d	2021	100
Method 2-d	2021	100
Ibuprofen	207 ± 5	87.6 ± 1.0

6.4.4. *In Vitro* Drug Release

The drug release profiles of the caffeine-loaded chitosan–cellulose nanocrystal PEC particles are shown in Figure 6.6. The PEC particles loaded by Method 1-d released 63% of the loaded caffeine within the first 2 h and 100% within 8 h. The release profile for

these particles was almost identical to that obtained for sole caffeine at a comparable concentration, indicating that the release profiles were governed by the diffusion of caffeine through the dialysis membrane. The fact that the release profiles for caffeine and the particles loaded by Method 1-d were almost identical also indicated the absence of strong molecular interactions between caffeine and the PEC particles. This finding is in accordance with the observation by Vachoud *et al.* (2001) that caffeine has no or only weak interactions with chitin networks prepared by acetylation of chitosan. The release values for PEC particles prepared by Method 2-d were slightly lower than those for PEC particles prepared by Method 1-d, indicating a minor effect of the polyelectrolyte mixing sequence during drug loading.

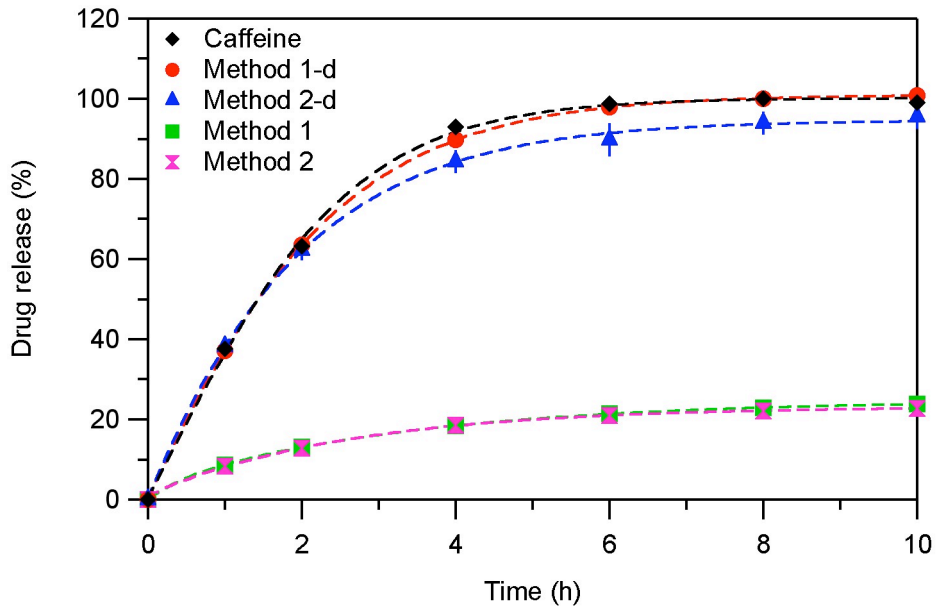

Figure 6.6. *In vitro* release profiles of caffeine-loaded chitosan–cellulose nanocrystal PEC particles for different loading methods and for sole caffeine. (See text for details. Data points are means of three measurements. Error bars represent ± one standard deviation.)

The release profiles of PEC particles loaded by Methods 1 and 2, involving separation of the loaded particles from the caffeine solution by centrifugation prior to freeze-drying, were nearly identical and differed significantly from those of particles

loaded by Methods 1-d and 2-d. Release from these particles proceeded much more slowly and reached a maximum of 23–24% after 10 h. The most probable explanation for these low release values is that the drug loadings at the beginning of the release experiments were actually lower than assumed, due to a loss of caffeine in the freeze-drying process. Following isolation by centrifugation, the loaded PEC particles were resuspended in deionized water. Since caffeine is highly soluble in deionized water, a portion of the loaded caffeine might have been released from the PEC particles and either been carried out of the flask by the subliming water molecules or deposited onto the flask walls, yielding PEC particles with much reduced drug loadings.

The drug release profiles of the ibuprofen-loaded PEC particles in simulated gastric and intestinal fluid are shown in Figure 6.7. Nearly no release of ibuprofen was observed in simulated gastric fluid, indicating that the PEC particles had no effect on the low solubility of ibuprofen in acidic aqueous media (Shaw *et al.*, 2005). In simulated intestinal fluid, ibuprofen release was rapid initially, reaching a value of 76% within 4 h, and then leveled off to approach a value of 85% after 10 h. The incomplete (< 100%) release of ibuprofen from the PEC particles in simulated intestinal fluid could have the same reason as the low release values observed for the caffeine-loaded PEC particles, loaded by Methods 1 and 2. Alternatively, the incomplete release could be due to attractive Coulomb interactions between the ibuprofen carboxylate groups and the chitosan ammonium groups. At a pH of 7.4 ibuprofen is completely ionized whereas chitosan is approximately 9% ionized (see Chapter 4). Nevertheless, this low degree of ionization may be enough to prevent complete release of the loaded ibuprofen molecules. Ionic complexes of chitosan and ibuprofen have been reported in the literature (Qandil *et al.*, 2009).

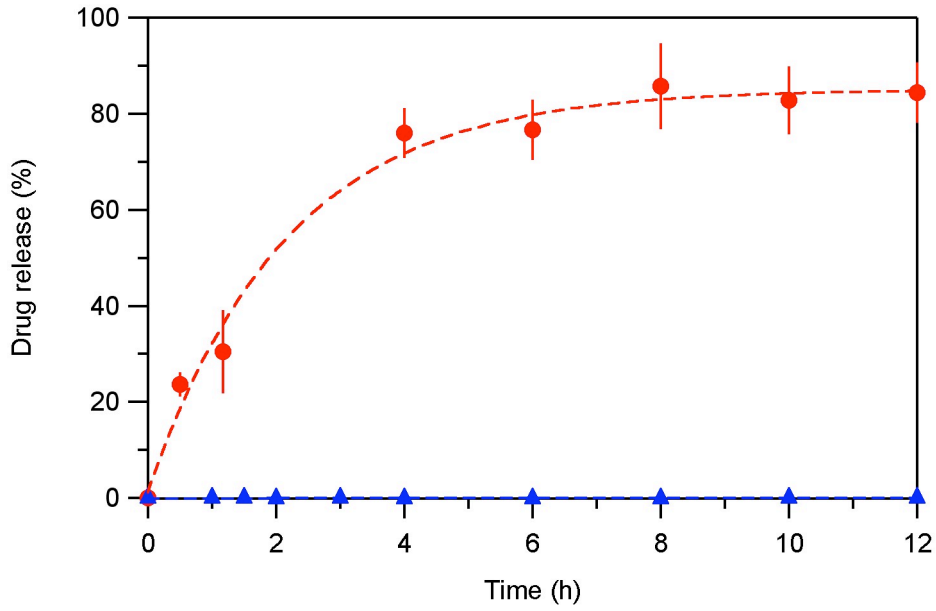

Figure 6.7. *In vitro* release profiles of ibuprofen-loaded chitosan–cellulose nanocrystal PEC particles in simulated gastric fluid (pH 1.2, ▲) and simulated intestinal fluid (pH 7.4, ●) at 37 °C. (Data points are means of three measurements. Error bars represent ± one standard deviation.)

6.5. CONCLUSIONS

Chitosan–cellulose nanocrystal PEC particles provide no control over the release rates of caffeine and ibuprofen and do not noticeably enhance the solubility of ibuprofen in simulated gastric fluid. Further evaluation studies should focus on the expected mucoadhesive and permeability-enhancing properties.

Acknowledgement

This material is based upon work supported in part by the USDA/CSREES under Grant No. 2005-35504-16088, the National Science Foundation under Grant No. CHE-0724126, and the Institute for Critical Technology and Applied Science at Virginia Tech. Additional support from Omnova, Inc. and Tembec, Inc. is also acknowledged. Furthermore, HW thanks the staff of the Nanoscale Characterization and Fabrication Laboratory for assistance with the SEM images.

6.6. REFERENCES

Agnihotri, S. A., N. N. Mallikarjuna and T. M. Aminabhavi (2004). "Recent advances on chitosan-based micro- and nanoparticles in drug delivery." Journal of Controlled Release **100**(1): 5–28.

Al-Maaieh, A. and D. R. Flanagan (2002). "Salt effects on caffeine solubility, distribution, and self-association." Journal of Pharmaceutical Sciences **91**(4): 1000–1008.

Arangoa, M. A., M. A. Campanero, M. J. Renedo, G. Ponchel and J. M. Irache (2001). "Gliadin nanoparticles as carriers for the oral administration of lipophilic drugs: Relationships between bioadhesion and pharmacokinetics." Pharmaceutical Research **18**(11): 1521–1527.

Belay, A., K. Ture, M. Redi and A. Asfaw (2008). "Measurement of caffeine in coffee beans with UV/vis spectrometer." Food Chemistry **108**(1): 310–315.

Berth, G., A. Voigt, H. Dautzenberg, E. Donath and H. Mohwald (2002). "Polyelectrolyte complexes and layer-by-layer capsules from chitosan/chitosan sulfate." Biomacromolecules **3**(3): 579–590.

Callender, D. P., N. Jayaprakash, A. Bell, V. Petraitis, R. Petratienes, M. Candelario, R. Schaufele, J. M. Dunn, S. Sei, T. J. Walsh and F. M. Balis (1999). "Pharmacokinetics of oral zidovudine entrapped in biodegradable nanospheres in rabbits." Antimicrobial Agents and Chemotherapy **43**(4): 972–974.

Cekic, N. D., S. D. Savic, J. Milic, M. M. Savic, Z. Jovic and M. Malesevic (2007). "Preparation and characterisation of phenytoin-loaded alginate and alginate-chitosan microparticles." Drug Delivery **14**(8): 483–490.

Chellat, F., M. Tabrizian, S. Dumitriu, E. Chornet, P. Magny, C. H. Rivard and L. Yahia (2000a). "*In vitro* and *in vivo* biocompatibility of chitosan-xanthan polyionic complex." Journal of Biomedical Materials Research **51**(1): 107–116.

Chellat, F., M. Tabrizian, S. Dumitriu, E. Chornet, C.-H. Rivard and L. H. Yahia (2000b). "Study of biodegradation behavior of chitosan-xanthan microspheres in simulated physiological media." Journal of Biomedical Materials Research **53**(5): 592–599.

Chen, Y., V. J. Mohanraj, F. Wang and H. A. E. Benson (2007). "Designing chitosan-dextran sulfate nanoparticles using charge ratios." AAPS PharmSciTech **8**(4): 131–139.

Dai, Y. N., P. Li, J. P. Zhang, A. O. Wang and Q. Wei (2008). "Swelling characteristics and drug delivery properties of nifedipine-loaded pH sensitive alginate-chitosan hydrogel beads." Journal of Biomedical Materials Research Part B-Applied Biomaterials **86B**(2): 493–500.

Dai, Z. Z., J. B. Yin, S. F. Yan, T. Cao, J. Ma and X. Chen (2007). "Polyelectrolyte complexes based on chitosan and poly(L-glutamic acid)." Polymer International **56**(9): 1122–1127.

de la Fuente, M., B. Seijo and M. J. Alonso (2008a). "Design of novel polysaccharidic nanostructures for gene delivery." Nanotechnology **19**(7): 1–9.

de la Fuente, M., B. Seijo and M. J. Alonso (2008b). "Novel hyaluronan-based nanocarriers for transmucosal delivery of macromolecules." Macromolecular Bioscience **8**(5): 441–450.

Domanska, U., A. Pobudkowska, A. Pelczarska and P. Gierycz (2009). "pK(a) and solubility of drugs in water, ethanol, and 1-octanol." Journal of Physical Chemistry B **113**(26): 8941–8947.

Drogoz, A., L. David, C. Rochas, A. Domard and T. Delair (2007). "Polyelectrolyte complexes from polysaccharides: Formation and stoichiometry monitoring." Langmuir **23**(22): 10950–10958.

Drogoz, A., S. Munier, B. Verrier, L. David, A. Dornard and T. Delair (2008). "Towards biocompatible vaccine delivery systems: Interactions of colloidal PECs based on polysaccharides with HIV-1 p24 antigen." Biomacromolecules **9**(2): 583–591.

Du, L. W., X. H. Liu, W. M. Huang and E. K. Wang (2006). "A study on the interaction between ibuprofen and bilayer lipid membrane." Electrochimica Acta **51**(26): 5754–5760.

Dunn, J. M. and A. S. Hollister (1995). "Oral bioavailability of heparin using a novel delivery system." Current Therapeutic Research-Clinical and Experimental **56**(8): 738–745.

El-Shabouri, M. H. (2002). "Positively charged nanoparticles for improving the oral bioavailability of cyclosporin-A." International Journal of Pharmaceutics **249**(1-2): 101–108.

Galindo-Rodriguez, S. A., E. Allemann, H. Fessi and E. Doelker (2005). "Polymeric nanoparticles for oral delivery of drugs and vaccines: A critical evaluation of *in vivo* studies." Critical Reviews in Therapeutic Drug Carrier Systems **22**(5): 419–463.

Gomez-Burgaz, M., B. Garcia-Ochoa and S. Torrado-Santiago (2008). "Chitosan-carboxymethylcellulose interpolymer complexes for gastric-specific delivery of clarithromycin." International Journal of Pharmaceutics **359**(1-2): 135–143.

Hajdu, I., M. Bodnar, G. Filipcsei, J. F. Hartmann, L. Daroczi, M. Zrinyi and J. Borbely (2008). "Nanoparticles prepared by self-assembly of chitosan and poly-gamma-glutamic acid." Colloid and Polymer Science **286**(3): 343–350.

Hinterstoisser, B. and L. Salmén (1999). "Two-dimensional step-scan FTIR: A tool to unravel the OH-valency-range of the spectrum of cellulose I." Cellulose **6**(3): 251–263.

Illum, L., N. F. Farraj and S. S. Davis (1994). "Chitosan as a novel nasal delivery system for peptide drugs." Pharmaceutical Research **11**(8): 1186–1189.

Jiao, Y. Y., N. Ubrich, M. Marchand-Arvier, C. Vigneron, M. Hoffman, T. Lecompte and P. Maincent (2002). "*In vitro* and *in vivo* evaluation of oral heparin-loaded polymeric nanoparticles in rabbits." Circulation **105**(2): 230–235.

Junginger, H. E. and J. C. Verhoef (1998). "Macromolecules as safe penetration enhancers for hydrophilic drugs - a fiction?" Pharmaceutical Science & Technology Today **1**(9): 370–376.

Katsu, T., Y. Tsunamoto, N. Hanioka, K. Komagoe, K. Masuda and S. Narimatsu (2008). "A caffeine-sensitive membrane electrode: Previous misleading report and present approach." Analytica Chimica Acta **620**(1-2): 50–54.

Kawashima, Y., H. Yamamoto, H. Takeuchi and Y. Kuno (2000). "Mucoadhesive DL-lactide/glycolide copolymer nanospheres coated with chitosan to improve oral delivery of elcatonin." Pharmaceutical Development and Technology **5**(1): 77–85.

Kesimli, B., A. Topacli and C. Topacli (2003). "An interaction of caffeine and sulfamethoxazole: studied by IR spectroscopy and PM3 method." Journal of Molecular Structure **645**(2-3): 199–204.

Kondo, T. and C. Sawatari (1996). "A Fourier transform infra-red spectroscopic analysis of the character of hydrogen bonds in amorphous cellulose." Polymer **37**(3): 393–399.

Kotze, A. F., B. J. de Leeuw, H. L. Luessen, A. G. de Boer, J. C. Verhoef and H. E. Junginger (1997). "Chitosans for enhanced delivery of therapeutic peptides across intestinal epithelia: *In vitro* evaluation in Caco-2 cell monolayers." International Journal of Pharmaceutics **159**(2): 243–253.

Kreuter, J., U. Muller and K. Munz (1989). "Quantitative and microautoradiographic study on mouse intestinal distribution of polycyanoacrylate nanoparticles." International Journal of Pharmaceutics **55**(1): 39–45.

Krzek, J., M. Starek and D. Jelonkiewicz (2005). "RP-TLC determination of S(+) and R(-) ibuprofen in drugs with the application of chiral mobile phase and UV densitometric detection." Chromatographia **62**(11-12): 653–657.

Li, S., J. Berger and S. Hartland (1990). "UV spectrophotometric determination of theobromine and caffeine in cocoa beans." Analytica Chimica Acta **232**(2): 409–412.

Liu, X. D., W. T. Yu, W. Wang, Y. Xiong, X. J. Ma and Q. A. Yuan (2008). "Polyelectrolyte microcapsules prepared by alginate and chitosan for biomedical application." Progress in Chemistry **20**(1): 126–139.

Liu, X. Z. and Z. L. Fang (1998). "Sequential-injection system for drug-dissolution studies of ibuprofen tablets and sustained-release formulations." Analytica Chimica Acta **358**(2): 103–110.

Liu, Z. G., Y. P. Jiao, F. Liu and Z. Y. Zhang (2007). "Heparin/chitosan nanoparticle carriers prepared by polyelectrolyte complexation." Journal of Biomedical Materials Research Part A **83A**(3): 806–812.

Lopez-Martinez, L., P. L. Lopez-de-Alba, R. Garcia-Campos and L. M. De Leon-Rodriguez (2003). "Simultaneous determination of methylxanthines in coffees and teas by UV-Vis spectrophotometry and partial least squares." Analytica Chimica Acta **493**(1): 83–94.

Ma, Z. S., T. M. Lim and L. Y. Lim (2005). "Pharmacological activity of peroral chitosan-insulin nanoparticles in diabetic rats." International Journal of Pharmaceutics **293**(1-2): 271–280.

Marchessault, R. H. and C. Y. Liang (1960). "Infrared spectra of crystalline polysaccharides. III. Mercerized cellulose." Journal of Polymer Science **43**: 71–84.

Maréchal, Y. and H. Chanzy (2000). "The hydrogen bond network in I-beta cellulose as observed by infrared spectrometry." Journal of Molecular Structure **523**: 183–196.

Matkovic, S. R., G. M. Valle and L. E. Briand (2005). "Quantitative analysis of ibuprofen in pharmaceutical formulations through FTIR spectroscopy." Latin American Applied Research **35**(3): 189–195.

Morrow, P. E., H. C. Hodge, W. F. Neuman, E. A. Maynard, H. J. Blanchet, Jr., D. W. Fassett, R. E. Birk and S. Manrodt (1952). "Gastrointestinal non-absorption of sodium cellulose sulfate labeled with sulfur-35." Journal of Pharmacology and Experimental Therapeutics **105**(3): 273–281.

Motwani, S. K., S. Chopra, S. Talegaonkar, K. Kohl, F. J. Ahmad and R. K. Khar (2008). "Chitosan-sodium alginate nanoparticles as submicroscopic reservoirs for ocular delivery: Formulation, optimisation and *in vitro* characterisation." European Journal of Pharmaceutics and Biopharmaceutics **68**(3): 513–525.

Nikonenko, N. A., D. K. Buslov, N. I. Sushko and R. G. Zhbankov (2000). "Investigation of stretching vibrations of glycosidic linkages in disaccharides and polysaccarides with use of IR spectra deconvolution." Biopolymers **57**(4): 257–262.

Nikonenko, N. A., D. K. Buslov, N. I. Sushko and R. G. Zhbankov (2005). "Spectroscopic manifestation of stretching vibrations of glycosidic linkage in polysaccharides." Journal of Molecular Structure **752**(1-3): 20–24.

Oh, S. Y., D. I. Yoo, Y. Shin, H. C. Kim, H. Y. Kim, Y. S. Chung, W. H. Park and J. H. Youk (2005). "Crystalline structure analysis of cellulose treated with sodium hydroxide and carbon dioxide by means of X-ray diffraction and FTIR spectroscopy." Carbohydrate Research **340**(15): 2376–2391.

Pan, Y., Y.-J. Li, H.-Y. Zhao, J.-M. Zheng, H. Xu, G. Wei, J.-S. Hao and F.-D. Cui (2002). "Bioadhesive polysaccharide in protein delivery system: chitosan nanoparticles improve the intestinal absorption of insulin *in vivo*." International Journal of Pharmaceutics **249**(1-2): 139–147.

Piyakulawat, P., N. Praphairaksit, N. Chantarasiri and N. Muangsin (2007). "Preparation and evaluation of chitosan/carrageenan beads for controlled release of sodium diclofenac." AAPS PharmSciTech **8**(4): 120–130.

Qandil, A. M., A. A. Obaidat, M. A. M. Ali, B. M. Al-Taani, B. M. Tashtoush, N. D. Al-Jbour, M. M. Al Remawi, K. A. Al-Sou'od and A. A. Badwan (2009). "Investigation of the interactions in complexes of low molecular weight chitosan with ibuprofen." Journal of Solution Chemistry **38**(6): 695–712.

Sano, M., O. Hosoya, S. Taoka, T. Seki, T. Kawaguchi, K. Sugibayashi, K. Juni and Y. Morimoto (1999). "Relationship between solubility of chitosan in alcoholic solution and its gelation." Chemical & Pharmaceutical Bulletin **47**(7): 1044–1046.

Sarmento, B., A. Ribeiro, F. Veiga and D. Ferreira (2006). "Development and characterization of new insulin containing polysaccharide nanoparticles." Colloids and Surfaces, B: Biointerfaces **53**(2): 193–202.

Sarmento, B., A. Ribeiro, F. Veiga, D. Ferreira and R. Neufeld (2007a). "Oral bioavailability of insulin contained in polysaccharide nanoparticles." Biomacromolecules **8**(10): 3054–3060.

Sarmento, B., A. Ribeiro, F. Veiga, P. Sampaio, R. Neufeld and D. Ferreira (2007b). "Alginate/chitosan nanoparticles are effective for oral insulin delivery." Pharmaceutical Research **24**(12): 2198–2206.

Sarmento, B., A. J. Ribeiro, F. Veiga, D. C. Ferreira and R. J. Neufeld (2007c). "Insulin-loaded nanoparticles are prepared by alginate ionotropic pre-gelation followed by chitosan polyelectrolyte complexation." Journal of Nanoscience and Nanotechnology **7**(8): 2833–2841.

Save, T. K., D. V. Parmar and P. V. Devarajan (1997). "High-performance thin-layer chromatographic determination of ibuprofen in plasma." Journal of Chromatography, B: Biomedical Sciences and Applications **690**(1-2): 315–319.

Schatz, C., A. Domard, C. Viton, C. Pichot and T. Delair (2004a). "Versatile and efficient formation of colloids of biopolymer-based polyelectrolyte complexes." Biomacromolecules **5**(5): 1882–1892.

Schatz, C., J. M. Lucas, C. Viton, A. Domard, C. Pichot and T. Delair (2004b). "Formation and properties of positively charged colloids based on polyelectrolyte complexes of biopolymers." Langmuir **20**(18): 7766–7778.

Schipper, N. G. M., S. Olsson, J. A. Hoogstraate, A. G. deBoer, K. M. Varum and P. Artursson (1997). "Chitosans as absorption enhancers for poorly absorbable drugs. 2. Mechanism of absorption enhancement." Pharmaceutical Research **14**(7): 923–929.

Shaw, L. R., W. J. Irwin, T. J. Grattan and B. R. Conway (2005). "The effect of selected water-soluble excipients on the dissolution of paracetamol and ibuprofen." Drug Development and Industrial Pharmacy **31**(6): 515–525.

Sochor, J., J. Klimes, J. Sedlacek and M. Zahradnicek (1995). "Determination of ibuprofen in erythrocytes and plasma by high-performance liquid-chromatography." Journal of Pharmaceutical and Biomedical Analysis **13**(7): 899–903.

Sochor, J., J. Klimes, M. Zahradnicek and J. Sedlacek (1994). "High-performance liquid-chromatography assay for ibuprofen in whole-blood using solid-phase extraction." Journal of Chromatography, B: Biomedical Sciences and Applications **654**(2): 282–286.

Steele, D. F., S. Edge, M. J. Tobyn, R. C. Moreton and J. N. Staniforth (2003). "Adsorption of an amine drug onto microcrystalline cellulose and silicified microcrystalline cellulose samples." Drug Development and Industrial Pharmacy **29**(4): 475–487.

Sui, W., L. L. Huang, J. Wang and Q. B. Bo (2008). "Preparation and properties of chitosan chondroitin sulfate complex microcapsules." Colloids and Surfaces, B: Biointerfaces **65**(1): 69–73.

Tusing, T. W., O. E. Paynter and O. A. Battista (1964). "Birefringence of plant fibrous cellulose and microcrystalline cellulose in human stools freezer-stored immediately after evacuation." Agriculture and Food Chemistry **12**(3): 284–287.

Vachoud, L., N. Zydowicz and A. Domard (2001). "Sorption and desorption studies on chitin gels." International Journal of Biological Macromolecules **28**(2): 93–101.

Veselkov, D. A., V. V. Kodintsev, V. I. Pakhomov, L. N. Dymant, D. B. Davies and A. N. Veselkov (2000). "1H-NMR analysis of heteroassociation of caffeine with antibiotic actinomycin D in aqueous solution." Biofizika **45**(2): 197–206.

Wang, X. Q., J. D. Dai, Z. Chen, T. Zhang, G. M. Xia, T. Nagai and Q. Zhang (2004). "Bioavailability and pharmacokinetics of cyclosporine A-loaded pH-sensitive

nanoparticles for oral administration." Journal of Controlled Release **97**(3): 421–429.

Wei, W., L. Y. Wang, L. Yuan, X. D. Yang, Z. G. Su and G. H. Ma (2008). "Bioprocess of uniform-sized crosslinked chitosan microspheres in rats following oral administration." European Journal of Pharmaceutics and Biopharmaceutics **69**(3): 878–886.

Wong, T. W. and S. Nurjaya (2008). "Drug release property of chitosan-pectinate beads and its changes under the influence of microwave." European Journal of Pharmaceutics and Biopharmaceutics **69**(1): 176–188.

Yamauchi, Y., A. Nakamura, I. Kohno, M. Kitai, K. Hatanaka and T. Tanimoto (2008). "Simple and rapid UV spectrophotometry of caffeine in tea coupled with sample pre-treatment using a cartridge column filled with polyvinylpolypyrrolidone (PVPP)." Chemical & Pharmaceutical Bulletin **56**(2): 185–188.

Zhang, L., Y. Jin, H. Q. Liu and Y. M. Du (2001). "Structure and control release of chitosan/carboxymethyl cellulose microcapsules." Journal of Applied Polymer Science **82**(3): 584–592.

CHAPTER 7

CONCLUSIONS

The formation and properties of PEC particles from chitosan and cellulose nanocrystals are governed by the strong mismatch in the densities of ionizable groups. The particles are composed primarily of cellulose nanocrystals. The composition, shape, and size strongly depend on the mixing ratio and pH of the surrounding medium. The ionic strength of the surrounding medium, and the molecular weight and degree of deacetylation of chitosan have a minor effect on the formation and properties of the particles.

Chitosan–cellulose nanocrystal PEC particles provide no control over the release rates of caffeine and ibuprofen and do not noticeably enhance the solubility of ibuprofen in simulated gastric fluid. Further evaluation studies should focus on the expected mucoadhesive and permeability-enhancing properties of chitosan–cellulose nanocrystal PEC particles.